FACIES, STRATIGRAPHIC ARCHITECTURE, AND LAKE EVOLUTION OF THE OIL SHALE BEARING GREEN RIVER FORMATION, EASTERN UINTA BASIN, UTAH

by

Morgan Joshua Rosenberg

A thesis submitted to the faculty of
The University of Utah
in partial fulfillment of the requirements for the degree of

Master of Science

in

Geology

Department of Geology and Geophysics

The University of Utah

August 2013

The University of Utah Graduate School

STATEMENT OF THESIS APPROVAL

The thesis of **Morgan Joshua Rosenberg**

has been approved by the following supervisory committee members:

Lauren Birgenheier	, Chair	**6/01/2013** Date Approved
Cari Johnson	, Member	**3/22/2013** Date Approved
Michael Vanden Berg	, Member	**3/22/2013** Date Approved

and by **D. Kip Solomon** , Chair of

the Department of **Geology and Geophysics**

and by Donna M. White, Interim Dean of The Graduate School.

ABSTRACT

Lacustrine basin systems have historically been valued for their abundant conventional oil and gas reserves, but they also contain a vast potential for unconventional petroleum development. To better understand the evolution of Utah's Eocene Lake Uinta and to help facilitate prudent and economic development of its oil shale resource, a predictive genetic model of the basin's lacustrine strata has been refined here. This model provides a better understanding of facies distribution, stratigraphic architecture, and a precise history of depositional evolution of Lake Uinta in eastern Utah.

This study evaluates the upper Douglas Creek and Parachute Creek Members of the Green River Formation, exposed along the Evacuation Creek outcrop on the eastern flank of the Uinta Basin. In addition to the outcrop, the Asphalt Wash-1 core, located about 13.7 km (8.5 mi) to the northwest of Evacuation Creek, was described. Ten different facies are defined and grouped into four facies associations: siliciclastics, carbonates, saline deposits, and volcanic-derived deposits. These datasets provide an exceptional opportunity to highlight lateral changes in facies architecture on the east side of the basin. The sections record meter-scale shallowing upward successions, with an overall shallow to deep to shallower transformation of the lake system. Periods of high sediment supply are recorded by laterally extensive sandstone associations, whereas low

siliciclastic sediment supply conditions are recorded by carbonate-dominated organic-rich zones and organic-poor microbialite intervals.

This research further defines a genetic framework that recognizes small-scale phases in lake evolution which are defined by the relationship between absolute lake level, accommodation, siliciclastic input, and salinity. The combination of short-term climatic changes and longer-term tectonics shaped the evolution of Lake Uinta from an overfilled basin with fluctuations in sediment supply and accommodation that vary in both frequency and length (lake phases 1a and 1b), to a balance-filled basin with little to no sediment input with a high lake level (lake phases 2a, 2b, and 3a), to an underfilled basin with abundant saline minerals (lake phase 3b). This research provides a key dataset towards developing a regional genetic framework for lake evolution in the eastern Uinta Basin.

TABLE OF CONTENTS

LIST OF TABLES

LIST OF FIGURES

ACKNOWLEDGMENTS

Acknowledging everyone who has impacted my academic career over the last two years is an unmanageable task, but there are a handful of individuals whose influence should not go unnoticed. First and foremost, I want to thank my loving and supportive parents, Dena and David Rosenberg, who raised me with unparalleled determination and work ethic, which were essential for completing this project. I also want to thank my family at Kennesaw First Baptist Church in Kennesaw, Georgia whose nonstop moral support, encouragement, and prayers reached me on a daily basis; specifically: John Dyal, Philip Stephenson, Timmy K. Thai, George Carlton, and Joseph Fowler. Lastly for my personal acknowledgements, I want to thank Hyatt Howard, Elliott Ream, David Harris, and Mike McCrary, whose friendships and conversations I value immensely.

On an academic level, I first want to acknowledge John Schafer, Earth Science instructor at Kennesaw Mountain High School. Mr. Schafer first sparked my interest in geology by introducing me to field-based problem solving. I also want to thank Rob Hawman and Steve Holland from the University of Georgia for their guidance and instruction while I was an undergraduate student.

At the University of Utah, I first want to thank my advisor Lauren Birgenheier for giving me the opportunity to come to Salt Lake City and work on a project that I have enjoyed thoroughly from day one. Lauren motivated me and often pushed me to the academic limit on a weekly basis, this kept my interest and focus level high. I will always

be grateful for my experience working with Lauren. I also want to acknowledge the other two members of my advisory committee: Cari Johnson and Mike Vanden Berg. Cari and Mike both taught me a great deal during the last two years and have both provided vast contributions towards this project. I will never forget the hours and hours Mike and I spent driving on dirt roads in the Uinta Basin the last two years listening to the "basin rock" radio station. I want to acknowledge Jon Primm for providing me with professional field assistance. Waking up and doing fieldwork in the dark to watch our Dawgs whip the jean-short-wearing Gators in the Lamplighter Inn is a memory I will never forget. Last, but not least, I want to thank all my classmates at the University of Utah for their support: James Taylor for his help with CorelDraw and field assistance, Andrew McCauley and Brendan Horton for their many shared workroom hours, Mason Edwards for his ArcGIS assistance, Leah Toms for her field assistance, and finally all of the office supporters: Mark Gorenc, Pat Dooling, Luke Pettinga, Tyler Szwarc, Tommy Good, Jim Lehane, Alex Gonzalez, Alex Turner, and Kelly Good. Isaiah 41:10/ Matthew 16:26/ Romans 1:16

INTRODUCTION

Increasing oil prices along with concerns of declining conventional oil reserves have led to an increased emphasis on unconventional petroleum research. The thermally immature lacustrine oil shale deposits of the Green River Formation in Utah, Colorado, and Wyoming provide a substantial unconventional resource. Oil shale contains an abundance of thermally-immature organic matter called kerogen, formed predominately by the deposition and preservation of algae found in lacustrine settings (Dyni, 2006; Ruble and Philp, 1998). Oil shale has the potential to be an important energy resource if economic and environmentally sound retorting technologies can be developed (Dyni, 2006). The upper Green River Formation in the Uinta Basin hosts one of the largest deposits of oil shale in the world; estimated in-place resources total 1.32 trillion barrels of oil (USGS, 2010) with approximately 77 billion barrels as a potential economic resource (Vanden Berg, 2008; Cashion, 1967). Within the Mahogany zone, the interval with the highest organic-richness, beds can surpass 70 gallons of oil per ton of rock (GPT) (Vanden Berg, 2008). The Mahogany zone typically averages between 20 and 25 GPT, while other rich zones average between 5 and 15 GPT (Birgenheier and Vanden Berg, 2011).

Throughout the last century, emphasis on oil shale research has mirrored trends in petroleum prices. In 1973, the Organization of Arab Petroleum Exporting Countries placed an oil embargo on the United States, causing oil prices to climb abruptly

(Andrews, 2006). Not knowing the duration of the embargo, oil shale research intensified. However, in the early 1980s, oil prices dropped and so did oil shale related research (Andrews, 2006). Since the early 2000s, oil prices have again been climbing, stimulating yet another resurgence in oil shale research.

Despite decades of research, controls on the shorter-term cyclicity of organic-rich and lean zones, combined with longer-term changes in stratigraphy, are still lacking for the eastern Uinta Basin. Tänavsuu-Milkeviciene and Sarg (2012) performed a detailed study of the evolution of the Piceance Creek Basin and studies of Wyoming's Greater Green River Basin, in large part, formed the basis for Carroll and Bohacs' (1999, 2001) seminal model of lake facies and depositional controls that categorizes overfilled, balance filled and underfilled lake conditions relative to the balance of water and sediment input.

In the Uinta Basin, numerous studies have been completed in the south-central region, in the Sunnyside Delta interval (middle Green River Formation) of Nine Mile Canyon. Keighley (2002, 2003), Schomaker et al. (2010), and Moore et al. (2012) focused on the sedimentology, stratigraphic architecture, and presented a high resolution sequence stratigraphic model of a discrete interval within the Sunnyside Delta Interval. Detailed comparative analysis of the Douglas Creek Member on the eastern side of the basin, which is largely correlative with the Sunnyside Delta Interval, is lacking. Taylor and Ritts (2004) performed a reservoir characterization study comparing and contrasting short intervals of fluvial-deltaic shoreline deposits from Nine Mile Canyon, as well as wave-modified shoreline deposits from Raven Ridge in the northeastern Uinta Basin. Morgan et al. (2003) has provided a detailed outcrop characterization and log correlation study of the lower to middle Green River Formation across the basin. Vanden Berg

(2008) has conducted a resource evaluation of the organic-rich oil-shale zones within the Uinta Basin, but this excludes detailed facies descriptions and interpretations of the organic-rich and lean zones. Despite this research, there are no studies to date that highlight the detailed facies changes and stratigraphic architecture of the alternating rich and lean zones in the Parachute Creek Member that overlies the Douglas Creek Member. Specifically a predictable sequence stratigraphic model from a significant thickness of the formation on the eastern side of the basin is needed, with a focus on sedimentologic processes, lateral facies architecture, and controls on lake deposition. Existing studies reveal numerous stratigraphic and geographic knowledge gaps in the eastern side of the Uinta Basin, which are essential for developing basin wide genetic models and interpretations.

The long-term evolution of Lake Uinta is thought to have been controlled by a combination of climatic and tectonic factors that resulted in different phases in lake evolution, due to changes in the balance between lake accommodation as well as sediment and water influx, resulting in basins that are either overfilled, balance filled, or underfilled with water and sediment relative to neighboring basins (Carroll and Bohacs, 1999; Smith et al., 2008; Keighley et al., 2003; Fouch et al., 1992; Moncure and Surdam, 1980; Morgan et al., 2003; Picard and High, 1972; Ryder et al., 1976; Birgenheier and Vanden Berg, 2011). This model accurately reflects the long term changes in the Green River Formation in the Uinta Basin, but does not appropriately explain the controls on the more detailed facies changes and architecture, as well as the stratigraphic packaging.

Very recent studies in the Uinta Basin have established a relationship between lean zone deposition and early Eocene abrupt global warming events (hyperthermals)

(Plink-Bjorklund et al., 2010; Foreman et al., 2012; Birgenheier, L. P. et al., 2009; Plink-Bjorklund and Birgenheier, 2012). During these global warming events, an overall arid climate is thought to produce highly seasonal, flashy discharge events such as monsoons. These events quickly deposit high volumes of siliciclastic material at high energy levels that resulted in deposition of the lean zones seen in outcrop (Plink-Bjorklund et al., 2009; Birgenheier and Vanden Berg, 2011; Birgenheier, L.P. et al., 2009; Plink-Bjorklund and Birgenheier, 2012).

The main objective of this study is to use a high quality, laterally extensive outcrop section to constrain the controls on rich and lean zone deposition in the eastern Uinta Basin. The nearby Asphalt Wash-1 core was used to examine the details of mud-rich lithologies that are poorly exposed in outcrop. This research aims to further define a genetic framework that recognizes small-scale phases in lake evolution that could be applied throughout the basin and used to better predict facies distribution as it relates to Utah's oil shale development. Specifically, the superb outcrop quality allows for a unique evaluation of lateral and stratigraphic changes in facies architecture in the oil shale bearing interval of the Green River Formation.

GEOLOGIC BACKGROUND AND LOCATION

The Green River Formation is an Eocene lacustrine deposit that spans northeastern Utah (Uinta Basin), southwestern Wyoming (Green River and Washakie Basins), and northwestern Colorado (Piceance Creek Basin) (Figure 1) (Blakey and Ranney, 2008). These isolated intermontane basins are part of the Colorado Plateau province of the western United States and were formed by a combination of Sevier and Laramide orogenic events (Dickinson et al., 1988). Although formed by similar mechanisms, these basins have different attributes when compared to the Uinta Basin. The Piceance Creek Basin is smaller, deeper, and more organic-rich than the Uinta Basin, whereas the Green River Basin is shallower and has the highest fluvial siliciclastic sediment supply (Tänavsuu-Milkeviciene and Sarg, 2012).

During the Late Cretaceous, Laramide deformation broke up the broad foreland province previously occupied by the Western Interior Seaway (east of the Sevier orogenic belt) into sedimentologically isolated basins. These isolated basins were separated and confined by basement-cored uplifts and primarily occupied by nonmarine environments such as lakes (Dickinson et al., 1988; Blackstone, 1983; Hagen et al., 1985; Crews and Ethridge, 1993; Osmond, 1965; DeCelles, 1994; Johnson, 1985; Fouch, 1975). Laramide deformation is attributed to continued subduction of the Farallon plate beneath the North American plate, but is distinguished by a series of basement-cored, thick-skinned contractional uplifts, which served as local sediment sources (Crews and Ethridge, 1993;

Figure 1 – Paleogeographic map of the Colorado Plateau during the Eocene Epoch. This map illustrates the regional extent of the Green River Formation with the field area marked in red. Modified from Blakey, 2008.

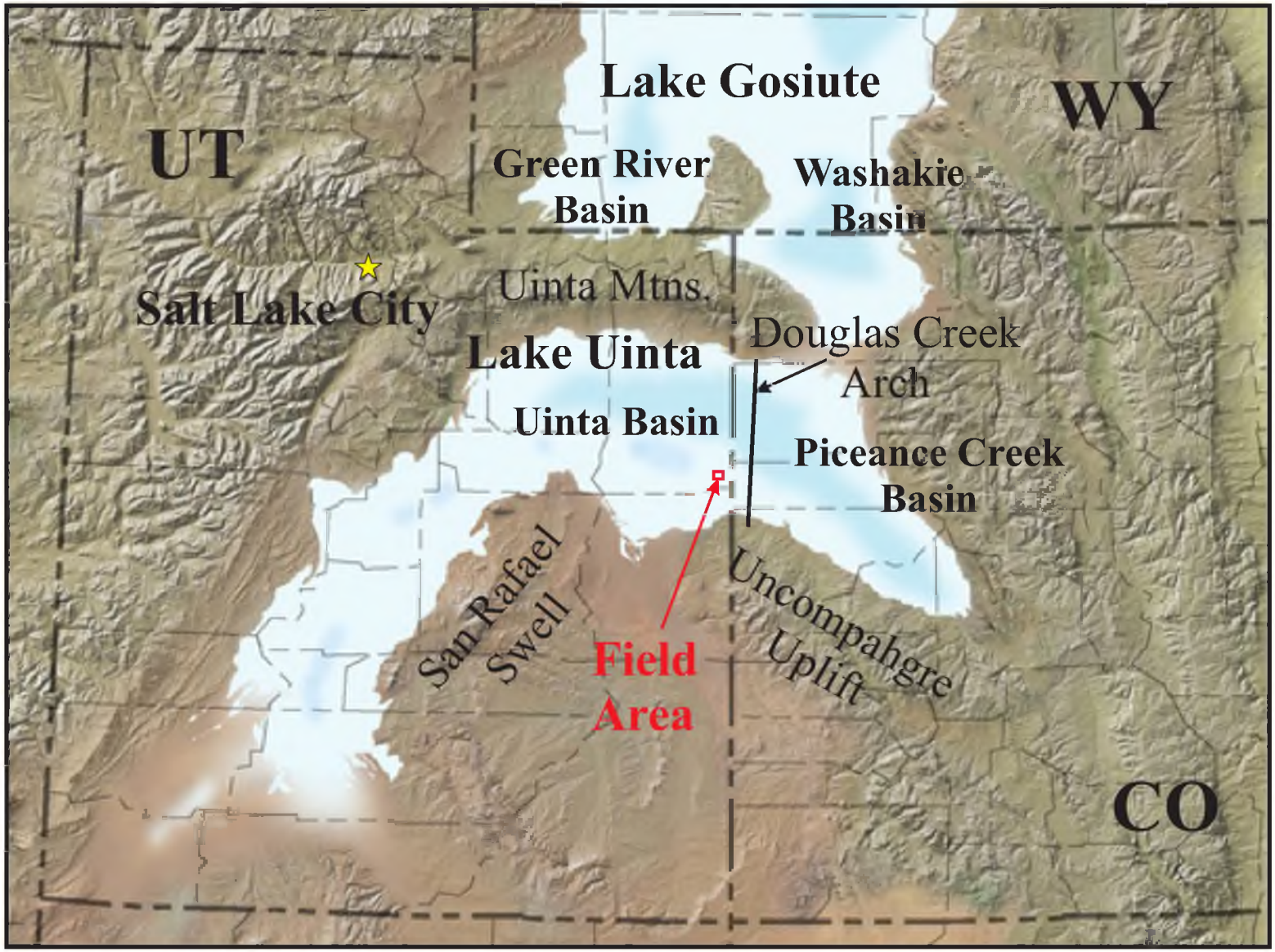
Lake Gosiute
WY
UT
Green River Basin
Washakie Basin
Uinta Mtns.
Salt Lake City
Lake Uinta
Douglas Creek Arch
Uinta Basin
Piceance Creek Basin
San Rafael Swell
Uncompahgre Uplift
Field Area
CO

Blackstone, 1983. The irregular distribution, shape and size of the uplifts across the central Rocky Mountain region cause many of the basins, like the Uinta Basin, to be asymmetric in cross-section (Abbott, 1957; Cashion, 1967; Dickinson et al., 1988). Subsidence of these basins is presumed to be in response to thrust-thickened loading along basin-margin uplifts (Crews and Ethridge, 1993; Hagen et al., 1985). The Uinta Basin is an intermontane low that is constrained by the Uinta uplift to the north and San Rafael and Uncompahgre uplifts to the south (Figure 1) (Abbott, 1957). Sevier orogenic events generated Jurassic through early Cenozoic thrusted uplifts that border the Uinta Basin to the west (Johnson, 1985). The Douglas Creek arch is a structural high on the eastern flank of the Uinta Basin that periodically served as an emergent topographic high and acted as a sill separating the Uinta and Piceance Creek Basins. This faulted anticline extends approximately 75 km from north to south and is about 35 km wide (Bader, 2009). At the end of the Cretaceous, the basins on either side of the arch began to subside, while the arch remained a positive structural feature (Osmond, 1965). During the Eocene, the Uinta and Piceance Creek Basins were occupied by Lake Uinta (Figure 1). During periods of high lake level, the Douglas Creek arch was submerged, and the Uinta and Piceance Creek lake basins were in water mass communication. In contrast, during periods of low lake level, these lake basins were isolated from one another (Carroll and Bohacs, 1999; Ruble and Philp, 1998; Birgenheier and Vanden Berg, 2011; Keighley et al., 2003; Tänavsuu-Milkeviciene and Sarg, 2012; Surdam and Stanley, 1980; Smith et al., 2008).

The Green River Formation in the Uinta Basin is separated into the lower, middle, and upper members (Figure 2) (Witkind, 1995). The lower member is characterized by

Figure 2 – Stratigraphy of the middle and upper Green River Formation. The studied interval is highlighted in red. Uinta Basin general stratigraphy from Keighley (2002), based on map by Witkind et al. (1995). Radiogenic dates from Smith and others (2010).

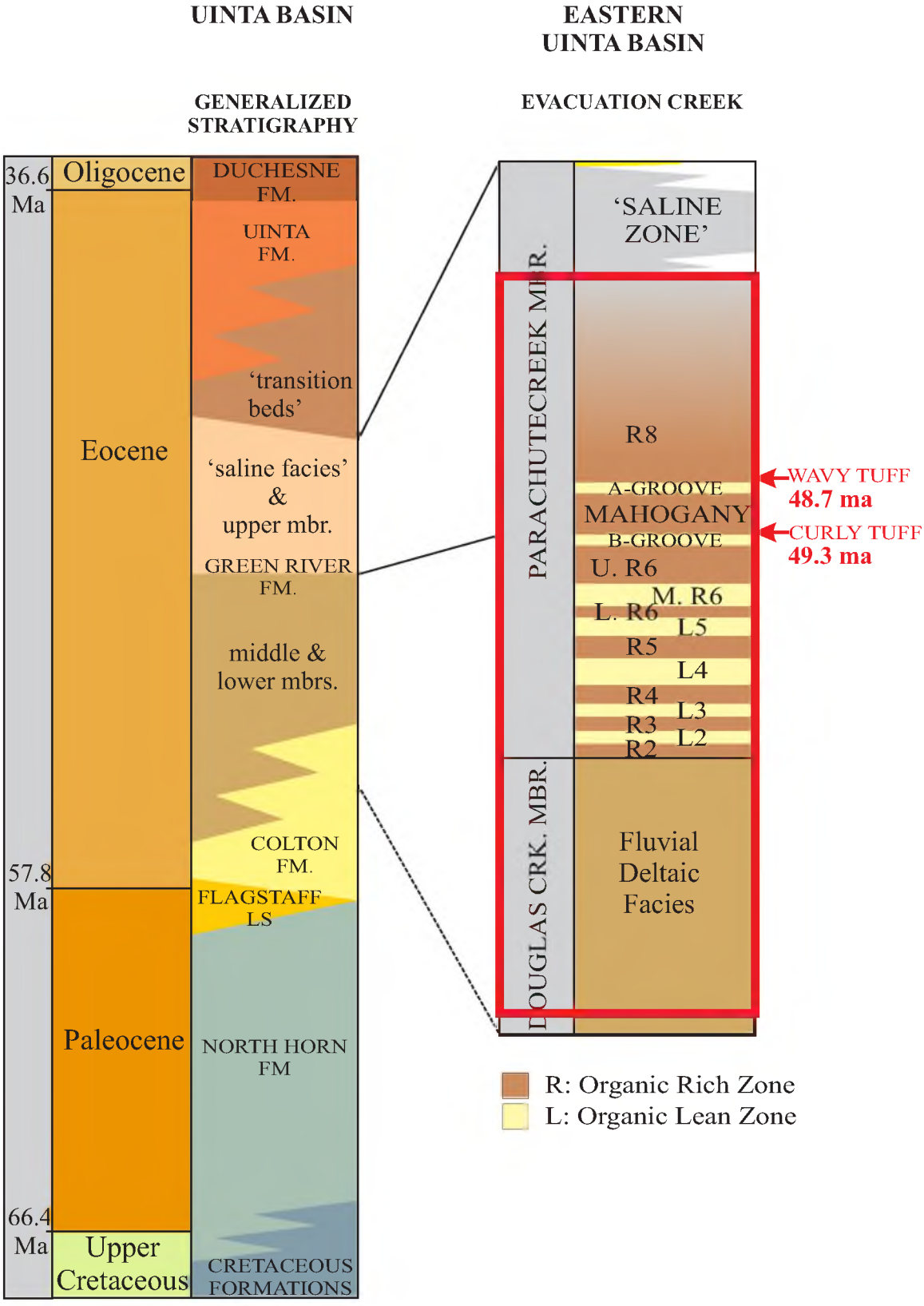
UINTA BASIN
EASTERN UINTA BASIN
GENERALIZED STRATIGRAPHY
EVACUATION CREEK
36.6 Ma
Oligocene
DUCHESNE FM.
UINTA FM.
'transition beds'
Eocene
'saline facies' & upper mbr.
GREEN RIVER FM.
middle & lower mbrs.
COLTON FM.
57.8 Ma
FLAGSTAFF LS
Paleocene
NORTH HORN FM
66.4 Ma
Upper Cretaceous
CRETACEOUS FORMATIONS
'SALINE ZONE'
PARACHUTE CREEK MBR.
R8
A-GROOVE
MAHOGANY
B-GROOVE
U. R6
M. R6
L. R6
L5
R5
L4
R4
L3
R3
L2
R2
DOUGLAS CRK. MBR.
Fluvial Deltaic Facies
WAVY TUFF
48.7 ma
CURLY TUFF
49.3 ma
R: Organic Rich Zone
L: Organic Lean Zone

regionally extensive lacustrine carbonate units and locally extensive fluvial-deltaic sandstone facies that commonly interfinger with the underlying Colton/Wasatch Formation (Ryder et al., 1976; Morgan et al., 2003; Birgenheier and Vanden Berg, 2011; Abbott, 1957). The carbonate marker bed, a regionally extensive dolomitic organic-rich unit, marks the top of the lower member. The middle and upper members of the Green River Formation, the focus of this study, are designated as the Douglas Creek Member overlain by the Parachute Creek Member (Figure 2). The Douglas Creek Member is characterized by fluvial-deltaic and carbonate facies, whereas the Parachute Creek Member is characterized by alternating rich (R) and lean (L) oil shale zones (R2 – R8 in stratigraphic order), with the Mahogany zone (R7) being the most organic-rich, and a saline facies within the middle R8 (Figure 2; (Ryder et al., 1976; Birgenheier and Vanden Berg, 2011).

The study area is located on the southeastern edge of the Uinta Basin, just west of the Douglas Creek Arch. A 6.4 km (4 mi) laterally extensive northwest to southeast trending outcrop of the middle Douglas Creek Member to the lower R8 is well exposed at Evacuation Creek. The Asphalt Wash-1 core is located approximately 13.7 km (8.5 mi) to the northwest of the Evacuation Creek outcrop (T11S, R24E, Sec. 7; 39° 52' 37.5" N 109° 16' 9.9" W) (Figure 3) and records the upper Douglas Creek Member through the basal portion of the saline zone within the middle R8.

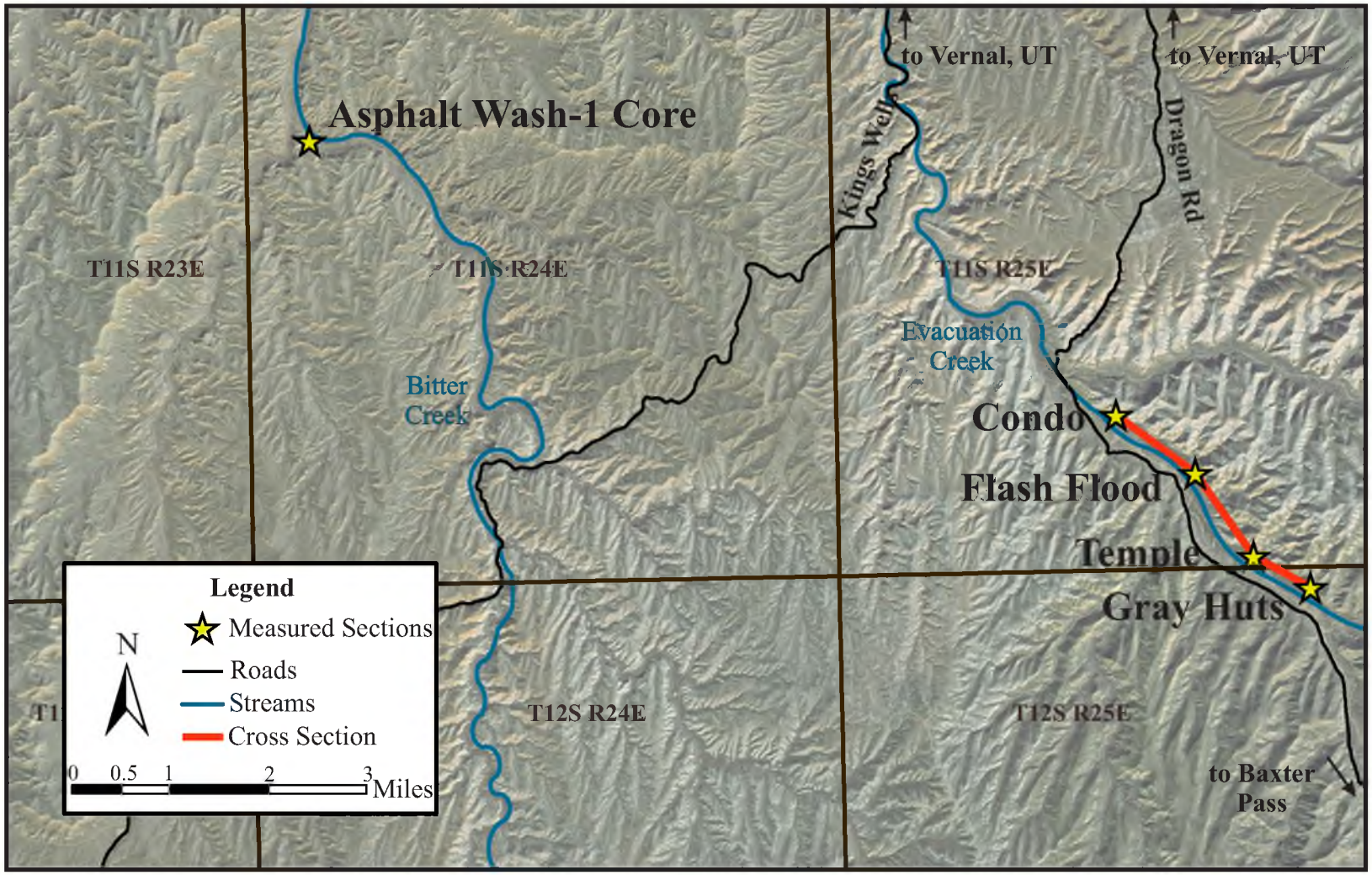

Figure 3 – Map showing the locations of measured sections along Evacuation Creek and the Asphalt Wash-1 core.

METHODS

Four detailed sections were measured along the Evacuation Creek outcrop (Figure 3). This northwest to southeast trending outcrop is about 6.4 km (4 mi) long, with 4.4 km (2.7 mi) between all measured sections, informally named (from NW to SE): Condo, Flash Flood, Temple, and Gray Huts. Each section was described using a 1.5 m measuring ruler while noting lithology, sedimentary structures, organic-richness, presence of fossils, nature of contacts, and architecture at the centimeter to meter scale. The thickness of these sections ranges from 135 m (442.9 ft) to 209 m (685.7 ft) and averages about 180 m (590.6 ft). Additionally, high-resolution gigapan photographs were taken at each measured section location and used to highlight facies architecture, mainly sandstone bodies, laterally along the Evacuation Creek outcrop (Figure 4). Key units were traced between measured sections to document lateral changes on the gigapans.

Handheld spectral gamma ray measurements were taken at 1-meter intervals at the northwestern most Condo section and southwestern most Gray Huts section. These measurements provide relative abundance of the radioactive elements thorium, potassium, and uranium, which are valuable for assessing changes in source material and can aid in the interpretation of lithology and depositional environment.

In addition to the Evacuation Creek outcrop descriptions; the Asphalt Wash-1 core was similarly described in terms of lithology, sedimentary structures, and level of

Figure 4 – Gigapan photographs of Evacuation Creek outcrop moving from NW (A) to SE (D). Sandstone bodies highlighted in yellow and Mahogany zone (R7) highlighted in green. A. Condo section. B. Flash Flood section. C. Temple section. D. Grey Huts section. Vertical scales vary and were estimated from measured section locations.

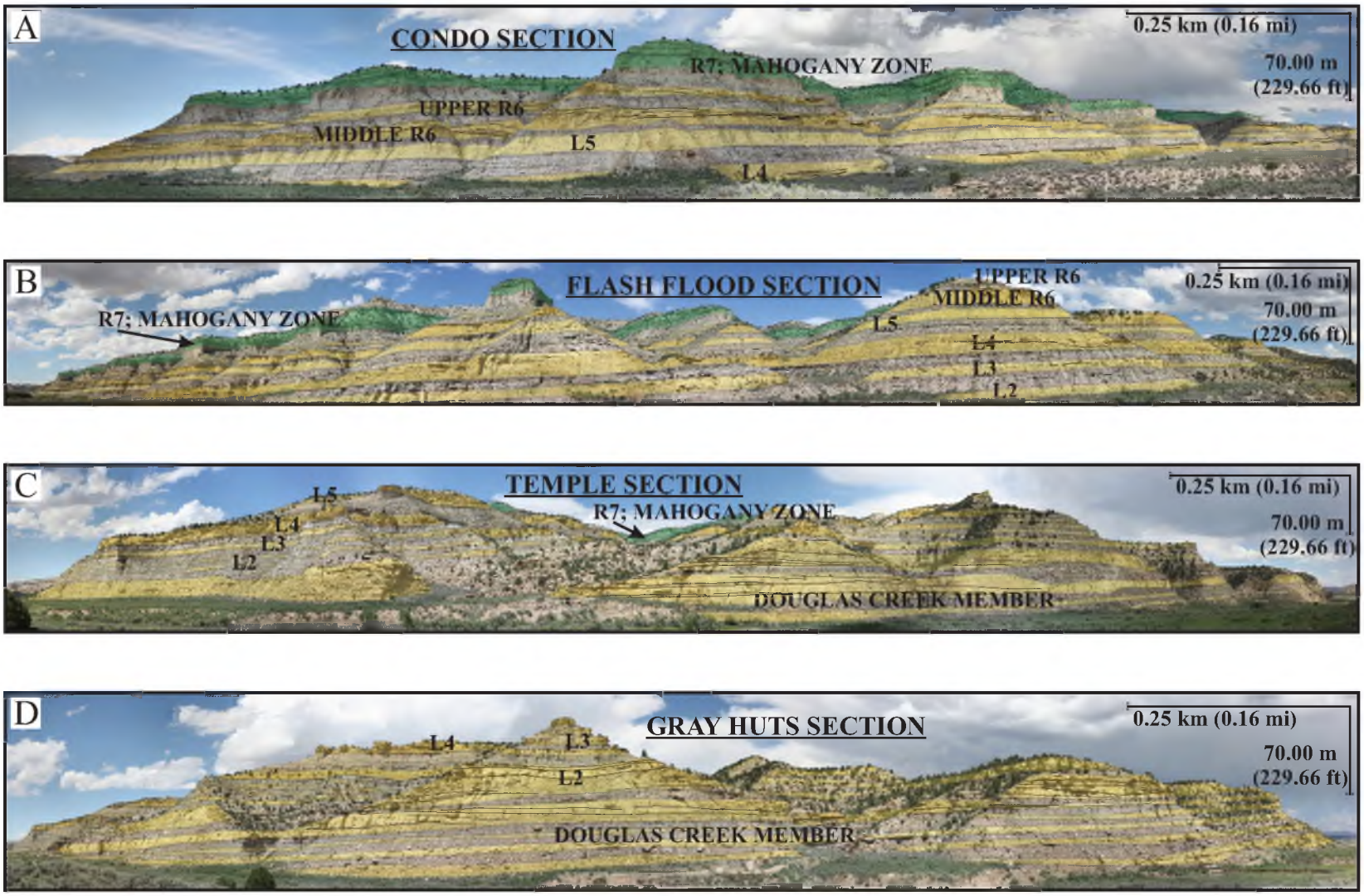
A
CONDO SECTION
R7; MAHOGANY ZONE
UPPER R6
MIDDLE R6
L5
L4
0.25 km (0.16 mi)
70.00 m
(229.66 ft)
B
FLASH FLOOD SECTION
R7; MAHOGANY ZONE
UPPER R6
MIDDLE R6
L5
L4
L3
L2
0.25 km (0.16 mi)
70.00 m
(229.66 ft)
C
TEMPLE SECTION
L5
L4
L3
L2
R7; MAHOGANY ZONE
DOUGLAS CREEK MEMBER
0.25 km (0.16 mi)
70.00 m
(229.66 ft)
D
GRAY HUTS SECTION
L4
L3
L2
DOUGLAS CREEK MEMBER
0.25 km (0.16 mi)
70.00 m
(229.66 ft)

detail. The Asphalt Wash-1 core spans two nonadjacent stratigraphic intervals from 636 to 612 m (2088 to 2007 ft) and 416 to 94 m (1364 to 307 ft).

RESULTS

Facies and Facies Associations

Detailed measured section and core descriptions are documented in Appendix A. Ten facies were defined based on lithology, sedimentary structures, organic-richness, presence of fossils, and bed geometry (Table 1; Figures 5, 6, and 7). These ten facies were grouped into four facies associations: siliciclastics, carbonates, saline deposits, and volcanic-derived deposits. The siliciclastic facies association is interpreted as a low-gradient deltaic complex composed of terminal distributary channels and fluvial mouthbars with evidence of wave influence. The carbonate facies association is typical of lacustrine carbonate ramp shorelines ranging from littoral (high energy) to sublittoral to profundal (low energy) deposits (Renaut and Gierlowski-Kordesch, 2010). Carbonate benches are characterized by a very gently sloping terrace, which subsequently have steeply sloping transitions into deeper water, resulting in abrupt facies changes. Carbonate ramps, as seen here, are characterized by a constant, gradual slope from the littoral zone, into deeper water, resulting in gradual facies transitions. The saline deposits are associated with a deep (i.e., profundal) hypersaline lacustrine environments with minimal siliciclastic input. Numerous tuff beds throughout the interval record volcanic activity in the form of both fallout tuffs and volcanic sediment sourced from the Absaroka Volcanic Province (Smith et al., 2008). The ten facies that make up the facies associations are described in detail below.

Table 1 – Faces Table

Facies	Description	Lake Zonation	Depositional Environment
F1.1	Erosionally based, channelized fine to medium grained sandstone, rip-up clasts common at base, low angle laminations to current ripples present	Littoral	Terminal distributary channel
F1.2	Massive, tabular, fine grained sandstone with some low angle laminations present	Littoral	Proximal fluvial mouthbar
F1.3	Organic poor claystone to siltstone, parallel laminated, some rip up clasts, few ripples	Sublittoral to Profundal	Distal fluvial mouthbar
F2.1	Carbonate grainstone, ooids to peloids to oncolites	Littoral	Carbonate ramp (high energy)
F2.2	Microbialites; ranging from stromatolites to thrombolites	Littoral	Carbonate ramp (high energy)
F2.3	Organic poor carbonate mudstone	Sublittoral	Carbonate ramp (low energy)
F2.4	Organic-rich carbonate mudstone, commonly associated with fish scales/bones	Profundal	Carbonate ramp (low energy)
F2.5	Organic-rich carbonate mudstone, very few fossils, parallel to wavy laminations	Profundal	Laminated, deep open water
F3.1	Organic-rich carbonate mudstone with abundant hypersaline precipitant minerals	Profundal	Laminated, deep open water
F4.1	Tuff	Volcanic ash	Volcanic ash deposit

Descriptions of the ten facies identified from the Evacuation Creek outcrop and Asphalt Wash-1 core. Facies association 1 is composed of siliciclastic deposits; facies association 2 is composed of carbonate deposits; facies association 3 is composed of saline deposits; facies association 4 is composed of volcanic-derived deposits.

Figure 5 – Facies association 1; siliciclastic deposits. A: Facies 1.1 from Gray Huts section; erosionally-based (highlighted by white dotted line), fine to medium grained sandstone channel, rip-up clasts common at base, low-angle laminations to current ripples common; interpreted as littoral, terminal distributary channel. B: Facies 1.2 from Gray Huts section; massive, fine grained sandstone (red arrow) with few ripples, low angle laminations; interpreted as proximal, fluvial mouthbar. C: Facies 1.1 from Flash Flood section; close up of medium grained sandstone. D: Facies 1.1 from Flash Flood section; close up of medium grained sandstone with current ripples. E: Facies 1.2 from Flash Flood section; massive, fine grained sandstone. F: Facies 1.1 from Asphalt Wash-1 core; fine grained sandstone with abundant current ripples, from Asphalt Wash-1 core. G: Facies 1.3 from Gray Huts section; organic poor claystone to siltstone, parallel laminations, some rip-up clasts, few ripples; interpreted as sublittoral to profundal, distal, fluvial mouthbar.

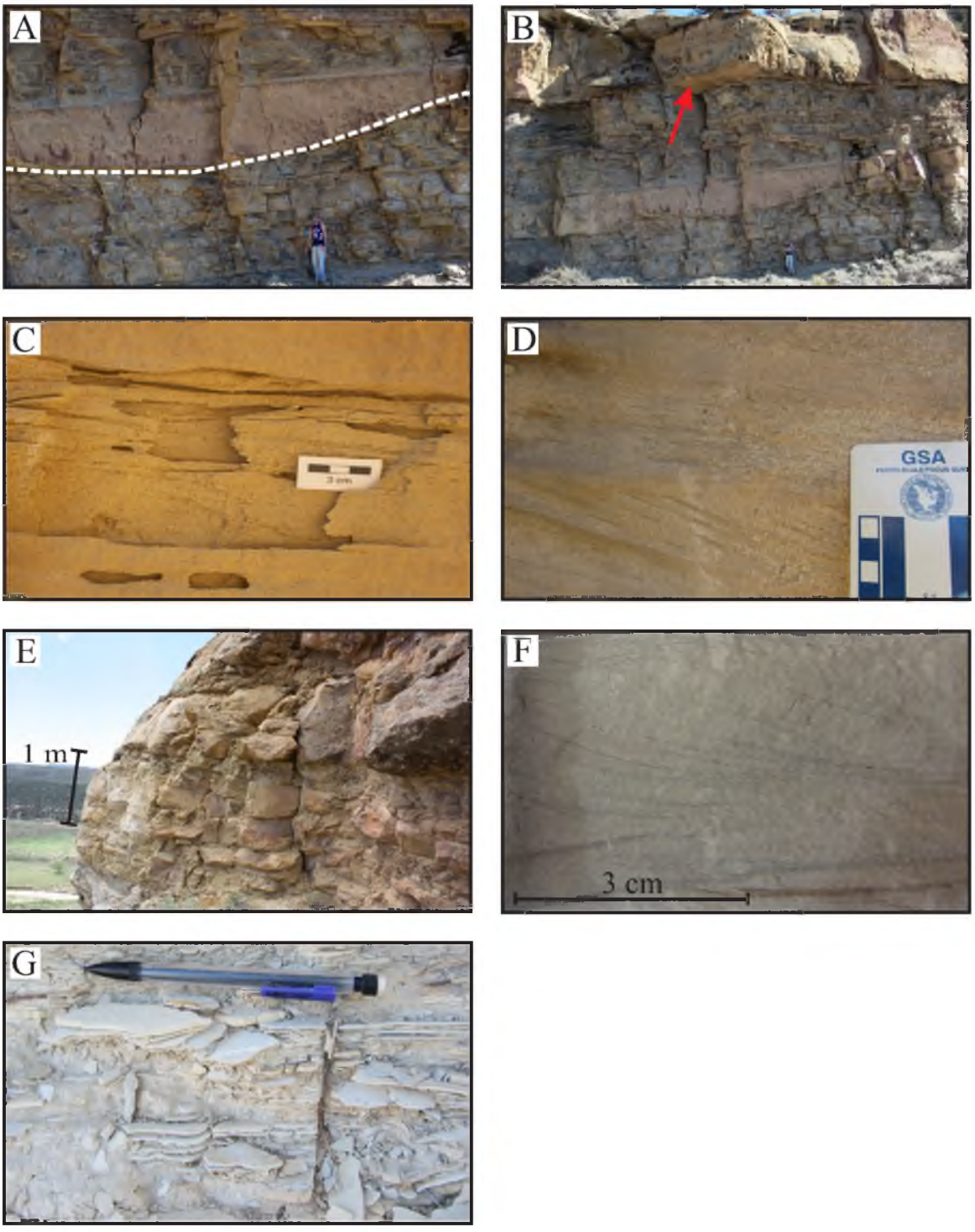
A
B
C
D
GSA
E
1 m
F
3 cm
G

Figure 6 – Facies association 2; carbonate deposits. A: Facies 2.1 from Gray Huts section; carbonate grainstone, ooids/ peloids and oncolites in base of Gray Huts section; interpreted as littoral, high-energy carbonate ramp. B: Facies 2.2 from Temple section; stromatolites; interpreted as littoral, high-energy carbonate ramp. C: Facies 2.2 and 2.3 from Gray Huts section; stromatolite heads overlaying organic poor carbonate mudstone; interpreted as sublittoral, low-energy carbonate ramp. D: Facies 2.4 from Gray Huts section; organic-rich carbonate mudstone with articulated fish scales (circled), plant debris common (right of hammer); interpreted as profundal, low-energy carbonate ramp. E: Facies 2.4 from Asphalt Wash-1 core; organic-rich carbonate mudstone with abundant fish scales. F: Facies 2.2 from Gray Huts section; thick (~1 m) thrombolite build-up which can be traced along the entire Evacuation Creek outcrop. G: Facies 2.5 from Condo section; finely laminated, organic-rich carbonate mudstone, parallel to wavy laminations; interpreted as profundal, "deep" open water, found in Mahogany Zone. H: Facies 2.5 from Asphalt Wash-1 core; finely laminated, organic-rich carbonate mudstone from the Mahogany zone.

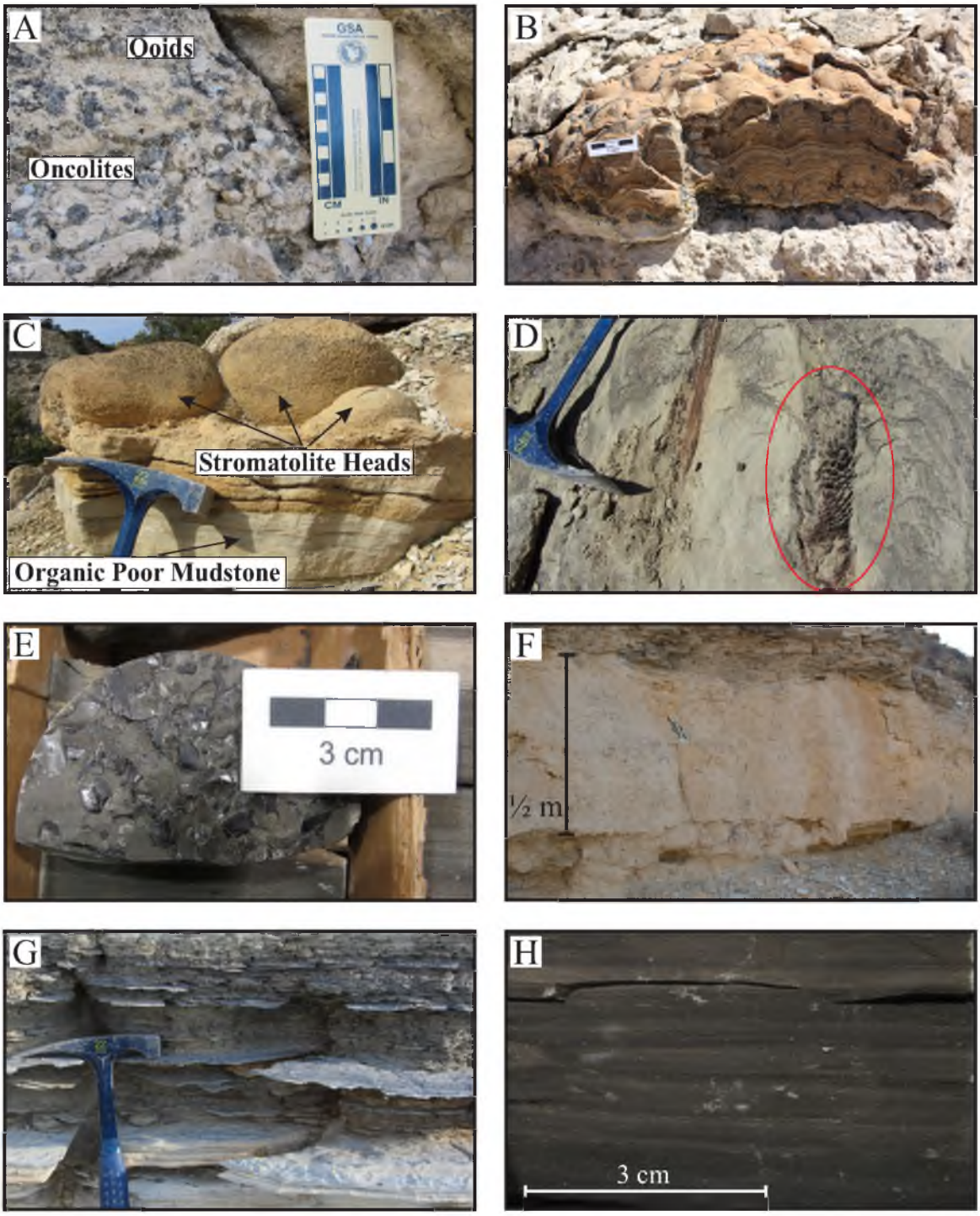
A
Ooids
Oncolites
GSA
CM
IN
B
C
Stromatolite Heads
Organic Poor Mudstone
D
E
3 cm
F
½ m
G
H
3 cm

Figure 7 – Facies association 3 and 4; saline deposits and volcanic-derived deposits; A: Facies 3.1 from Asphalt Wash-1 core; organic-rich carbonate mudstone with abundant disseminated saline mineral crystals; interpreted as profundal, laminated "deep" open hypersaline water. B: Facies 4.1 from Condo section; Curly Tuff. C: Facies 4.1 from Gray Huts section; fine to medium grained volcanic ash deposit.

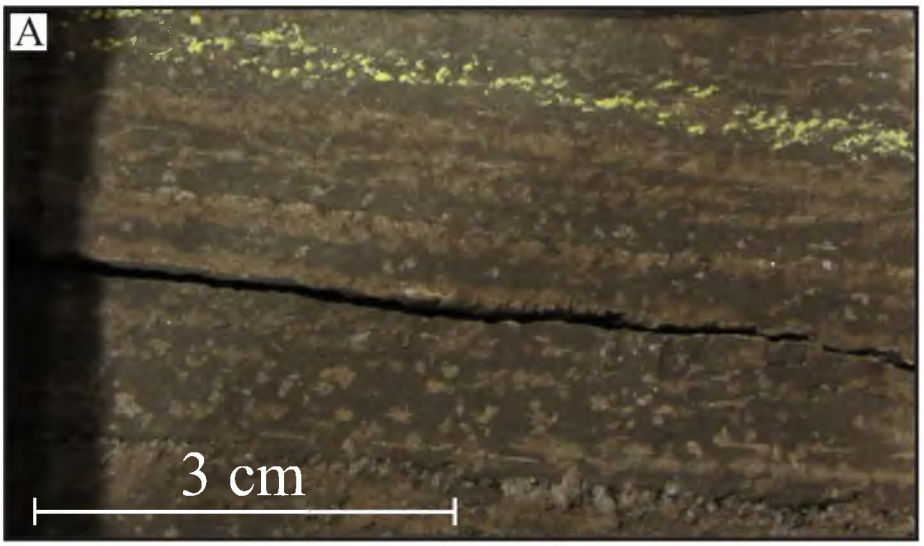
A
3 cm


B


C
GSA
CM
IN
mm

Facies Association 1: Siliciclastic deposits

Facies 1.1 (F1.1)

Facies 1.1 consists of erosionally-based, fine to medium sandstone channels (Table 1; Figure 5). Color ranges from light tan to yellow or orange. Rip-up clasts are common along the base of channel bodies. Parallel to low-angle laminations are common towards the bottom of the channel bodies, whereas current ripples tend to be more common towards the upper half. Individual channel bodies average about 3 to 4 m thick, but range from less than a meter to 7 meters in thickness. Channel bodies are on average 10 to 20 m wide, but range from about 5 to up to many tens of meters wide. These bodies can be single storied, or multistoried. Thickness of individual stories ranges from 1 to ~12 m. Channel bodies are commonly amalgamated in both the vertical and horizontal direction with other sandstones. Some channel bodies contain evidence of lateral migration (Figures 8 and 9). Dewatering structures and soft sediment deformation are also common, indicating rapid sedimentation rates. Paleocurrent data (n=25) indicate a prominent average flow direction to the northwest, with less prominent flow direction to the northeast (Appendix).

Facies 1.2 (F1.2)

Facies 1.2 is composed of massive, fine sandstone (Table 1; Figure 5). Sandstone bodies are commonly tabular and sharp-based. Facies 1.2 consistently overlies facies 1.1 and commonly transitions into facies 1.1 laterally at sharp boundaries (Figures 9 and 10). Colors range from light tan to yellow or orange. Bed thickness is commonly meter scale, and multiple beds are often stacked, forming tabular packages. These packages range in

Figure 8 – Example of a terminal distributary channel (F1.1) from the Gray Huts section in the L2 zone.

Figure 9 – Example of a terminal distributary channel (F1.1) and fluvial mouthbar (F1.2) from the Condo section in the upper R6 zone.

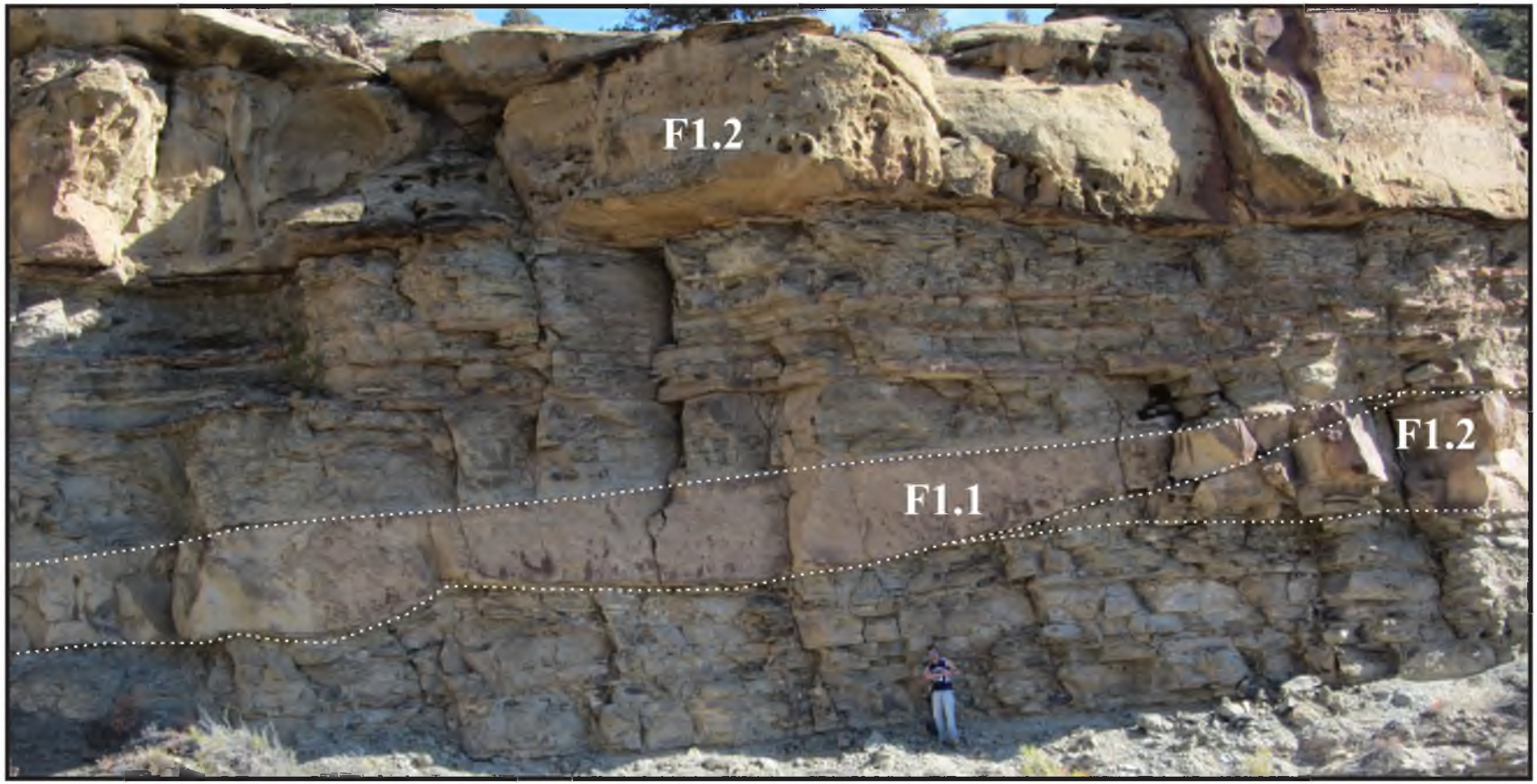

Figure 10 – Example of a terminal distributary channel (F1.1) and fluvial mouthbar (F1.2) from the Gray Huts section in the Douglas Creek Member.

thicknesses from 1 to 7 m. Where sedimentary structures are visible, parallel to low-angle laminations are found locally (Figure 5). Soft sediment deformation is also extensive in some beds.

Facies 1.3 (F1.3)

Facies 1.3 consists of finely laminated, organic-poor claystone to siltstone (Table 1; Figure 5). The base of this facies is commonly gradational rather than sharp and overlies many other facies, including organic-rich carbonate mudstone (F2.5), microbialites (F2.2), and sandstones (F1.1 and F1.2). Color is usually light tan to light gray. Plane parallel laminations are common. Ripples are present in the siltstone, but are uncommon relative to plane parallel laminations. Few *Lithophypoderm sp.* fossils (commonly called "botfly" larvae) are present. Some dewatering structures and soft sediment deformation are also present. This facies also commonly contains thin (<5 mm), very fine sandstone interlaminations, which contain some ripples that range from NNE to SW paleoflow directions.

Facies Association 1 Interpretation

The three siliciclastic facies observed in this study have been interpreted to comprise different components of a fluvial-dominated deltaic complex that expresses some wave influence. These components are all closely associated with one another and show evidence of a fluvial influence with wave modification.

The sandstone facies (F1.1 and F1.2) occur in laterally extensive units that can be followed across the entirety of the Evacuation Creek outcrop (Figure 4). Within these

siliciclastic units, there is a complex relationship between facies 1.1, 1.2, and 1.3 in both the lateral and vertical direction (Figure 11). Facies 1.2 and 1.3 are interpreted as fluvial mouthbar complexes that were deposited slightly downdip of their updip counterparts, terminal distributary channels (F1.1).

Fluvial mouthbars are sediment bodies that form where a river (terminal distributary channel) meets a large standing water body, such as a lake (Schomacker et al., 2010). The sediment transport velocity of the river drops dramatically upon entering the body of water, causing deposition of coarser sand proximal to the shoreline of the lake and finer sediments in more distal settings (Olariu and Bhattacharya, 2006; Moore et al., 2012). The distal siliciclastic input was probably deposited as hyperpycnal flows due density differences between the incoming sediment-laden freshwater and lakewater. Thin stratified beds are observed in the profundal siliciclastic deposits in the Asphalt Wash-1 core. Sorting within the mouthbar deposits is very good, due to reworking by lacustrine and fluvial processes after initial deposition (Moore et al., 2012). The term "mouthbar" is used instead of "delta" because of the low gradient in which the fluvial system entered the shallow lake. Due to the interpreted low gradient, full delta systems were not able to form, but instead a series of mouthbar complexes were deposited. These complex siliciclastic packages were predominantly sourced from the south of Lake Uinta (Cashion, 1967; Picard and High, 1972; Ryder et al., 1976; Dickinson et al., 1988; Moore et al., 2012). Paleocurrents indicate a prominent northwestern flow direction in the lower part of the sandstone packages, with an increasing northeastern to southwestern flow direction higher up in the sandstone packages (Appendix). This transition in paleoflow direction is an indication of both primarily fluvial and secondarily wave processes

Figure 11 – Simplified image of terminal distributary channel and fluvial mouthbar system. Modified from Schomacker et al. (2010), Bhattachurya and Giosan (2003), and Olariu and Bhattachurya (2006).

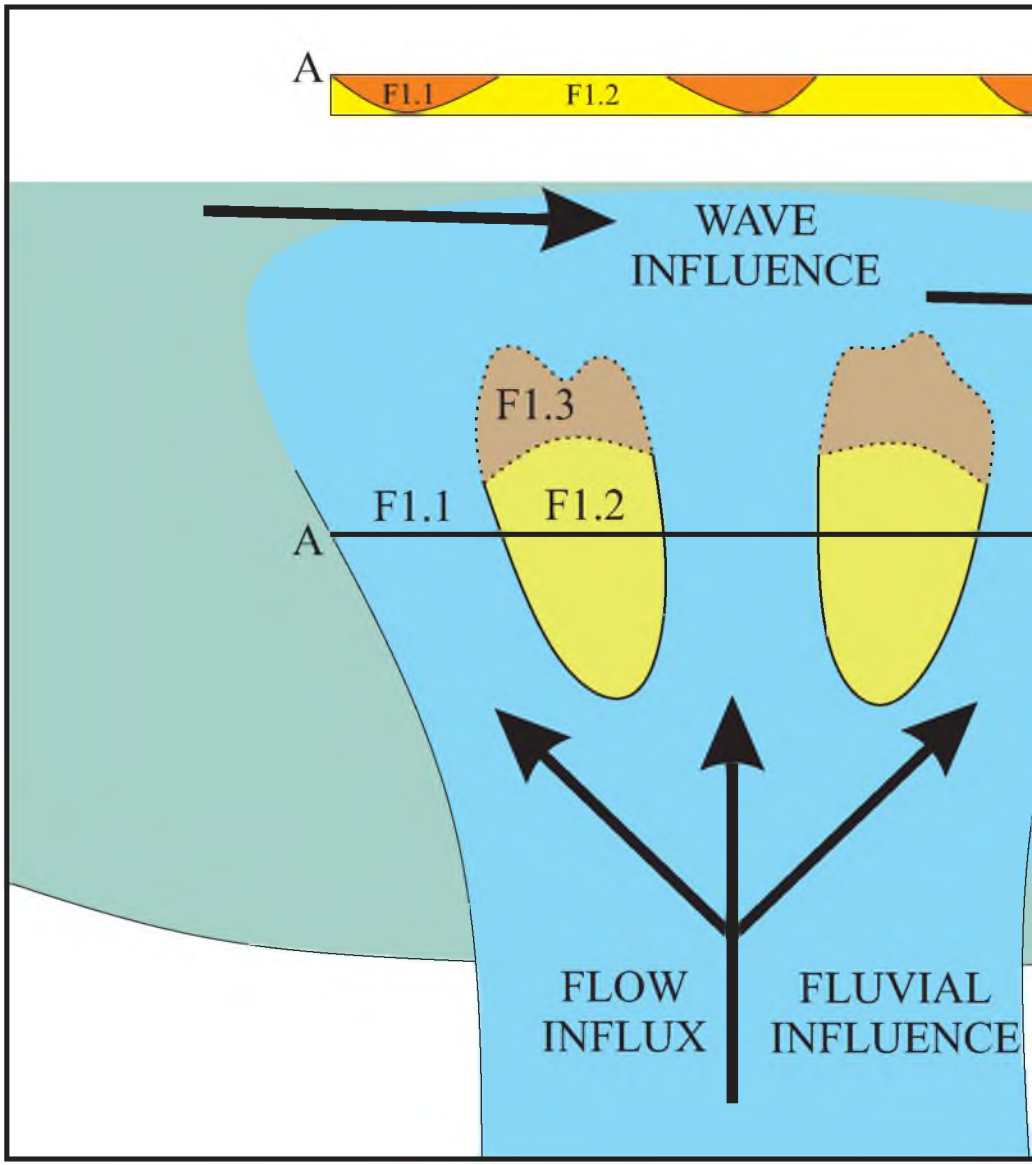
A
F1.1
F1.2
WAVE
INFLUENCE
F1.3
F1.1
F1.2
A
FLOW
INFLUX
FLUVIAL
INFLUENCE


A'
A'

affecting sand deposition as progradation into the basin occurs. The distal siliciclastic deposits have a greater influence from longshore wave action (as fluvial discharge energy decreases), generating flow indicators perpendicular to the fluvial onset direction (Bhattacharya and Giosan, 2003).

Numerous fluvial channel splits, due to the formation of fluvial mouthbars, generate terminal distributary channels (Figure 8) (Olariu and Bhattacharya, 2006). These channels are the most distal features of a distributive system, so it is nearly impossible to count the number of channel splits (Olariu and Bhattacharya, 2006). These lenticular sandstone channels are almost always observed incising into underlying tabular mouthbars (Figures 8-10). Figure 11 illustrates a simplified model of the association of siliciclastic deposits that are interpreted to comprise these deltaic complexes. Initially, the main river channel is bifurcated by a single mouthbar as it enters the lake system. The formation of the mouthbar diverts the main channel into two smaller channels, which are the terminal distributary channels. The terminal distributary channels represent the final splits of the main channel.

Facies 1.2 and 1.3 are distinguished by their difference in grain size. The proximity of the fluvial mouthbar to the lake margin can be interpreted by looking at the lower bounding surface, as well as the internal structure and grain size. Proximal mouthbar sandstone bodies are typically sharp and erosionally based. In distal fluvial mouthbars, the lower bounding surface is more depositional than erosional, so it appears slightly undulating and nearly horizontal (Schomacker et al., 2010). Distal mouthbars also show evidence of wave modification. This wave modification is observed in the upper portions of the sandstone packages, as they prograded into the basin. In the distal

claystone and siltstone packages, there is no direct evidence of wave modification because these were deposited below wave base. There are however, numerous very fine sandstone interlaminations within these claystones and siltstones that do show wave modification. Similar to the interpretations by Moore et al. (2012) in Nine Mile Canyon, these facies are interpreted as fluvial mouthbars based on the lack of subaerial exposure indicators (especially in the lower portion of the Parachute Creek Member), lack of basal erosional surfaces, and abundant soft-sediment deformation.

Where the main distributary channel becomes terminal, there is a high degree of division within the channel that occurs, generating an intimate relationship between the channel and mouthbar deposits, as seen across Evacuation Creek. Numerous channel bodies alternating with mouthbar deposits represent many thin, migrating channels entering the lake system from the south. The orientation of these channels varies more in terminal distributary channels than in proximal distributary channels due to their extremely low gradients farther from the shoreline (Moore et al., 2012).

Across the Evacuation Creek outcrop, these facies relationships can be seen within the extensive sandstone bodies (Figures 8, 9, and 10). Laterally, distributary channels (F1.1) and proximal mouthbars (F1.2) often transition back and forth, reflecting an instance where numerous mouthbars are dividing these channels and vice versa (Figure 11). Vertically, mouthbars (F1.2) and channels (F1.1) always alternate, which is an indication of additional mouthbars being generated with channel movement. As progradation occurs in this siliciclastic setting, facies 1.1 will then overlie facies 1.2, creating an alternating vertical pattern between facies 1.1 and 1.2 (Figure 12).

Figure 12 – Lithostratigraphic cross section of rocks exposed along Evacuation Creek outcrop.

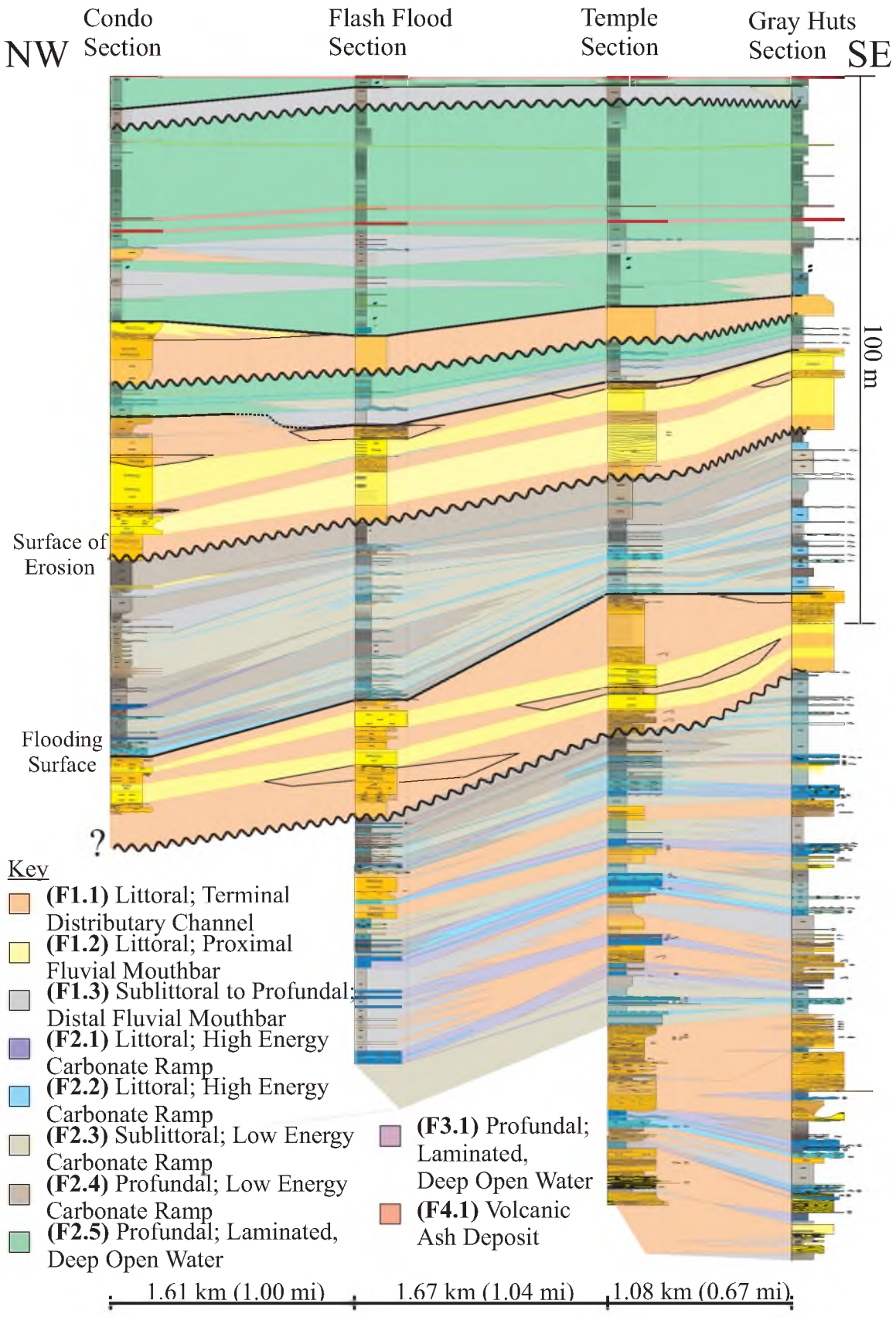
NW
Condo Section
Flash Flood Section
Temple Section
Gray Huts Section
SE
100 m
Surface of Erosion
Flooding Surface
?
Key
(F1.1) Littoral; Terminal Distributary Channel
(F1.2) Littoral; Proximal Fluvial Mouthbar
(F1.3) Sublittoral to Profundal; Distal Fluvial Mouthbar
(F2.1) Littoral; High Energy Carbonate Ramp
(F2.2) Littoral; High Energy Carbonate Ramp
(F2.3) Sublittoral; Low Energy Carbonate Ramp
(F2.4) Profundal; Low Energy Carbonate Ramp
(F2.5) Profundal; Laminated, Deep Open Water
(F3.1) Profundal; Laminated, Deep Open Water
(F4.1) Volcanic Ash Deposit
1.61 km (1.00 mi)
1.67 km (1.04 mi)
1.08 km (0.67 mi)

Taylor and Ritts (2004) surveyed lacustrine sandstone deposits by examining the depositional geometries and heterogeneity within both fluvial-deltaic and wave dominated shorelines. Datasets for their study were from outcrops within Nine Mile Canyon in the south-central part of the Uinta Basin and Raven Ridge, located in the northeastern part of the basin. Generally, the fluvial-deltaic lacustrine shorelines are dominant in the gently-dipping southern margin of the basin, where there is less subsidence and more sediment influx. These shorelines are observed in the Nine Mile Canyon localities. The wave-modified shorelines are dominant at the steeper gradient, northern margin of the basin, where there are higher subsidence rates and lower sediment influx. These are observed at the Raven Ridge localities.

There are similarities from both types of lacustrine shorelines that are observed within the Evacuation Creek sandstone deposits, but overall there are more similarities with the fluvial deltaic shoreline, suggesting a dominance of fluvial deltaic processes with secondary wave influence characteristics. In the deltaic facies described from Nine Mile Canyon, amalgamated undulatory distributary channels have been described to have an intimate relationship with distributary mouthbar deposits similar to what is observed at Evacuation Creek (Taylor and Ritts, 2004). These channels, as described by Taylor and Ritts, typically truncate and amalgamate with distributary mouthbar deposits and can also be truncated themselves by additional distributary channels. The basal bounding surfaces are sharp and erosive when underlain by carbonates or mudstones. They describe the distributary mouthbars as tabular and laterally extensive across the outcrop. Their lower bounding surfaces are sharp, and erosive or nonerosive. These mouthbars, incised by the

amalgamated undulatory distributary channels are very similar to what is observed in the Evacuation Creek lean zones.

In the wave-dominated facies described from Raven Ridge in the northeastern part of the Uinta Basin, shallow-lacustrine sheet sand deposits are described by Taylor and Ritts (2004) as extremely thin, tabular, laterally extensive sandstones with sharp bounding surfaces. Few of these thin sandstone beds are observed interbedded with lacustrine carbonate deposits at Evacuation Creek and interpreted as mouthbar complexes. These interpreted mouthbar complexes show additional wave modification in the form of broad symmetrical ripples, indicating current flow.

Facies Association 2: Carbonate deposits

Facies 2.1 (F2.1)

Facies 2.1 is composed of carbonate grainstone ranging in "grain size" from ooids to oncolites (Table 1; Figure 6). Oncolites are only found in the lower Gray Huts section in the Douglas Creek Member. The carbonate grains are light gray in color. Some units contain broad wave ripples with a west to southwest paleocurrent direction (Figure 13); these are known as ooid shoals. Some ostracodal grainstones are also present. Many beds coarsen upward and are associated with microbialite layers that vary in thickness from millimeters to over one meter (F2.2).

Facies 2.1 is interpreted as being deposited in a high-energy carbonate ramp setting in the littoral zone of the lake, more specifically a shoal. The geometry of the lake margin, as well as the energy level, is indicated by the carbonate facies present. The abundance of ooids to oncolites suggests a high energy wave reworking of the carbonate

Figure 13 – Ooid grainstone (F2.1) with ripples from the Flash Flood section in the R4 zone. The dashed lines highlight the ripple crests, and the wavy line follows the bedding plane topography.

grains during carbonate formation in relatively shallow water of the littoral zone (Renaut and Gierlowski-Kordesch, 2010). Shoal environments are characterized by relatively strong, consistent currents evidenced by lithologies that indicate agitation. The absence of fluvial, siliciclastic input in this facies indicates that all paleocurrent indicators are from wave influence. Algal microbialites are often seen in association with shoal environments (Williamson and Picard, 1974). This association helps to determine the shoreline geometry. Lakes with steep margins generate carbonate bench profiles and sharp facies transitions, whereas lakes with gentler-sloped margins generate carbonate ramp profiles and more gradual facies transitions. Facies 2.1 is interpreted as a high-energy carbonate ramp because of the common, gradational association with microbialites, as well as the presence of ooid shoals, indicating reworked ooids along the shoreline (Renaut and Gierlowski-Kordesch, 2010). These shoals illustrate that the depositional environment was wave-influenced, as well as having a ramp-style geometry suitable for microbialites.

Facies 2.2 (F2.2)

Facies 2.2 consists of microbialites, forms ranging from stromatolites to thrombolites (Table 1; Figure 6). Color is commonly light gray to tan. Bed thickness ranges from mm to over 1 m. This lithofacies commonly contains rip-up clasts of other microbialite fragments near the base of units. Well-preserved stromatolites in the form of low-relief domes or bioherms (commonly referred to as "heads") are found in some beds. These heads are commonly 10-15 cm in diameter. The growth of these heads was promoted by sufficient carbonate sediment supply and the amount of oxygen available based on proximity to the photic zone (Williamson and Picard, 1974).

Facies 2.2 is also interpreted as deposited in a high-energy carbonate ramp setting in the littoral zone. Key features of this facies are carbonate bioherms that can be up to 1 m thick. The larger buildups are commonly interbedded stromatolites and thrombolites. Algal buildups of this nature are present as autochthonous growth structures (Williamson and Picard, 1974). The necessity for a stable substrate for these buildups indicates a low-angle shoreline geometry during deposition (Renaut and Gierlowski-Kordesch, 2010). The thick nature of some of the algal mats suggests a constant carbonate sediment flux, evident by a constant reworking in a high-energy environment. The energy level was thus high enough to provide a carbonate influx, but low enough to promote algal mat construction.

Facies 2.3 (F2.3)

Facies 2.3 consists of finely laminated, organic-poor carbonate mudstone (Table 1; Figure 6). Color ranges from light tan to light gray. Plane parallel laminations are common in this lithofacies. Fossils found in this facies include few "botfly" larvae, fish scales/bones, plant debris, and rare bird feathers. This facies is often associated with thin microbialite layers (F2.2).

Facies 2.3 is interpreted as low energy carbonate ramp deposits found in the sublittoral lake zone. The interpretation of a low energy setting is due to the sublittoral nature of the deposits, where wave influence is more infrequent. Possible reasons for this facies' lack of preserved organic material include: low rates of plankton productivity, dilution by relatively high rates of carbonate production, conditions not conducive to

organic matter preservation, or a combination of these factors (Renaut and Gierlowski-Kordesch, 2010).

Facies 2.4 (F2.4)

Facies 2.4 consists of finely laminated, organic-rich carbonate mudstone, commonly known as "oil shale" (Table 1; Figure 6). Color ranges from light gray in outcrop to black in core. Plane parallel laminations are very common in this lithofacies. Numerous fish scales and bones are found in this lithofacies and it is commonly associated with thin (0.1 to 0.3 m) microbialite layers (F2.2). Organic-richness is moderate to high, with beds ranging from 10 – 30 GPT (Vanden Berg, 2008).

Facies 2.4 is interpreted as low energy carbonate ramp deposits, found in the distal sublittoral to profundal lake zones. Organic-rich carbonate muds can be deposited in a range of lake depth conditions. The low wave energy in this gently sloping environment allows for carbonate mud deposition (Renaut and Gierlowski-Kordesch, 2010). Its association with thin microbialites (facies 2.2) indicates the transition on the ramp between high and low wave energy or littoral to sublittoral (or profundal) environments, respectively. The presence and size of these associated thin microbialites (F2.2) helps to define the lake zone of deposition. Due to the shallow-angle of carbonate ramp environments, a slight vertical change in lake level can result in a significant lateral shift in facies deposition from a littoral microbialite deposit, to a sublittoral or even profundal carbonate mudstone, which is recorded in a short stratigraphic distance (Williamson and Picard, 1974). The fact that thin microbialites can be interbedded is an indication of an episodically shallower environment, but the thin nature of these

microbialites indicates that they likely formed in the deeper realm of the littoral or even shallow sublittoral zone. Increased organic material preservation in this facies is the result of increased biologic activity, with only minor dilution from detrital input.

Facies 2.5 (F2.5)

This facies consists of finely laminated, organic-rich carbonate mudstone (Table 1; Figure 6). Color ranges from light gray to black, but is typically dark gray and similar to facies 2.4. It is also commonly termed "oil shale." Plane parallel to wavy laminations are very common in this lithofacies. Fossil abundance varies by zone, but fossilized "botfly" larvae (found in specific stratigraphic intervals within the upper R6 and lower R8), insects, and plants are common, whereas fish fossils are very rare, as compared to facies 2.4. Also in contrast to facies 2.4, microbialites (F2.2) are not typically associated with this facies. Soft sediment deformation is common, and some particularly organic-rich intervals are brecciated, containing oil shale rip-up intraclasts. Facies 2.5 is generally more organic-rich than facies 2.4, with individual beds reaching up to 70 GPT in the Mahogany zone (Vanden Berg, 2008). Facies 2.4 and 2.5 are similar, but exhibit a clear geochemical difference. X-ray fluorescence data measured on the Asphalt Wash-1 core at approximately 1.5 to 4.6 m (5 to 15 ft.) intervals illustrates that facies 2.5 is more calcium rich than facies 2.4 (Figure 14) (Birgenheier and Vanden Berg, 2011).

Facies 2.5 is interpreted as deep, open water deposits found in the profundal lake zone (Ryder et al., 1976; Ruble and Philp, 1998). These finely laminated carbonate mudstones are indicative of a deep lacustrine environment in which there was minimal siliclastic input, along with high plankton and algal production and preservation rates that

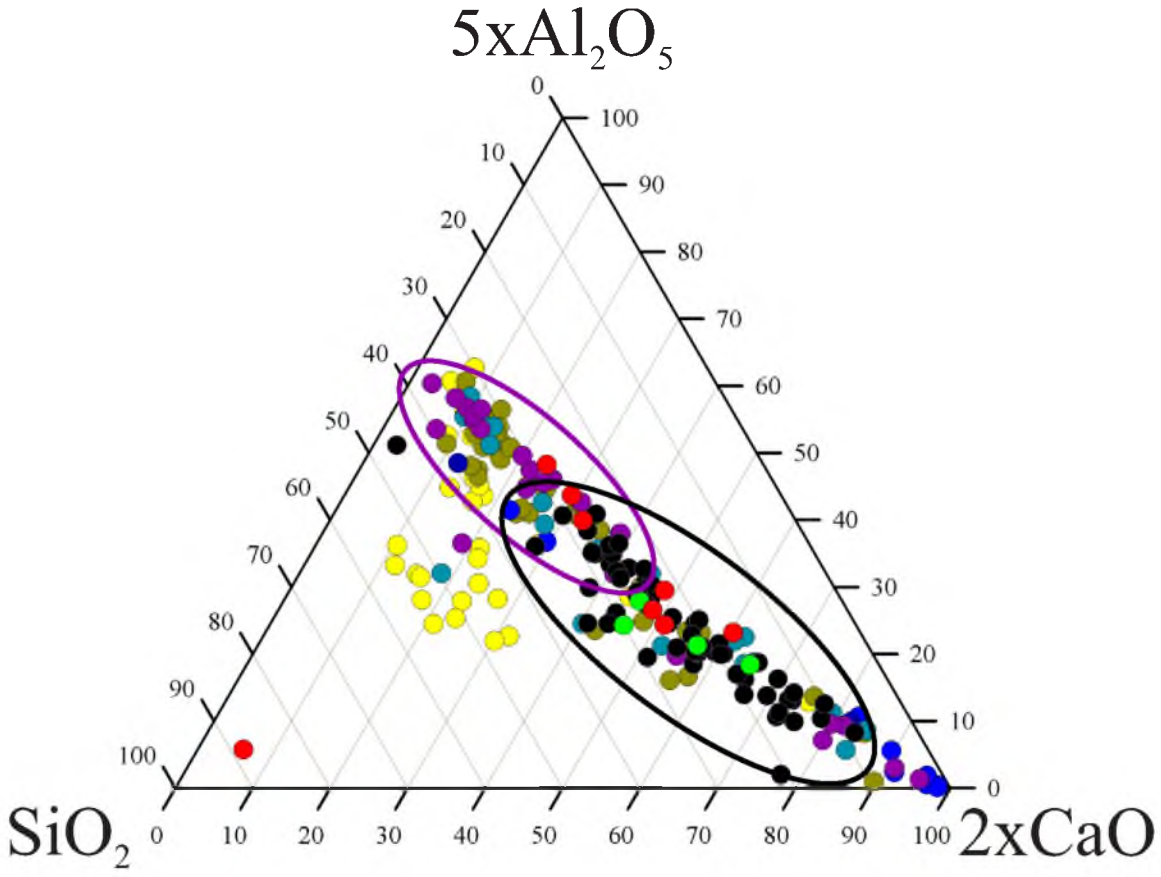

Key
- Facies 1.2; Sandstone
- Facies 1.3; Siltstone
- Facies 2.1; Grainstone
- Facies 2.2; Microbialite
- Facies 2.3; Organic-Poor Mudstone
- Facies 2.4; Profundal, Organic-Rich Mudstone
- Facies 2.5; Profundal, Organic-Rich Mudstone
- Facies 3.1; Saline-Rich Mudstone
- Facies 4.1; Volcanic Deposits

Figure 14 – Ternary diagram that illustrates the geochemical differences between facies. This diagram suggests geochemical difference between F2.4 and F2.5 where F2.4 is more carbonate poor, while F2.5 is more carbonate rich.

outpaced carbonate production overall (Renaut and Gierlowski-Kordesch, 2010). The soft sediment deformation and oil-shale breccia beds formed through downslope migration and failure of the organic-rich material. The organic-rich carbonate sediment was saturated with water during deposition. As compaction occurred, the beds fail, promoting soft sediment deformation and downslope movement. The general absence of fish material relative to facies 2.4 suggests a chemically or biologically stressed environment, perhaps a density stratified saline and/or anoxic water column. The geochemical distinction between F2.4 and F2.5 seen in Figure 14 suggests a transition from proximal to a more distal organic-rich environment within the profundal zone. Higher clay content would be expected in a more proximal location, closer to the source of detrital input, whereas higher carbonate production and less detrital input would be expected in more distal environments.

Facies Association 3: Saline deposits

Facies 3.1 (F3.1)

Facies 3.1 is composed of finely laminated organic-rich carbonate mudstone, similar to facies 2.5, but with abundant saline minerals (Table 1; Figure 7). The most common saline minerals found in the Green River Formation include shortite and nahcolite (Fahey, 1962). These saline minerals occur in a variety of forms including small to large nodules, thin beds, or small disseminated crystals along bedding planes. The nodules average a few centimeters in diameter, but can be more than a decimeter. The saline minerals themselves are white to clear to grey. The background sediment in this facies is medium to dark gray in color and consists of moderately organic-rich

carbonate mudstone that is faintly laminated or massive. Facies 3.1 is eroded at Evacuation Creek, but exposed in outcrops nearby to the north and is captured at the top of the Asphalt Wash-1 core.

Facies 3.1 is interpreted as deep, open water deposits found in the profundal lake zone, with minimal siliciclastic disturbance. Overall, high lake salinity resulted in saline mineral precipitation at or near the sediment-water interface of the deep lake (Johnson, 1985; Ruble and Philp, 1998; Vanden Berg et al., 2012). Precipitation of saline minerals in solution resulted as the lake water became supersaturated due to a low freshwater input and relatively high evaporation rates. Stratification ensued and dense brines accumulated at the bottom of the lake (Fahey, 1962). Relatively high lake levels precluded evaporite mineral deposition in this environment.

Facies Association 4: Volcanic-derived Deposits

Facies 4.1 (F4.1)

Facies 4.1 is composed of fine to medium grained volcanic ash deposits (reworked and ash-falls) (Table 1; Figure 7) (Smith et al., 2010). Colors range from light tan to light yellow. Most beds are less than 10 cm thick, but few are close to half a meter thick. This lithofacies contains abundant igneous crystals visible in hand specimen, such as biotite.

The two thickest and most prominent tuff beds present along Evacuation Creek, and the eastern Uinta Basin include the Curly and Wavy tuffs, which are also present regionally. The Curly tuff lies near the base of the Mahogany zone, whereas the Wavy tuff lies in the lower part of the R8 zone. These tuffs were sourced by the Absaroka

Volcanic province to the north, beginning at about 49 million years ago (Ma) (Smith et al., 2008; Smith et al., 2010). Both of these beds are about a half-meter thick and are present in all measured sections (Figure 12). The Curly and Wavy tuffs are probably reworked volcanic material brought into the lake by fluvial processes, as they contain bedding, lamination, and swirled textures. The thinner tuffs are massive and, hence, more likely to be ash fall deposits. The regionally-extensive Mahogany marker is a 15 cm thick tuff that is located 2 to 3 m above the Mahogany bed, the richest bed within the Mahogany zone (Cashion, 1967).

Smith and others (2008; 2010) determined ages, using $^{40}Ar/^{39}Ar$ methods, for 22 ash beds and 3 volcaniclastic sand beds throughout the Greater Green River, Piceance Creek, and Uinta Basins. These ages allowed for a comparative study between all Green River Formation deposits and were used to determine accumulation rates, draining patterns, and evolutionary trends on an inter-basin scale. Constraints on the Curly and Wavy tuffs indicate ages of 49.3 Ma and 48.7 Ma, respectively (Smith et al. 2008; 2010). No reliable age dates on tuffs from the Uinta Basin stratigraphically below the Curly tuff are available, despite numerous attempts at age dating of stratigraphically lower tuffs (Birgenheier and Smith, pers. comm.).

Stratigraphy and Facies Architecture

The lateral extent and geometry of facies architecture and stratigraphic units across the Evacuation Creek outcrop are shown in cross section in Figures 12 and 15. This facies architecture and stratigraphic units were also correlated to the Asphalt Wash-1 core (Figure 16 and 17).

Figure 15 – Cross section of interpreted stratigraphic units present along Evacuation Creek outcrop.

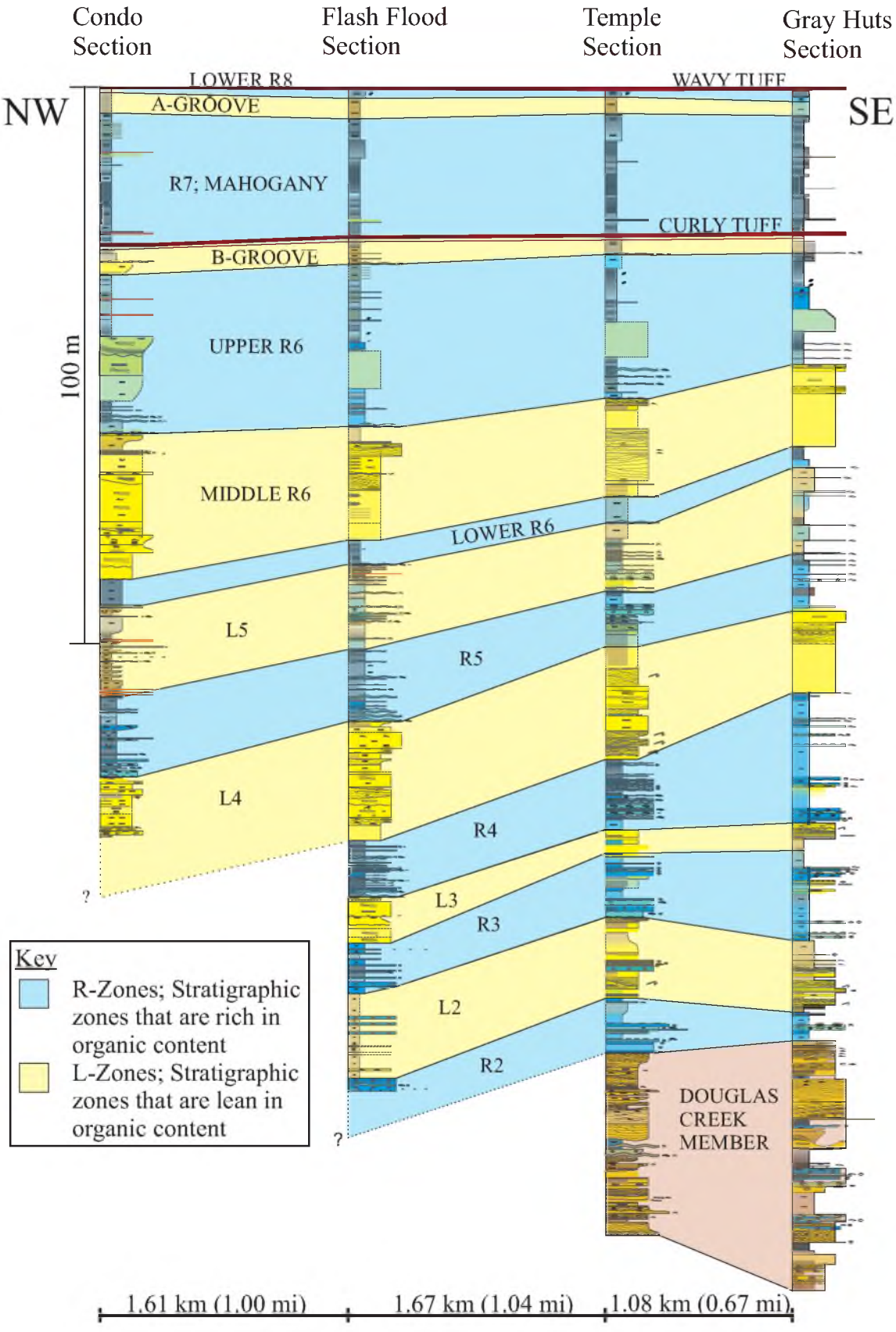
Condo Section
Flash Flood Section
Temple Section
Gray Huts Section
NW
SE
LOWER R8
WAVY TUFF
A-GROOVE
R7; MAHOGANY
CURLY TUFF
B-GROOVE
UPPER R6
100 m
MIDDLE R6
LOWER R6
L5
R5
L4
R4
L3
R3
L2
R2
DOUGLAS CREEK MEMBER
?
?
Key
R-Zones; Stratigraphic zones that are rich in organic content
L-Zones; Stratigraphic zones that are lean in organic content
1.61 km (1.00 mi)
1.67 km (1.04 mi)
1.08 km (0.67 mi)

Figure 16 – Lithostratigraphic cross section of Evacuation Creek outcrop and Asphalt Wash-1 core.

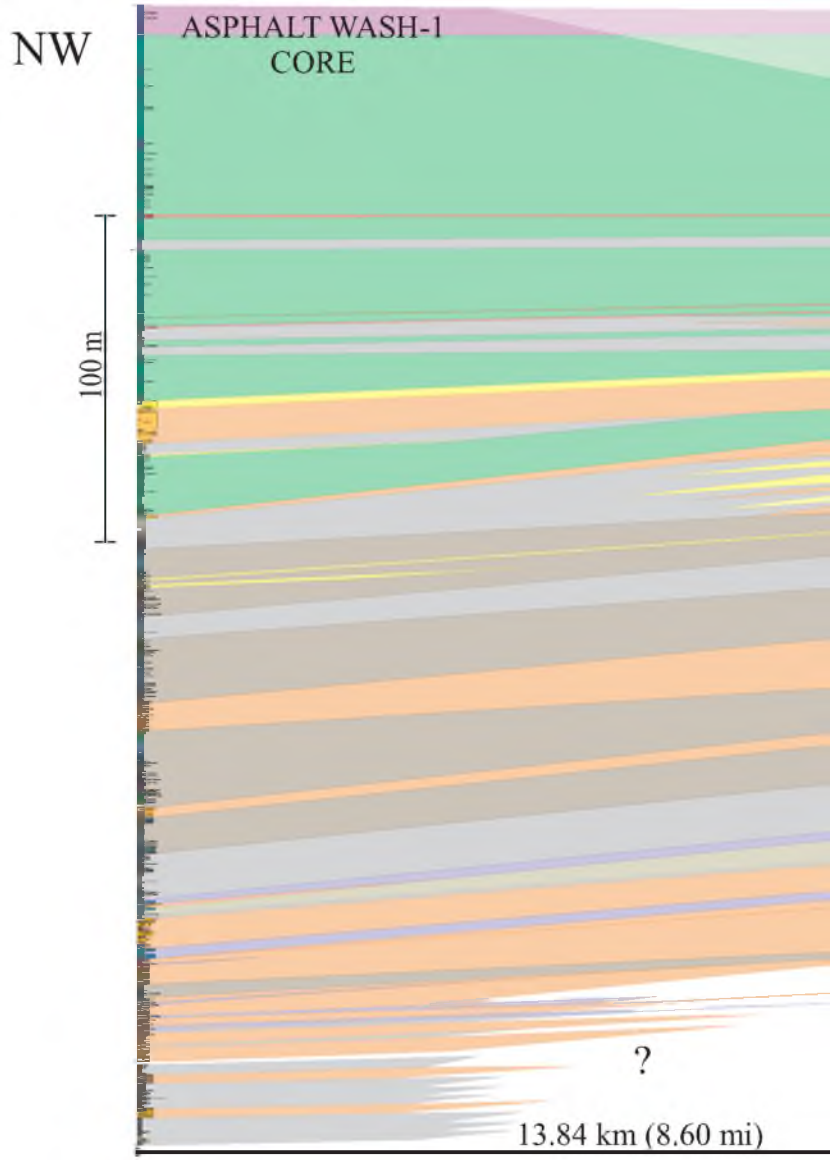
NW
ASPHALT WASH-1
CORE
100 m
?
13.84 km (8.60 mi)

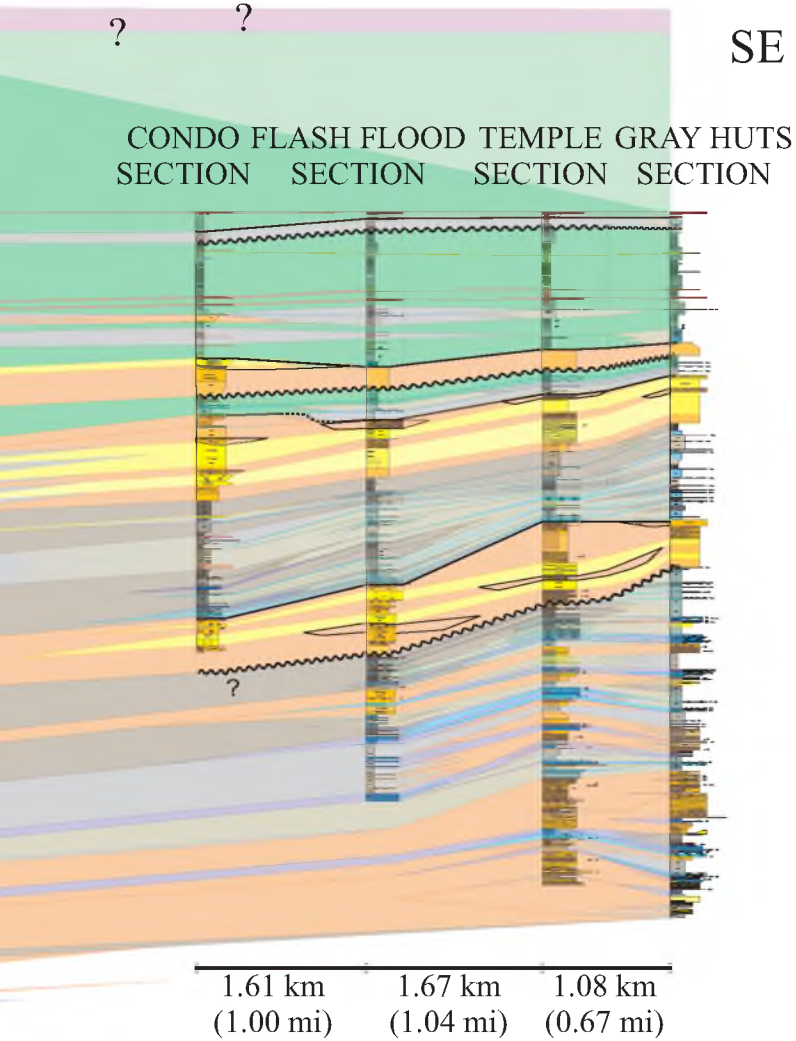
?
?
SE
CONDO FLASH FLOOD TEMPLE GRAY HUTS
SECTION SECTION SECTION SECTION
?
1.61 km
(1.00 mi)
1.67 km
(1.04 mi)
1.08 km
(0.67 mi)

Figure 17 – Cross section of interpreted stratigraphic units present in Evacuation Creek outcrop and Asphalt Wash-1 core.

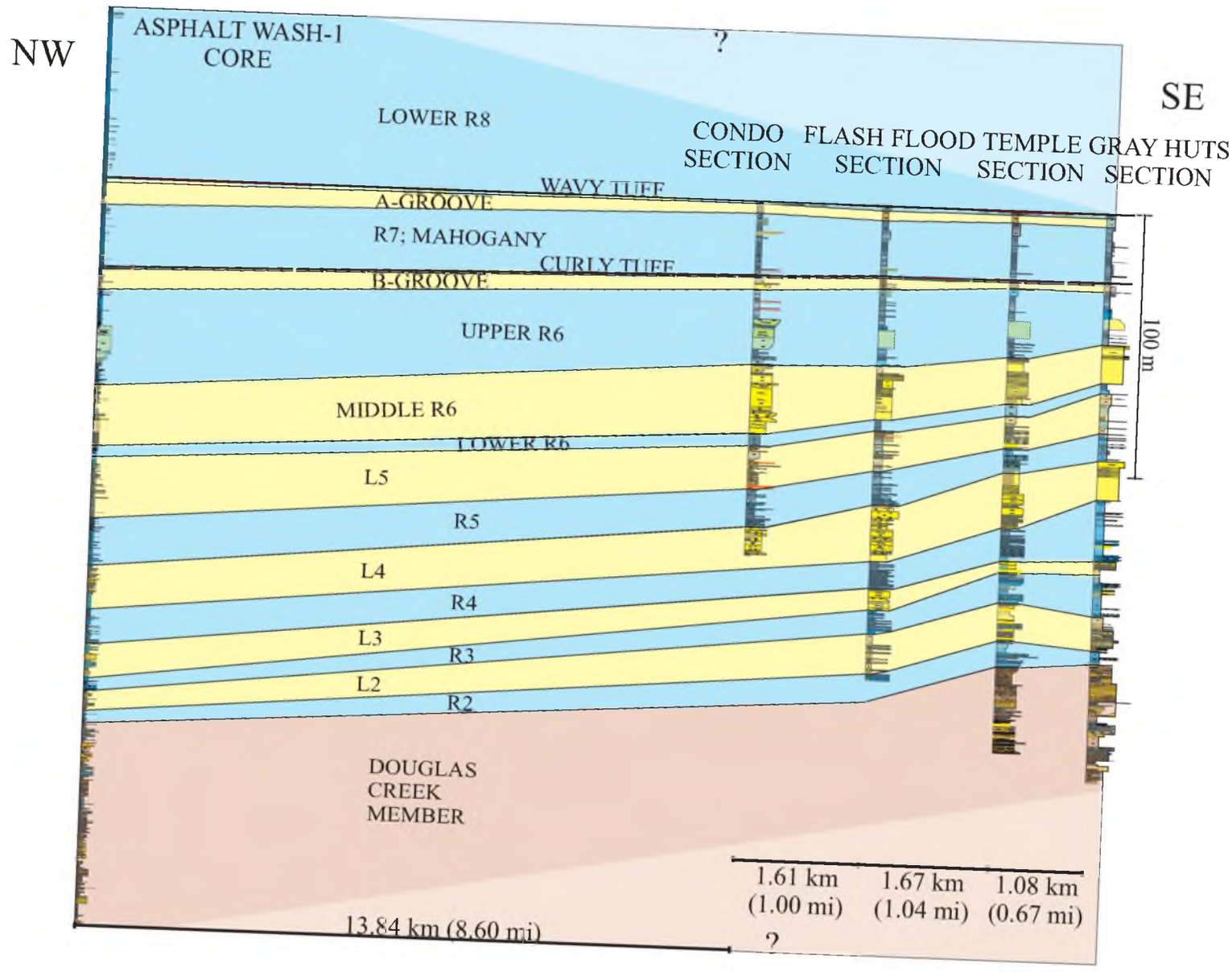
NW
ASPHALT WASH-1
CORE
?
SE
LOWER R8
CONDO
SECTION
FLASH FLOOD
SECTION
TEMPLE GRAY
SECTION
HUTS
SECTION
WAVY TUFF
A-GROOVE
R7; MAHOGANY
CURLY TUFF
B-GROOVE
UPPER R6
MIDDLE R6
LOWER R6
L5
R5
L4
R4
L3
R3
L2
R2
DOUGLAS
CREEK
MEMBER
100 m
1.61 km
(1.00 mi)
1.67 km
(1.04 mi)
1.08 km
(0.67 mi)
13.84 km (8.60 mi)
?

The lowest stratigraphic unit, the Douglas Creek Member, is only exposed at the base of the Temple and Gray Huts sections at the southeast end of the Evacuation Creek outcrop. The thickness of the exposed Douglas Creek Member is 33 m in the Temple section and 45 m in the Gray Huts section (Figure 15). The Asphalt Wash-1 core contains a much thicker record of the Douglas Creek Member, spanning 76 m (250 ft) (Figure 17). Lithologies present in the Douglas Creek Member range from facies association 1, siliciclastic deposits, including sandstone to claystone (F1.1 to F1.3), as well as facies association 2, carbonate deposits, including stromatolities and thrombolites, ooid packstones to grainstones, and carbonate mudstones (F2.1 to F2.5) (Figure 12). High heterogeneity is observed in the Douglas Creek Member throughout all Green River Formation depositional localities (Cashion, 1967). Individual sandstone bodies of facies association 1 are laterally extensive, but individual carbonate units of facies association 2 are not. Fish scales/bones and plant debris fossils are found in select beds within this member. The Douglas Creek Member has the largest range of lithologies within the Evacuation Creek section, reflecting a highly variable environment with periods and regions of fluvial input, but also periods and regions ideal for carbonate generation. The Douglas Creek Member in the Asphalt Wash-1 core contains the same lithologies identified in Evacuation Creek, but grades from siliciclastic-dominated at the base of the core (which is not the base of the Douglas Creek Member), with an increase in carbonate facies towards the top of the unit (Figure 16). The Asphalt Wash-1 core contains a thin, rooted, paleosol bed near its base (0.5 m or 1.6 ft), which is below the exposed rocks at the Evacuation Creek section.

The Parachute Creek Member, which overlies the Douglas Creek, is defined as a succession of alternating organic-rich (R) and lean (L) units with varying lithologies (Figures 15 and 17). Generally, organic-rich zones are identified as facies association 2 (carbonate deposits), whereas lean zones contain mostly facies association 1 (siliciclastic deposits), except the A and B-Grooves, which are mostly carbonate dominated. There are a number of different trends that are found in these units across the Evacuation Creek sections. The upper, siliciclastic, lean zones (L5, middle R6, and B-Groove) tend to thicken from the southeast to the northwest, whereas the upper, organic-rich zones (R5, lower R6, upper R6, R7, and R8) maintain a relatively consistent thickness across the study area. The lower, siliciclastic lean zones (L2, L3, and L4) fluctuate in thickness, which causes the lower, organic-rich zones (R2, R3, and R4) to also fluctuate at the more proximal Evacuation Creek section. These lower, organic rich zones thin to the northwest at the Asphalt Wash-1 core as the volume of littoral to sublittoral carbonate deposits decrease at this more distal location. These changes are due to the proximity of the shoreline and incoming fluvial mouthbars, as well as the available accommodation due to the Douglas Creek Arch structural high to the east. Paleocurrent data indicate a dominant northwest flow direction; this implies that fluvial inputs carried the siliciclastic material towards the northwest from a southern sourced shoreline. As the lake deepened to the northwest, accommodation necessary to preserve the channel and mouthbar deposits increased.

The R2 zone is the lowermost laterally extensive organic-rich zone and is defined by this study as the base of the Parachute Creek Member. R2 is relatively thin and is only exposed in the Flash Flood (partially exposed), Temple, and Gray Huts sections. It is also

present in the Asphalt Wash-1 core. The R2 zone averages about 6.4 m thick; ranging from about 5.0 m thick in the Gray Huts section to about 10.2 m thick in the Temple section to 4.0 m thick in the Asphalt Wash-1 core (Figures 15 and 17). The unit thins basinward (to the NW). Lithologies in the R2 unit are primarily littoral, organic-rich carbonate mudstones, ooid grainstones, and microbialites (F2.1, F2.2, and F2.4) (Figures 12 and 16). There are few, thin sandstone beds (F1.1 and F1.3) present, but they are not laterally extensive between measured sections. F1.1 commonly erodes into F2.1, whereas F1.3 laterally grades into F2.3.

The L2 organic-lean zone is the lowermost lean zone recognized in the Parachute Creek Member. L2 averages about 12.7 m in thickness and ranges from 13.0 m in the Gray Huts section to 15.0 m in Flash Flood to 8.8 m thick in the Asphalt Wash-1 core, the latter of which contains similar facies as found in outcrop. L2 is primarily composed of F1.1, fining up to claystone and siltstone at the top (F1.3), representing the deposition of a mouthbar complex (Figures 12 and 16). There are three thin carbonate, ooid grainstone beds (F2.1) that can be traced across all three sections. These represent pauses in siliciclastic mouthbar deposition or lateral switches in the location of the mouthbar lobe, during which carbonates developed locally.

The R3, which is present in the Flash Flood, Temple, and Gray Huts sections, as well as the Asphalt Wash-1 core, averages about 10.6 m thick and ranges from 9.5 m in Flash Flood to about 12.6 m in Temple, 16.0 m in Gray Huts, and 4.3 m thick in the Asphalt Wash-1 core (Figures 15 and 17). Overall, the R3 unit thins from the most southeast section (Gray Huts) to the most northwest section (Asphalt Wash-1). The thinning along Evacuation Creek and then into the Asphalt Wash-1 core could be due to

the irregular erosional patterns of the overlying lean units, but is most likely due to the down-dip transition to a more distal setting, not suitable for significant littoral carbonate accumulations. Lithologies in R3 are primarily littoral carbonate mudstones, grainstones, and microbialites (F2.1 – F2.4), but there are minor thin sandstone beds (F1.1) towards the top of the unit and minor siltstone to claystone beds (F1.3) (Figures 12 and 16). The carbonate intervals specifically also thin from southeast to northwest, away from the paleoshoreline, but are laterally traceable along all sections. F1.1 and F1.3 are very thin in the R3 unit and only present locally, pinching out laterally within the carbonate facies.

The overlying L3, which is present in the Flash Flood, Temple, and Gray Huts sections, as well as the Asphalt Wash-1 core, has an average thickness of about 7.4 m and ranges from 3.5 m in the Temple section to about 8.0 m in Flash Flood to 13.1 m in the Asphalt Wash-1 core (Figures 15 and 16). L3 is composed almost entirely of sandstone and siltstone (F1.1 and F1.3) in outcrop, except for a thin carbonate mudstone bed (F2.3) in the middle of the unit (Figure 12). The sandstone (F1.1) transitions to a finer grained facies (F1.3) laterally, which then transitions gradually to an organic-lean carbonate mudstone (F2.3). This demonstrates the lateral relationships between siliciclastic and carbonate facies at the local scale. The lithology of L3 in the Asphalt Wash-1 core consists of numerous coarsening-upward claystone to fine sandstone packages, which are interpreted as distal mouthbar packages (Figure 16).

The R4 zone outcrops in the Flash Flood, Temple, and Gray Huts sections, and is also found in the Asphalt Wash-1 core. The average thickness of the R4 unit is about 15.0 m and ranges from 10.5 m in Flash Flood to 23.7 m in Gray Huts to 12.8 m in the Asphalt Wash-1 core (Figures 15 and 17). The thinning at the Flash Flood section could be

attributed to the overlying channels cutting down into the R4 zone at this section. In outcrop, R4 consists of dark, organic-rich carbonate mudstones (F2.4) interbedded with light-colored dolomitic mudstones with abundant microbialites and carbonate grainstones (F2.1 and F2.3) (Figures 12 and 16). Within R4, F2.4 becomes less organic-rich laterally and gradually grades to F2.3. The microbialite layers often pinch out along the outcrop, whereas the F2.1 layers are laterally traceable. Fish scales/bones and shell debris are commonly found in R4, typically in F2.4. The Asphalt Wash-1 core contains layers of shell debris and numerous fish scales, but microbialites are less common than near Evacuation Creek, evidence of a more basinward location.

L4 is present in all four sections at Evacuation Creek as well as Asphalt Wash-1, but it is only partially exposed in the Condo section. The average thickness of L4 is about 18.0 m and ranges from 14.8 m in the Gray Huts section to 21.0 m in the Flash Flood section to 16.5 m in Asphalt Wash-1 (Figures 15 and 17). L4 is almost entirely composed of sandstone (F1.1 and 1.2) near Evacuation Creek, but outcrop quality degrades as it thins from the northwest (NW) to southeast (SE). The only facies present in L4 near Evacuation Creek are F1.1 and F1.2, which alternate vertically (Figure 12). Facies 1.1 forms the base of L4 and is erosional. These facies are laterally extensive and can be traced across the entire Evacuation Creek outcrop. L4 in the Asphalt Wash-1 core is thinner and composed entirely of claystones and siltstones (F1.3) (Figure 16). The transition from outcrop at Evacuation Creek down paleodepositional dip to the Asphalt Wash-1 core represents a down-dip facies change within a mouthbar complex.

R5, which is present in all four sections and the Asphalt Wash-1 core, averages a thickness of about 13.1 m. This unit ranges from 9.8 m in the Temple section to 14.0 m in

the Condo section to about 18.6 m in the Asphalt Wash-1 core (Figures 15 and 17). Near Evacuation Creek, R5 is composed primarily of organic-rich carbonate mudstone (F2.4) alternating with thin grainstone layers (F2.1), microbialites (F2.2), and some claystone to siltstone (F1.3). Similar lithologies are found in the Asphalt Wash-1 core (Figures 12 and 16). F2.1 and F2.2 are often very thin and pinch out laterally between the measured sections. However, a few microbialite beds can be traced through all four sections at Evacuation Creek (Figure 12). Trending northwest to southeast, F2.4 gradually transitions to F2.3, losing organic-richness towards the paleoshoreline. F1.3 also grades laterally into F2.3. R5 is the youngest stratigraphic unit within the Parachute Creek Member in which abundant fish scales and bones are found.

L5 is present in all four sections at Evacuation Creek, as well as the Asphalt Wash-1 core. It averages a thickness of about 16.5 m and ranges from 12.2 m at the Temple section to 17.0 m at the Condo section to 22.6 m at the Asphalt Wash-1 core, illustrating significant thinning from NW to SE from the core to outcrop sections (Figures 15 and 17). The lithology that composes the L5 unit is different from what is seen in the other lean stratigraphic units. Instead of sandstones, the L5 unit is primarily composed of claystone to siltstone (F1.3) to the northwest, with increasing carbonate facies (F2.2-F2.3) to the southeast.

The R6 zone is divided into lower, middle, and upper sections; the lower section and part of the upper section is relatively organic-rich, whereas the middle R6 and part of the upper section is composed of lean siliciclastics (Birgenheier and Vanden Berg, 2011; Vanden Berg, 2008). The lower R6 averages 4.4 m thick and ranges from 3.9 m in the Gray Huts section to 4.9 m in the Temple section to about 4.0 m in the Asphalt Wash-1

core (Figures 15 and 17). The lower R6 is composed of organic-rich carbonate mudstone (F2.4), lacking observable fossils. Other facies present include organic-lean carbonate mudstone (F2.3) thin microbialites (F2.2) (Figures 12 and 16). The middle R6 is mostly composed of sandstone (F1.1 and F1.2) and averages 20.2 m thick, ranging from 14.6 m at Gray Huts to 24.8 m at the Condo section to 23.5 m in the Asphalt Wash-1 core (Figures 15 and 17). The middle R6 is well exposed at the Condo section, but is poorly exposed in sections to the southeast. The middle R6 in the Asphalt Wash-1 core is similar in lithology to the Condo section (Figures 12 and 16).

Composed entirely of fine to medium sandstone in outcrop, the middle R6 transitions from blocky sandstone with numerous ripples and cross laminations in the northwestern-most Condo section to a thinner, poorly exposed sandstone in the Gray Huts section (Figure 12). In the Asphalt Wash-1 core, the middle R6 is composed primarily of siltstone, with some thin fine sandstone and lean mudstone beds, diagnostic of more distal basinward siliciclastic deposits (Figure 16). Near the top of the middle R6 unit is an extensive mudstone bed that contains mudcracks, which extends from the Condo section to the Gray Huts section of Evacuation Creek and represents a surface of subaerial exposure (Figure 18).

The upper R6 averages 27.7 m thick, ranging from 20.2 m in the Gray Huts section to 29.0 m in the Flash Flood section to 35.4 m in the Asphalt Wash-1 core (Figures 15 and 17). The upper R6 is composed of three "stories"; the first and third stories are primarily composed of organic-rich carbonate mudstone (F2.5) and claystone to siltstone (F1.3), with more minor organic-poor carbonate mudstone (F2.3) (Figures 12 and 16). The middle story is composed of fine to medium sandstone. At the Condo

Figure 18 – Photographs of mudcracks present along the Evacuation Creek outcrop. A. and B. Mudcracks at the top of the middle R6 unit of the Condo section. C., D., and E. Mudcracks at the top of the middle R6 unit of the Gray Huts section.

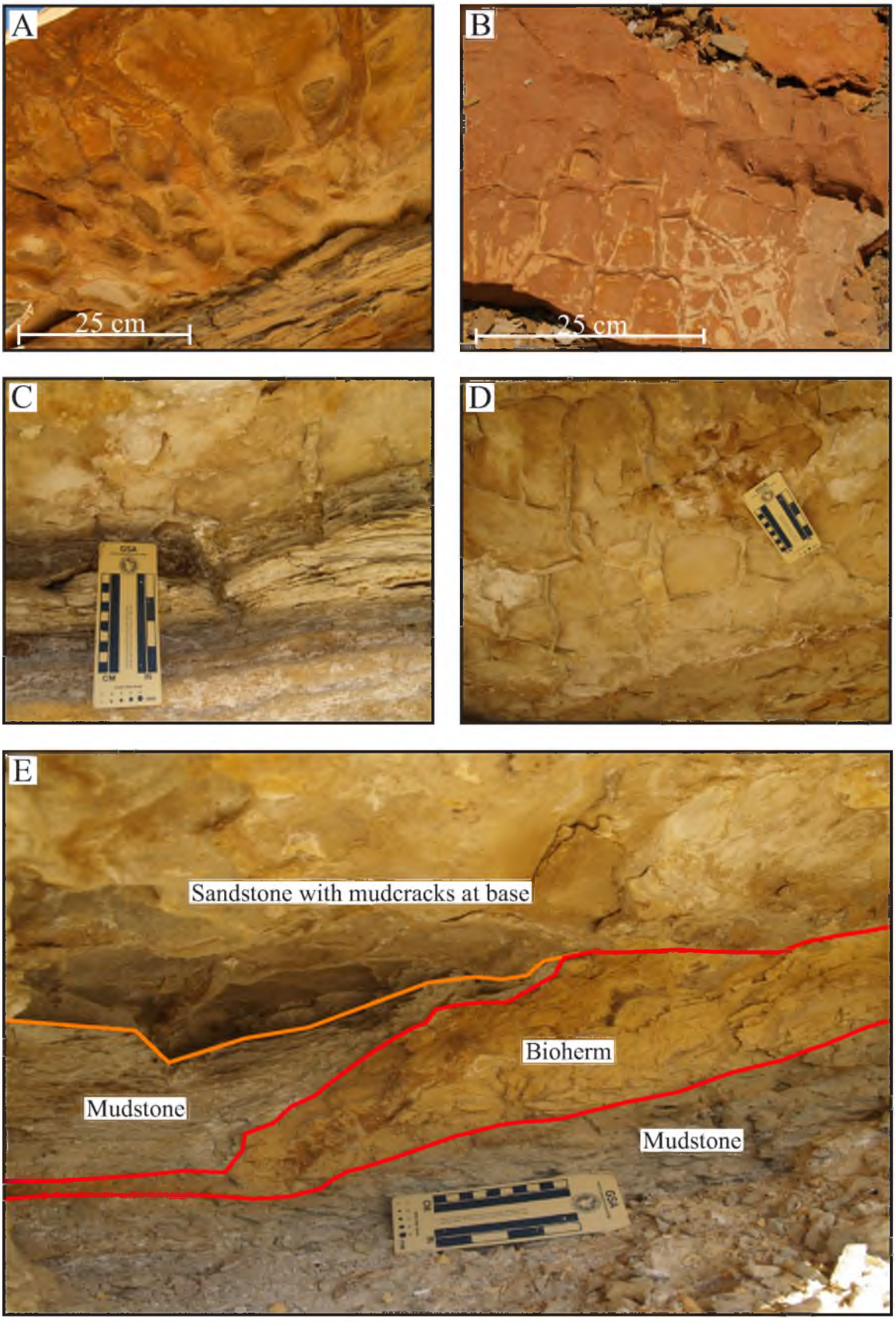
A
25 cm
B
25 cm
C
D
E
Sandstone with mudcracks at base
Bioherm
Mudstone
Mudstone

section, the fine to medium sandstone (F1.2) is erosional at its base and contains low angle cross bedding with ripples near the top. F1.2 is only present at the very top of the sand unit in the Condo section (Figures 12 and 16). F1.1 and F1.2 are laterally extensive across all measured sections, in alternating patterns; this is an example of a fluvial mouthbar, terminal distributary system that is extensive over the entire study area of at least 17.7 km (11 miles) along paleo-depositional dip. The upper R6 is one of two stratigraphic units that contain "botfly" larvae, making them excellent "index" fossils for determining stratigraphy. F2.5 is laterally extensive through all Evacuation Creek sections, whereas siltstone and claystone (F1.3) pinches out and organic-poor carbonate mudstone (F2.3) grades laterally into finely-laminated, organic-rich carbonate mudstone (F2.5), illustrating facies changes between siliciclastics, carbonate, and organic content in the sublittoral to littoral zone (Figures 12 and 16).

Above the upper R6 unit is the B-Groove, which is a thin lean unit. The B-Groove averages 4.5 m thick and ranges from 2.5 m in the Temple section to 4.5 m in the Condo section to 8.5 m in the Asphalt Wash-1 core (Figures 15 and 17). It is composed of claystone to fine sandstone to organic-poor carbonate mudstone. Laterally, there is a gradual facies transition from F1.1 in the northwest, to F1.3 in the middle, to F2.3 at the southeastern part of the outcrop (Figures 12 and 16). This illustrates the potential for unexpected lateral variations in facies relationships in the sublittoral zone. In this case, the lateral transition from siliciclastic to carbonate facies could be from a southerly, rather than southeasterly siliciclastic source.

The next unit is the R7, the rich zone commonly referred to as the Mahogany zone. In regards to resource extraction, this unit has the most economic potential because

it is the most organic-rich oil shale zone in Utah's Green River Formation. The Mahogany zone averages about 23.5 m thick, ranging from 20.9 m in the Gray Huts section to 28.0 m in the Condo section to 23.8 m in the Asphalt Wash-1 core (Figures 15 and 17). The Mahogany zone is composed almost entirely of very dark, organic-rich carbonate mudstone (F2.5) in all sections, including the Asphalt Wash-1 core (Figures 12 and 16). With the exception of a few thin tuff layers (F4.1) and the prominent Curly tuff near its base, F2.5 is the only facies that makes up the Mahogany zone in all locations (Figures 12 and 16). The Mahogany zone represents a prolonged period of extensive profundal sediment deposition.

Directly overlying the Mahogany zone is a thin lean zone, the A-Groove. The A-Groove averages 3.2 m thick, ranging from 3.0 m in the Gray Huts section to 3.6 m in the Flash Flood and Condo sections to 3.0 m in the Asphalt Wash-1 core (Figures 15 and 17). The A-Groove is composed of light tan to grey dolomite in all sections (F2.3) (Figures 12 and 16).

The uppermost unit in the Parachute Creek Member is the thick R8 section, which, for this study, is separated into lower, middle, and upper units. We define the lower R8 section as the top of the A-Groove to the first appearance of abundant saline minerals. The lower R8 section is composed mostly of organic-rich carbonate mudstone (F2.5). The middle R8 section is defined as the interval dominated by saline minerals (F3.1), whereas the overlaying upper R8 unit again lacks saline minerals and is composed of organic-rich carbonate mudstone that interfingers with the sandstones of the Uinta Formation near the top. Only the base of the lower R8 is exposed along Evacuation Creek (Figure 15). Similar to the upper R6, the lower R8 also contains a stratigraphically

distinct interval of "botfly" larvae fossils. The Wavy tuff (F4.1) is located 5 to 7 m above the base of the R8 unit and marks the top of the Evacuation Creek sections. A larger thickness of the R8 is captured in the Asphalt Wash-1 core (Figure 17). In the core, 71.9 (235.9 ft) m of the lower to middle R8 were recovered. The lithology is organic-rich carbonate mudstone (F2.5) with numerous, thin, tuff beds (F4.1) (Figure 16). Carbonate mudstone (F2.5), the most abundant facies within the lower R8, is laterally extensive through all four Evacuation Creek sections (Figure 12). The top 9 m of the middle R8 unit in the Asphalt Wash-1 core contains very abundant small saline crystals (F3.1) and marks the base of the saline zone and the establishment of hypersaline lake conditions (Figure 16).

Spectral Gamma Ray Signature

Handheld spectral gamma ray measurements were taken at 1-meter intervals through the Condo and Gray Huts sections. Spectral gamma ray is more advantageous over standard gamma ray because it measures the quantity of each individual element (Th, K, and U) that contributes towards the natural radiation (Rider, 2008). Further examination of the relative abundances of thorium, potassium, and uranium can benefit towards making interpretations about lithologies and depositional environments.

The elemental sources of natural radiation in rocks come from thorium, potassium, and uranium. Potassium is the most abundant element of the three, but they all have a relatively equal contribution to radioactivity (Rider, 2008). Results from the spectral gamma ray measurements provide thorium and uranium levels in parts per million, whereas potassium results are given in weight percent. The origin of thorium is

primarily from acids and intermediate igneous rocks. Thorium is stable and generally does not dissolve into solution (Rider, 2008)). Instead, it is transported to sites of sedimentation as clay fraction detrital grains and therefore is found in higher concentrations in terrestrial clay minerals. Potassium occurs in the silicate structure of clays and many rock-forming minerals, such as micas and feldspars. The potassium content within clay minerals varies considerably depending on the mineral, but overall it is considered to be a moderately good shale indicator. The primary source of uranium is igneous in origin. Uranium can be passed into sediment by direct chemical precipitation, but more commonly, it is extracted from solution by organic matter and therefore can help to identify source rocks or phosphate deposits (Rider, 2008). Although settings that favor inorganic uranium precipitation are rare, it can be found in reducing environments, such as stagnant, anoxic waters with slow sedimentation rates. Uranium commonly has an irregular distribution in logs because it behaves as an independent constituent, only associated with secondary components (Rider, 2008).

The standard gamma ray measurements (SGR; (3.93*1 ppm Th) + (16.32* 1% K) + (8.09* 1 ppm U)) and computed gamma ray measurements (CGR; which removes the irregular distribution of uranium (3.93*1 ppm Th) + (16.32* 1% K)) in combination with the individual thorium, potassium, and uranium elemental abundances are used here as supporting evidence for mineralogy, lithology, organic-richness, and even depositional environments (Figures 19-21). The heterogeneity in lithology, mineralogy, and organic-richness through the section generates complex results than can be explained by considering the individual elemental responses (Figures 19-21).

Figure 19 – Handheld spectral gamma ray data collected from the Condo section. The stratigraphic units (organic-rich and lean zones) have been highlighted, so that trends in the log response relative to organic-richness and dominant mineralogy are visible. The first track displays the standard gamma ray measurement ((3.93*1 ppm Th) + (16.32* 1% K) + (8.09* 1 ppm U)), as well as the computed gamma ray measurement, which removes the irregular distribution of uranium ((3.93*1 ppm Th) + (16.32* 1% K)) (Rider, 2008). The second and third tracks in these figures display the elemental abundances for thorium, potassium, and uranium. Red arrows indicate stacking patterns in rich and lean zones.

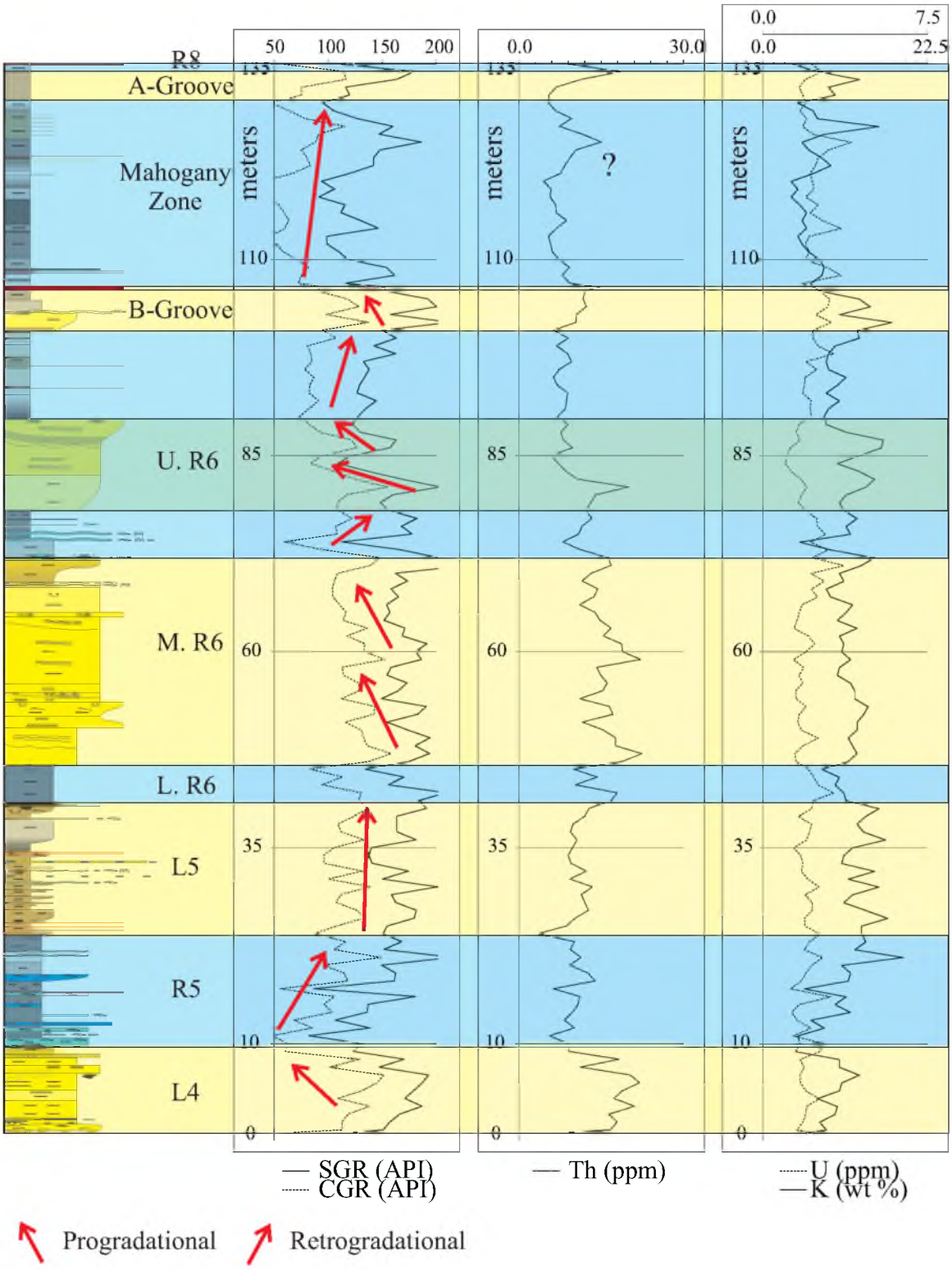
R8
A-Groove
Mahogany Zone
B-Groove
U. R6
M. R6
L. R6
L5
R5
L4
50
100
150
200
0.0
30.0
0.0
7.5
0.0
22.5
meters
meters
meters
?
135
110
85
60
35
10
0
SGR (API)
CGR (API)
Th (ppm)
U (ppm)
K (wt %)
Progradational
Retrogradational

Figure 20 – Handheld spectral gamma ray data collected from the Gray Huts section. The stratigraphic units (organic-rich and lean zones) have been highlighted, so that trends in the log response relative to organic-richness and dominant mineralogy are visible. The first track displays the standard gamma ray measurement ((3.93*1 ppm Th) + (16.32* 1% K) + (8.09* 1 ppm U)), as well as the computed gamma ray measurement, which removes the irregular distribution of uranium ((3.93*1 ppm Th) + (16.32* 1% K)) (Rider, 2008). The second and third tracks in these figures display the elemental abundances for thorium, potassium, and uranium. Red arrows indicate stacking patterns in rich and lean zones.

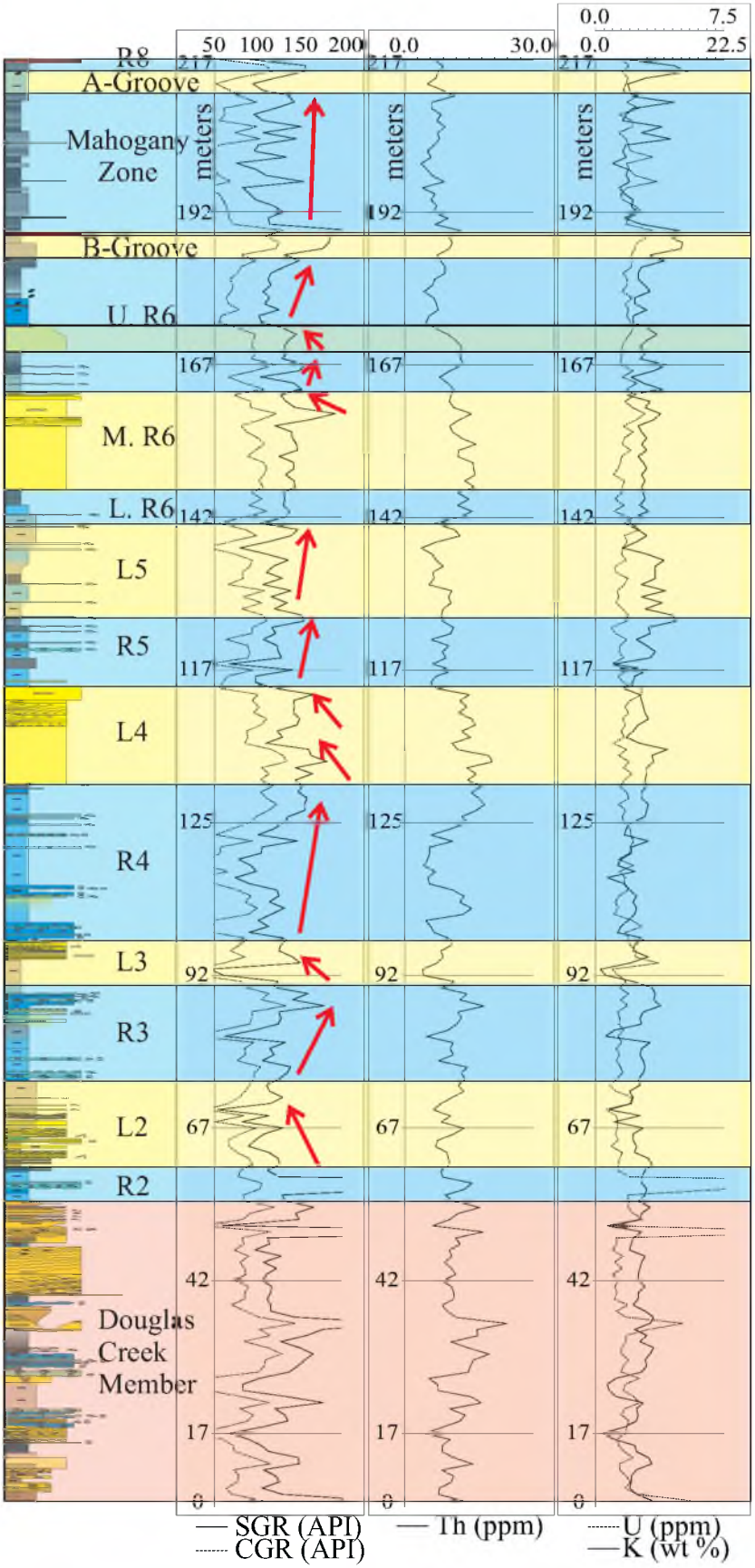
50 100 150 200
0.0 30.0
0.0 7.5
0.0 22.5
R8
A-Groove
Mahogany Zone
B-Groove
U. R6
M. R6
L. R6
L5
R5
L4
R4
L3
R3
L2
R2
Douglas Creek Member
meters
217
192
167
142
117
125
92
67
42
17
0
SGR (API)
CGR (API)
Th (ppm)
U (ppm)
K (wt %)

Figure 21 – Mean handheld gamma ray API values for each facies present along Evacuation Creek outcrop and Asphalt Wash-1 core. Top: Mean API values of standard gamma ray calculations for each facies present in the Condo and/or Gray Huts sections (colored box). Standard deviations are indicated by lines on either side of the mean values. Bottom: Mean API values of computed gamma ray calculations (Th + K) for each facies present in the Condo and/or Gray Huts sections (colored box). Standard deviations are indicated by lines on either side of the mean values. Note lower standard deviation values for CGR than SGR.

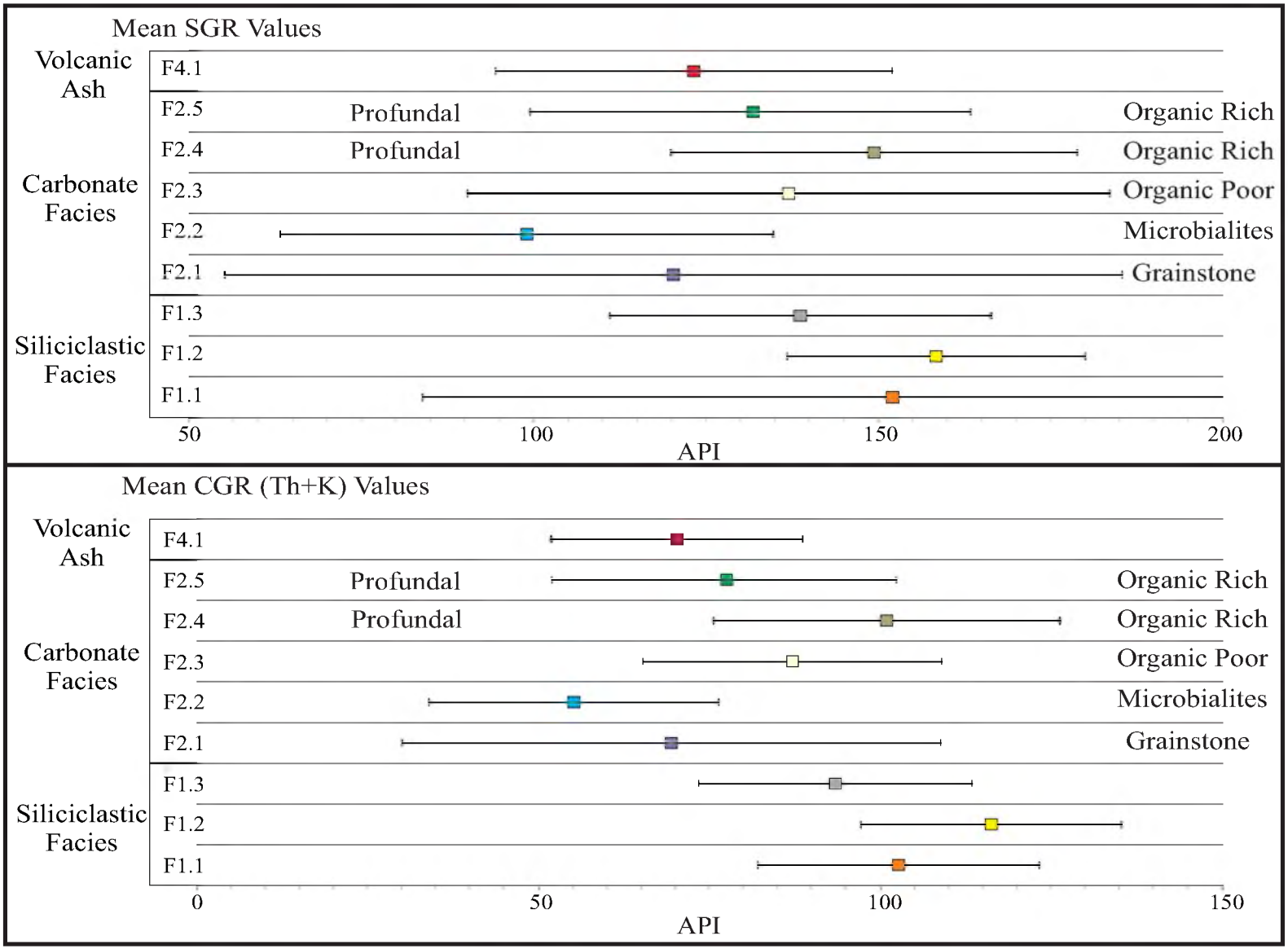
Mean SGR Values
Volcanic Ash
Carbonate Facies
Siliciclastic Facies
F4.1
F2.5
F2.4
F2.3
F2.2
F2.1
F1.3
F1.2
F1.1
Profundal
Profundal
Organic Rich
Organic Rich
Organic Poor
Microbialites
Grainstone
50
100
150
200
API
Mean CGR (Th+K) Values
Volcanic Ash
Carbonate Facies
Siliciclastic Facies
F4.1
F2.5
F2.4
F2.3
F2.2
F2.1
F1.3
F1.2
F1.1
Profundal
Profundal
Organic Rich
Organic Rich
Organic Poor
Microbialites
Grainstone
0
50
100
150
API

First, in both the Condo and Gray Huts sections, the SGR response is higher in the siliciclastic lean zones than in the carbonate, organic-rich zones (Figures 19 and 20). This trend is not in concert with conventional models that sandstone intervals have a lower gamma ray value than organic-rich intervals. However, these somewhat counterintuitive responses are confirmed by analyzing the data in terms of the API values of individual facies (Figure 21). The siliciclastic facies (F1.1-F1.3) display a relatively high API response (Table 2; Figure 21). Additionally, the thorium and potassium levels for each of the siliciclastic facies are above average (Table 2). The high levels of thorium and potassium in F1.1-F1.3 are responsible for the high SGR and CGR responses of the siliciclastic lean zones. Keighley and others (2003) performed a similar study and found the highest total gamma ray values in fluvial sandstone facies, which is in concert with the results of this dataset.

Vice versa, the organic-rich zones record lower SGR and CGR responses. These low values reflect higher carbonate contents of the organic-rich zones (F2.1-F2.5). In pure carbonates, thorium and potassium levels are expected to be negligible due to the lack of siliciclastic dilution (Glover, 2000). In the organic-poor carbonate facies (F2.1-F2.3), thorium and potassium levels are below average (Table 2), which in turn causes an overall lower SGR or CGR response. Facies 2.1 and 2.2 (Figure 21) display the lowest mean API values due to their lack of organic content and most "pure" carbonate content. Facies 2.3 and 2.4 have increasing mean API values as they are more organic-rich relative to Facies 2.1 and 2.2. F2.3 and F2.4 are defined as carbonate mudstones that differ in terms of organic-richness. These carbonates are both composed of more

Table 2 – Handheld Spectral Gamma Ray Data Organized by Facies

Facies	SGR (API)	CGR(API)	Th (ppm)	U (ppm)	K (wt %)
1.1 mean	152.1	102.6	**12.9**	**6.1**	**3.2**
St. Dev	68.2	20.6	3.6	7.9	0.8
1.2 mean	158.4	116.2	**15.2**	5.2	**3.5**
St. Dev	21.6	19.0	3.7	1.1	0.8
1.3 mean	138.7	93.4	**10.9**	5.6	**3.1**
St. Dev	27.7	19.9	2.9	2.0	0.9
2.1 mean	120.3	69.4	10.5	**6.3**	1.7
St. Dev	65.1	39.4	6.0	3.6	1.2
2.2 mean	99.0	55.1	7.7	5.4	1.5
St. Dev	35.8	21.2	2.9	2.1	0.9
2.3 mean	137.0	87.1	9.9	**6.2**	**2.9**
St. Dev	46.6	21.8	3.3	4.7	1.0
2.4 mean	149.4	100.9	**11.7**	6	**3.4**
St. Dev	29.5	25.3	3.7	1.5	1.1
2.5 mean	131.5	77.1	8.4	**6.7**	2.7
St. Dev	31.9	25.2	2.9	1.7	1.0
4.1 mean	123.3	70.2	9.7	**6.6**	1.9
St. Dev	28.8	18.4	3.1	1.6	0.6
Total Means	134.4	85.8	10.8	6.0	2.7

Handheld spectral gamma ray data organized by facies. Mean elemental values were highlighted as relatively high (bold) or relatively low (not bold) compared to overall averages.

dolomites and clays, rather than pure calcium carbonates (Figure 14). These impurities in F2.3 and F2.4 cause a higher API response relative to the other carbonate facies.

The Mahogany zone is almost entirely made up of F2.5, and its onset marks a transition from a dolomite and clay-rich carbonate system (F2.3 and F2.4), to a more calcium carbonate system (F2.5) (Figure 14). This facies transition marks a significant deepening in absolute lake level, where siliciclastic input decreases substantially and profundal, carbonate accumulation dominates (Ryder et al., 1976). This shift between F2.4 and F2.5 results in a decrease in SGR and CGR signature. The elemental differences between F2.4 and F2.5 illustrate a decrease of both Th and K concentrations due to the decrease in clay abundance, but the concentration of uranium increases between these facies (Table 2). This increase in uranium is due to the shift in the environment to an anoxic lake setting, which is one of the few environments ideal for uranium preservation (Rider, 2008). Although there is an increase in uranium, the decrease in thorium and potassium between F2.4 and F2.5 causes the mean SGR to be lower in F2.5 than F2.4. The abundant carbonates in the rich zones are the primary reason for the overall lower SGR responses than the thorium and potassium rich siliciclastic lean zones.

Another trend in the spectral gamma ray data, which is somewhat unexpected, is the lack of high signature in the tuff beds (F4.1). The individual elemental abundances in F4.1 show above average concentrations of uranium, but below average concentrations of thorium and potassium. Potassium values in the tuff beds would be expected to be low, but thorium and uranium values are expected to be high, due to their igneous source. In these sections, the original tuff matrix has been altered by the saline lake water,

decreasing the concentrations of uranium and thorium in the tuffs, resulting in lower SGR and CGR values in this facies (Smith et al., 2003; Smith et al., 2010).

Handheld spectral gamma ray measurements on outcrop can be extremely beneficial towards interpreting subsurface standard gamma ray data taken from the Green River Formation in other parts of the Uinta Basin. Unknown lithologies in the subsurface can be clarified by trends identified in this study. Siliciclastic lean zones generally have a higher API value than the carbonate, rich zones, due to the amounts of thorium, uranium, and potassium in each. These trends can be used to determine siliciclastic lean zones versus carbonate rich zones. More specifically, by separating the spectral gamma ray measurements into facies (Figure 21), further investigations can use subsurface API ranges to make broad interpretations about the facies and environments of deposition.

DISCUSSION

Genetic Stratigraphic Model

The nature of the surfaces that separate the rich and lean zones and the stacking patterns within are important for interpreting the genetic stratigraphy and lake evolution through time for the Parachute Creek Member of the Green River Formation (Table 3). Also important to this discussion is determining relative lake level changes that reflect accommodation as a result of tectonic subsidence, sediment supply, and absolute lake level changes. There are three major types of surfaces that are found in the Evacuation Creek outcrop. The first surface is a regional surface of erosion that is located at the base of the lean, siliciclastic units, at the top of the underlying organic-rich carbonate units. There are three main, laterally-extensive surfaces of erosion, found at the base of the L4, L5, middle R6, and upper R6 sandstone units (Figures 12, 15, and 17). The extent of these erosional surfaces not only encompasses this field area, but they are also observed on the basin and interbasin scale (Keighley et al., 2002; Keighley et al., 2003; Birgenheier and Vanden Berg, 2011; Tänavsuu-Milkeviciene and Sarg, 2012).

Depositionally, these laterally extensive surfaces of erosion mark the base of mouthbar complexes and terminal distributary channels that comprise the lean zones. The architecture and depositional nature of these siliciclastic complexes is similar to those described by (Taylor and Ritts, 2004). The inherent erosional nature of fluvial and mouthbar deposition does not necessitate an interpretation that includes a significant

Table 3 – Summary of Organic-rich and Organic-lean Zones

	Organic-Rich Zones	**Organic-Lean Zones**
Primary Lithology	Carbonate Facies	Siliciclastic Facies
Stacking Pattern	Aggradation or Retrogradation	Progradation
Basal Surface	Flooding Surface	Surface of Erosion
Top Surface	Surface of Erosion	Flooding Surface

Summary of the characteristics of the organic-rich and organic-lean zones observed in the study area. Features summarized include lithology, stacking patterns, and bounding surfaces typically observed.

change in absolute lake level at these regional surfaces of erosion. This is further supported by an overall similarity in littoral to sublittoral lake depth recorded in the bounding carbonate units as compared to the littoral to sublittoral lake depth interpreted from the siliciclastic distributary channel and proximal mouthbar units. Autocyclic deposition of channels and mouthbar facies throughout the succession would produce seemingly random and nonsystematic surfaces of erosion. Instead, the surfaces of erosion recorded here are regional in extent and stratigraphically systematic, suggesting an allocyclic control on siliciclastic deposition, mainly hinterland climate or tectonics. As such, the laterally extensive surfaces of erosion are interpreted to represent reduced accommodation (or a relative lake level fall) as a result of regional increased fluvial sediment supply and subsequent higher deposition rates, partially filling the available accommodation space in the lake basin (Figure 22). These surfaces of erosion are rather consistent with Keighley and others (2003) Type A sequence boundaries (Exxon type 1), indicating a basinward shift in facies across a regionally mappable surface. Fluvial incision of varying degrees are associated with these surfaces and are consistent with studies in the south-central Uinta Basin (Keighley et al., 2003). These contacts are best developed where lacustrine successions are truncated by laterally extensive, amalgamated fluvial channels, and are commonly at the top of well-developed paleosols. The main discrepancy between the regional surfaces of erosion at Evacuation Creek and these Type A sequence boundaries is that at Evacuation Creek, there are no paleosol beds to mark these surfaces, indicating that the underlying strata had more of a lacustrine origin. Additionally, in Keighley and others (2003) sequence stratigraphic model, Type A

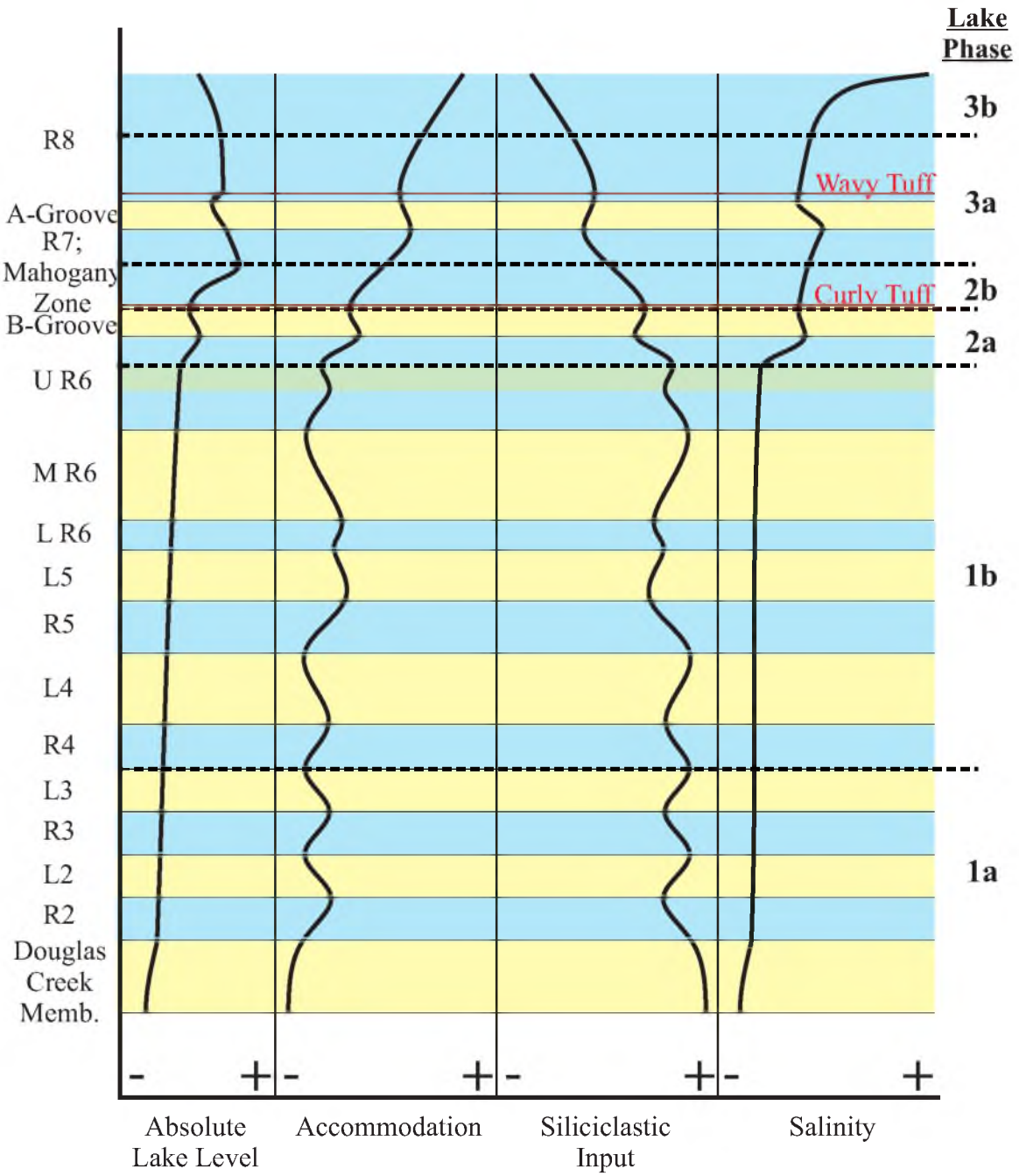

Figure 22 – Estimated stratigraphic changes in absolute lake level, accommodation, siliciclastic input, and salinity for the study area. Stratigraphic units are labeled to the left and lake phases are labeled to the right. The Curly and Wavy tuffs have age constraints of 49.3 Ma and 48.7 Ma, respectively (Source: Smith et al., 2010).

sequence boundaries are more common upsection, correlative to the lower section at Evacuation Creek.

Within the rich and lean depositional units, there are different types of stacking patterns that can be used to determine variations in sediment supply. The siliciclastic associations, or lean zones, are built of 3 to 5 m-scale parasequences that coarsen from very fine or fine to medium sandstone, indicating a vertical distal to proximal stacking trend within each parasequence. Parasequences stack repeatedly and exhibit an overall coarsening trend, indicating a progradational stacking pattern and an increase in sediment supply (or decrease in accommodation) upwards. Spectral gamma ray logs of the Condo and Gray Huts sections similarly display broadly progradational stacking patterns in the lean zones (Figures 19-21). Laterally, these progradational parasequences can be traced throughout the entirety of the Evacuation Creek outcrop, indicating a regional increase in sediment supply (or decrease in accommodation) over the lean zone depositional events. Progradational stacking patterns are also identified in the lake-margin clastic parasequences in Nine Mile Canyon by Keighley and others (2003).

The next major type of genetic surface is a regional surface of subaerial exposure, which is only observed in one stratigraphic horizon. Near the top of one of the progradationally stacked zones (middle R6) in multiple locations along the Evacuation Creek outcrop, there is an extensive mudcrack horizon indicating subaerial exposure (Figure 18). The mudcracks are in a thin mudstone layer near the top of the middle R6 zone, and are underlain and overlain by sandstone units. On top of the underlying sandstone unit, there are bioherms that protrude up through the mudstone layer (Figure 18, E). These bioherms developed on the sandy substrate, and were surrounded during

mud deposition. After bioherm growth, the mudstones were exposed for a period of time, stimulating crack formation.

The last major type of surface is a laterally extensive flooding surface, found at the base of the organic-rich carbonate units or rich zones (Figures 12, 15, and 17). These surfaces represent an increase in accommodation (or rise in relative lake level), following a basinward progradation of parasequences in the underlying mouthbar complexes and terminal distributary channels represented by lean zones. Following high rates of siliciclastic mouthbar deposition, siliciclastic sediment supply waned, and through a combination of low siliciclastic deposition rates and continued subsidence, relative flooding ensued. With low siliciclastic input, the carbonate factory switched on, and the overlying organic-rich carbonate units were deposited. Both organic preservation basinward and carbonate production on the shelf thrive in conditions of low siliciclastic sediment input. The flooding surfaces at the base of rich zones are laterally extensive (Figures 12, 15, and 17).

Keighley and others (2003) have described similar major flooding surfaces in Nine Mile Canyon. They have identified these surfaces at the base of lacustrine-dominated intervals where carbonates abruptly overlie sandstone deposits. These surfaces are consistent with the flooding surfaces at Evacuation Creek that lie at the top of the lean zones and base of the rich zones.

The stacking patterns in the organic-rich carbonate units are composed of retrogradational or aggradational stacked parasequences. These parasequences are on the 3 to 5 m-scale and comprise organic-rich carbonate mudstone (F2.4) that transitions upwards to organic-lean carbonate mudstones (F2.3) to microbialites (F2.2). These

shallowing-upward sequences are commonly capped by a carbonate grainstone (F2.1). Keighley and others (2003) identify ~10 m aggradational stacking patterns in their lacustrine parasequences. The facies transitions of the parasequences in these rich zones are often a result of the shallow-ramp geometry of the basin. Slight fluctuations in lake level resulted in significant facies changes from organic carbonate mudstone to microbialites or grainstones. Retrogradational or aggradational stacking patterns in the organic-rich zones are also exhibited in the spectral gamma ray logs from the Condo and Gray Huts sections (Figures 19 and 21). The absence of siliciclastic material, in addition to these stacked carbonate parasequences, illustrate a decrease in sediment supply (or increase in accommodation), relative to the siliciclastic packages below and above. Aggradational or retrogradational stacking patterns that are preserved reflect a system in which subsidence outpaced carbonate sedimentation rates, allowing for relative lake level rise. Laterally, individual carbonate parasequences are difficult to trace across a continuous distance such as the Evacuation Creek outcrop, suggesting local lateral changes in carbonate facies deposition, but at any given location, similar retrogradational or aggradational patterns are always exhibited, reflecting overall relative lake level rise.

Keighley and others (2003) present a high-resolution sequence stratigraphic interpretation of the strata present in Nine Mile Canyon. Their interpretations use traditional sequence stratigraphic terminology, which is not used in this study; however some of their concepts can be applied. They present lowstand systems tracts as occurring above Type A sequence boundaries and being capped by the first significant transgressive surface. These lowstand systems tract interpretations could be applied to some of the lower, well-defined lean zones such as L3 or L4. Transgressive and highstand systems

tracts are also included in this sequence stratigraphic model. Both of these systems tracts are bounded either at the base (TST) or top (HST) by maximum flooding surfaces, which they define as being present within oil shale of profundal origin. In the Evacuation Creek section, any maximum flooding surface would be interpreted higher in section than what can be loosely correlated to Nine Mile Canyon.

Stratigraphic Changes in Lake Level, Accommodation, and Sediment Supply

The upper Douglas Creek Member, which lies below the R2 unit, is highly variable in terms of lithology, containing large amounts of siliciclastic material (F1.1 and F1.2) and lesser amounts of coarse carbonate material (F2.1 and F2.2). Although there is a high degree of lithologic variability, most of the comprising facies reflect littoral deposition, so absolute lake level during Douglas Creek deposition is interpreted as the lowest during this study interval. There was minimal fluctuation in absolute lake level through the interval and more individual siliciclastic input events in comparison with overlying units (Figure 22). The upper Douglas Creek Member represents a laterally variable environment with multiple siliciclastic deposition events, separated by small-scale carbonate precipitation. The siliciclastic deposits have a high degree of fluvial influence that suggests a more proximal location to the source relative to overlying lean zones. The Douglas Creek Member contains some of the thickest (1+ m) and well-formed stromatolites in the section (F2.2), as well as the largest carbonate grainstones (oncolites) (F2.1). The siliciclastic input fluctuated both laterally and temporally, but overall was at its highest and accommodation at its lowest point in the study interval during the deposition of the Douglas Creek Member (Figure 22).

During deposition of the R2 to middle R6 units, the system records minimal fluctuations in absolute lake level illustrated by the dominance of interpreted littoral to sublittoral facies. There are some profundal facies present in the more distal outcrop locations, but the bulk volume of these units is littoral to sublittoral. These units record fluctuations in accommodation, which is controlled by tectonic subsidence and tectonically and climatically driven siliciclastic sediment supply and delivery (Figures 16 and 22). The available accommodation, however, fluctuated during this interval, increasing during the organic-rich periods and decreasing during organic-lean periods, with aggradation to retrogradation and progradation, respectively (Figure 22). The siliciclastic input also fluctuated, resulting in higher siliciclastic material in the lean zones and lower siliciclastics in the organic-rich zones (Figure 22). In the organic-rich zones, there does seem to be substantial lake level changes based on the presence of organic-rich carbonate mudstone as well as microbialite facies present. These are a result of slight vertical lake level fluctuations in low angle ramp, shallow lake environments that result in significant lateral shoreline translations and hence abrupt facies changes from the profundal to sublittoral or even littoral realm.

A rise in absolute lake level is interpreted above the sandstone in the upper R6 unit, as evidenced by a significant facies change from relatively shallow littoral and sublittoral to relatively deeper sublittoral and profundal facies (Figures 16 and 22). At this stratigraphic boundary, available accommodation began an increasing trend, whereas siliciclastic input began to decrease. The B-Groove indicates a small shallowing event, with a thin interval of more sublittoral facies. The base of the Mahogany zone (R7) represents another rise in absolute lake level marking the transition from sublittoral to

profundal to exclusively profundal facies (Figures 16 and 22). The highest lake level is within the Mahogany zone, near the Mahogany bed. The A-Groove indicates another shallowing event, with a decrease in organic matter production or preservation. Within the R8 unit, at the base of the middle R8, the absolute lake level began to fall again and salinity increased dramatically, creating a hyper-saline lake environment. There were no outlets from the lake system besides evaporation resulting in stratification of the water column. Dense, supersaturated brines accumulated at the bottom of the lake, where saline minerals precipitated.

Figure 22 illustrates two patterns in absolute lake level changes: 1) the longer term absolute lake level stability from the R2 through the upper R6 units, with alternating between rich and lean zones reflecting fluctuations in accommodation and siliciclastic input, and 2) the increase in absolute lake level that occurred midway through the upper R6 and R7 units, providing a shift from relatively shallow to profundal lake facies.

Lake Phases

The studied interval of the Douglas Creek and Parachute Creek Members at the Evacuation Creek outcrop and Asphalt Wash-1 core illustrate the long-term evolution of Lake Uinta in the Uinta Basin from a fluctuating "freshwater" lake with high fluvial input, to a rising, deep lake, and finally to a terminal lake system with hyper-saline conditions. The facies present demonstrate this evolutionary pattern and correspond to facies associations defined by Carroll and Bohacs (1999), as well as fit their model of lake phase evolution from an overfilled to balanced-fill to underfilled lake basin. These

lake phases are defined by the balance between the influx of water and sediment fill and potential accommodation present in the basin.

The Douglas Creek Member to the base of the upper R6 is interpreted as an overfilled lake basin consisting of fluvial-lacustrine facies. In an overfilled basin, the influx rate of water plus sedimentation is greater than potential accommodation (Carroll and Bohacs, 1999). During this overfilled time, the Uinta Basin was being supplied with sediment from the uprising mountains surrounding the basin, but was also spilling over the Douglas Creek Arch into the Piceance Creek Basin. Overall, accommodation was at its lowest in this lower stratigraphic interval (Figure 22). Overfilled basins have high amounts of inflows and outflows, but they are in relative equilibrium. These systems are described as freshwater lakes that are closely related to fluvial systems due to the high amount of siliciclastic, fluvial influx (Carroll and Bohacs, 1999). Since the inflows and outflows are relatively equal, any lake-level fluctuations are minimal and are climatically driven (Carroll and Bohacs, 1999). As evidenced above, in low-gradient carbonate ramp settings, minimal lake-level fluctuations can have a profound impact on the facies deposited.

Carroll and Bohacs (1999) describe "fluvial-lacustrine" facies as prograding parasequences, about 10 m thick that grade from mudstone or siltstone, to shelly coquina, to small sandy deltas. Similar parasequences are observed throughout these lower siliciclastic units, but there is much more variability in parasequence style and stacking patterns than described by the Carroll and Bohacs (1999) model. Progradation is recorded in these lower lean zones, but in the rich zones, aggradational or even retrogradational stacking patterns dominate. Although this entire interval can be termed "fluvial-

lacustrine" and overfilled, there is a significant amount of additional detailed information about lake evolution that is preserved.

The Douglas Creek Member through the L3 zone, termed here lake phase 1a, is highly variable, stratigraphically (laterally), in terms of lithology, and units are thinner relative to the overlying interval from the base of the R4 to the top of the upper R6 sandstone, termed here lake phase 1b, (Figures 12, 15-17). Below the R4 unit in lake phase 1a, there is a strong presence of fluvial facies as well as littoral lacustrine facies, but the architectural relationships between the two are highly heterogeneous and complex. The individual rich and lean zones in this interval are more difficult to define based on this high degree of variability in both the vertical and horizontal directions. High variability suggests fluctuations in siliciclastic input and accommodation were frequent and periods between fluctuations short-lived (Figure 22). In contrast, facies in the interval from the base of the R4 unit to the top of the upper R6 sandstone, which comprise lake phase 1b, are relatively more homogeneous and laterally continuous within each zone (Figures 12, 15-17). Within lake phase 1b, very clear organic-rich and lean zones can be defined by the lithology and stacking patterns. These zones are laterally continuous over the entire study area and stratigraphic boundaries between zones are easily defined. This suggests fluctuations in sediment supply and accommodation were less frequent and periods between fluctuations were longer-lived (Figure 22). Both lake phases 1a and 1b contain fish scales/bones and, as such, suggest fresher-water conditions were dominant. Oil shale preservation in the rich zones required persistent water column stratification conditions, either through means of stagnant water mass circulation,

temperature, oxygen, and/or salinity stratification. These conditions would be further encouraged by low siliciclastic sediment input.

Carroll and Bohacs' (1999) description for "fluctuating profundal" facies associations fits descriptions from Evacuation Creek and the Asphalt Wash-1 core from the top of the upper R6 zone up to the middle of the R8 zone. In a balanced-fill basin, water plus sediment influx is relatively equal to potential accommodation (Carroll and Bohacs, 1999). This balance of inputs and available space causes lake level to rise and therefore corresponds to the "fluctuating profundal" facies. Above the upper R6 unit, siliciclastic input decreases significantly and is absent altogether above the B-Groove. This fall in siliciclastic input is coupled with an increase in available accommodation. Above the upper R6 sandstone, absolute lake level increased, enough so that dominantly organic-rich carbonate mudstone (oil shale) was deposited. These facies are indicative of a deep lake environment. An absolute lake level rise is interpreted at the top of the upper R6 sandstone unit, and is marked by a shift in facies type from littoral/sublittoral to sublittoral/profundal facies (Figures 12, 15-17, and 22) (Ryder et al., 1976). As a balance-filled lake basin, lake level was above the Douglas Creek Arch and the Uinta and Piceance Creek Basins were connected. Preservation of abundant oil shale in this interval suggests long-lived water column stratification causing bottom water anoxia. Local preservation of saline minerals in cores outside of the study area within the Mahogany zone and the upper R6 suggest periodic salinity driven density stratification affected this system during this interval (Birgenheier and Vanden Berg, 2011). This water column stratification may have enhanced organic preservation and encouraged further anoxia.

Notably, the interval between the upper R6 sandstone and the middle of the R8 can be further divided. Below the Mahogany zone (top of the upper R6 sandstone to the top of the B-Groove), termed here lake phase 2a, there is a higher amount of siliciclastic input into these "fluctuating profundal" facies (Figures 12, 15-17, and 22). Within the upper R6 zone and the B-Groove, there are more sandstones and siltstones, whereas from the base of the Mahogany zone to the Mahogany bed, termed here, lake phase 2b, there is no evidence of siliciclastic input. The base of lake phase 2b (the base of the Mahogany zone) is interpreted to represent another increase in absolute lake level and accommodation, whereas siliciclastic input decreased. Lake level was highest during the deposition of the Mahogany zone, and reached its highest mark near the Mahogany bed (Figure 22). From the Mahogany bed to the base of the middle R8, termed here lake phase 3a, absolute lake level remained high and relatively stable outside of the A-Groove, which represents a slight shallowing event. Although this entire interval can be widely termed "fluctuating profundal," further subdivision of this interval based on facies variability helps to define a more precise model of lake evolution.

At the middle R8 unit of the Asphalt Wash-1 core, the organic-rich carbonate mudstones display abundant evaporate minerals at a distinct stratigraphic depth (336.3 ft), suggesting another shift in lake conditions (Figures 16, 17, and 22). The saline zone is not exposed in the area of the measured sections along Evacuation Creek, although it is documented in outcrop further to the north (Vanden Berg et al., 2012).

The final phase in lake evolution, termed here lake phase 3b, is interpreted as an underfilled basin comprising "evaporative facies" (Carroll and Bohacs, 1999). An underfilled basin is defined where potential accommodation is greater than water and

sediment influx and evaporative facies dominate these hypersaline environments (Carroll and Bohacs, 1999). This saline zone represents a time when Lake Uinta's only main outflow mechanism was evaporation and marked the transition to a terminal basin.

An interplay between climatic changes and tectonic activity drive the short and long term changes of lake evolution (Carroll and Bohacs, 1999). Based on the littoral to sublittoral facies preserved below the upper R6, the fluctuations in absolute lake level below the upper R6 are not significant, but there is a constant, steady rise in absolute lake level (Figure 22). However, the stratigraphic section below the upper R6 sandstone does display facies changes and systematic stacking patterns in the alternation between siliciclastic dominated lean zones and carbonate dominated rich zones. The facies changes and stacking patterns are attributed to changes in climate, which affected the amount of fluvial sediment delivery into the lake system from the hinterland. Organic-lean zones record periods in which fluvial siliciclastic transport into the lake system was high. These zones are attributed to episodes of high precipitation that carried a high volume of siliciclastic material into the basin (Birgenheier, L.P. et al., 2009; Plink-Bjorklund and Birgenheier, 2012; Birgenheier et al., 2013). Due to the exceptionally high siliciclastic sedimentation rate, carbonates were unable to form and the available accommodation space on the shallow lake margin was also quickly filled. The intermittent organic-rich carbonate zones resulted from a more stable climate between the periods of high siliciclastic input (Figure 22). The rich zones are characterized by lower siliciclastic sediment supply that encouraged the uninterrupted formation of carbonates. The relative lake level between the rich and lean zones is very similar since both zones

are composed of littoral to sublittoral facies, but climate via the rate of fluvial sediment delivery, is the driving factor that affects the short-term changes in lithology.

The meter-scale cyclic changes (stacked parasequences) in the rich and lean zones are an indication of the rates and types of lithologic deposition taking place. The lean zones are marked by prograding sandstones and siltstone dominated parasequences that are deposited in numerous pulses out into the basin. These sediment pulses are erosive and relatively short-lived. The progradational stacked parasequences imply that the sedimentation rate was greater than accommodation, allowing for shallowing cycles. The rich zones are marked by retrogradational or aggradational stacked carbonate parasequences. The retrogradational or aggradational stacking patterns imply that deposition rates in the rich zones could not keep up with accommodation, or subsidence. Since the accommodation rate is greater than the rate of carbonate precipitation, the cycles in the rich zones either progressively deepened or stayed relatively stable.

Longer-term evolutionary lake changes are more likely to have been driven by tectonic activities associated with basin formation and the interplay between basins (Carroll and Bohacs, 1999). However, the shorter-term changes and minor relative lake level fluctuations within these phases were likely driven by climatic activity.

Recent studies in the Uinta Basin have established a relationship between lean zone deposition and early Eocene abrupt global warming events (hyperthermals) (Plink-Bjorklund et al., 2009; Foreman et al., 2012). These events are well documented in the marine carbon isotope record, and are only recently documented in the terrestrial realm (Abels et al., 2012). Basin scale sedimentation events have previously been linked to Milankovitch-predicted periodicities with high confidence levels, but numerous non-

Milankovitch periods are also observed (Aswasereelert et al., 2013). Foreman and others (2012) document a basin-scale shift to multistoried sheet-sandstones at the onset of the Paleocene/ Eocene thermal maximum event. These sandstone deposits are dominated by upper flow regime sedimentary structures, indicating high-energy discharge events. Hyperthermal (global warming) events are characterized by increased precipitation intensities and seasonality, which cause an increase in weathering and sediment deposition (Plink-Bjorklund et al., 2009; Plink-Bjorklund et al., 2010; Birgenheier and Vanden Berg, 2011; Foreman et al., 2012; Birgenheier, L.P. et al., 2009; Plink-Bjorklund and Birgenheier, 2012). The climatic drivers for these lean zones are thought to be caused by global warming events that exhibit overall arid climates, with highly seasonal, flashy discharge events such as monsoons that quickly deposit high volumes of siliciclastic material at high energy levels (Plink-Bjorklund et al., 2009; Birgenheier and Vanden Berg, 2011; Birgenheier, L.P. et al., 2009; Plink-Bjorklund and Birgenheier, 2012).

Additionally, Tänavsuu-Milkeviciene and Sarg (2012) have developed a detailed evolutionary model of the Green River Formation in the Piceance Creek basin of Colorado. This model is based on detailed facies analysis, but also uses gamma ray and Fischer assay data to generate a basin-scale correlation to help understand the formation and paleoevolution that formed the organic-rich deposits present in the Piceance Creek basin. Within an overall deepening-upward trend in lake evolution, Tänavsuu-Milkeviciene and Sarg defined six lake stages based on facies associations. They determined that basinwide changes in oil shale richness and facies associations, evident by organic-rich and lean zones, were connected to the evolution and history of the lake. This model for lake evolution in the Piceance Creek basin is composed of six stages,

which include: (1) fresh lake, (2) transitional lake, (3) highly fluctuating lake, (4) rising lake, (5) high lake, and (6) closing lake. Generally, these stages are quite similar to the model developed here for the eastern Uinta basin. The section present at Evacuation Creek and Asphalt Wash-1 would span from stage 2 (transitional lake) to stage 6 (closing lake). The small scale phases of lake evolution developed in the Uinta Basin here mirror many of the lake stages presented by Tänavsuu-Milkeviciene and Sarg, with similar facies associations.

Stage 2, transitional lake, is described by an onset of numerous, laterally discontinuous deltaic sandstone deposits that are interbedded by microbial carbonates and littoral to sublittoral oil shales. This transitional lake stage marks where there is an increase in siliciclastic input that is interbedded with shallow lacustrine carbonates, as a slow transgression occurs. This stage is similar to what is observed in lake phase 1a in the Uinta Basin.

Stage 3, highly fluctuating lake, in the western Piceance Creek basin consists of channelized deltaic deposits that alternate with littoral to sublittoral microbial carbonates. In other parts of the Piceance Creek basin, this stage is marked by littoral to sublittoral oil shales and thick profundal oil shale breccias, generating the term "highly fluctuating." In the Uinta basin, this stage is quite similar to lake phase 1b, where clearly developed rich and lean zones are present. Lake phase 1b is most similar to the lithology and facies associations observed in the western Piceance Creek basin of stage 3. Tänavsuu-Milkeviciene and Sarg note that in the western Piceance Creek basin, stages 2 and 3 are very similar. This observation is consistent with the lake phases 1a and 1b defined here.

The next stage is a rising lake, or stage 4. This stage is marked by laterally continuous, organic-rich oil shale deposits, indicating an overall increase in profundal facies. This stage mimics lake phase 2a, defined in the Uinta basin, where there is a substantial rise in absolute lake level within the upper R6 zone.

Lake phases 2b and 3a defined in the Uinta basin correlate with lake stage 5 defined by Tänavsuu-Milkeviciene and Sarg in the Piceance Creek basin as a high lake. In this stage, there are no marginal lake deposits present, only thick laterally continuous organic-rich oil shale. This stage includes the Mahogany zone and can be traced across both the Piceance Creek and Uinta basins, suggesting a high lake level, under stable and open conditions. In this study in the Uinta basin, stage 5 has been split into two lake phases at the Mahogany marker (lake phase 2b and 3a). This signifies where the lake system rises to its deepest level, and then stabilizes.

Stage 6, closing lake, defined in the Piceance Creek basin is characterized by the introduction of more siliciclastic deposits, suggesting additional progradation. These siliciclastic deposits occur among profundal facies, indicating that deep water conditions still remained. In the Uinta basin, at Asphalt Wash-1, lake phase 3a is interpreted to indicate where the lake became terminal. There are no siliciclastic deposits in this lake phase, but instead numerous saline mineral deposits. Tänavsuu-Milkeviciene and Sarg indicate some saline mineral deposition in their stage 6, but ultimately call this stage an overfilled or balance-filled system due to the increased clastic input.

Controls on the depositional trends in the Piceance Creek basin are also considered by Tänavsuu-Milkeviciene and Sarg (2012) to be consistent with global Eocene climate patterns. During times of arid climates, depositional units are highly

cyclic, with sediments that are laterally heterogeneous, whereas during humid climates depositional units are laterally continuous.

One aim of this study was to develop a predictable evolutionary model for the eastern side of the Uinta Basin that could be used to help facilitate prudent and economic development of Utah's oil shale resource. Since this model is based on outcrop and core from the extreme eastern part of the basin, it would be prudent to see if there are similar patterns and changes throughout the section in other parts of the basin. The prime zones for oil shale development are those with the most homogenous rich zones and the highest grade of organic-richness. In our evolutionary model, these would be lake phase 2b and 3a. These phases include the Mahogany zone and represent when lake level was at its highest, and the most economical oil shale was being deposited. We find that the rich zones below the Mahogany zone are comprised of both organic-rich and poor carbonate parasequences. This heterogeneity within the rich zones poorly impacts their overall organic-richness, and could have a negative impact on their economic potential. Although these lower rich zones could suffer from the presence of organic poor carbonates, they are laterally extensive, so we interpret an external control on their deposition. We would expect to find these units across the basin, so although they might lack some in organic-richness, their volume would be extensive. From a geochemical view, the organic-rich carbonate mudstone below and above the Mahogany zone (F2.4 and F2.5) are distinct (Figure 14). These geochemical distinctions could impact geomechanical properties as well as chemical reactions during ex situ retorting or in situ heating. One benefit of studying such a laterally extensive and vertically complete section is the opportunity to

study the heterogeneities within the different rich zones and to consider how they could affect development.

CONCLUSIONS

The Evacuation Creek outcrop and the Asphalt Wash-1 core provide an exceptional dataset for interpreting the sedimentologic and sequence stratigraphic changes that occur within the Uinta Basin's Green River Formation. The high degree of heterogeneity in these sections illustrates the complexity of the mixed siliciclastic-carbonate lacustrine depositional system, yet further examination of the succession reveals predictability to the facies and stratigraphic stacking patterns. Ten different facies were deposited in four different facies associations: siliciclastics, carbonates, saline deposits, and volcanic-derived deposits. The combination of short-term climatic changes and longer-term tectonic mechanisms shaped the evolution of Lake Uinta from an overfilled basin with frequent and short-lived fluctuations in sediment supply and accommodation (lake phase 1a), to an overfilled basin with less frequent and longer-lived fluctuations in sediment supply and accommodation (lake phase 1b), to a balance-filled basin with little siliciclastic input (lake phase 2a), to a balance-filled basin with virtually no sediment supply and an increasing lake level (lake phase 2b), to a stable, high lake level (lake phase 3a), to an underfilled basin with abundant saline minerals (lake phase 3b). Spectral gamma ray analysis provides evidence for changes in lithologic composition that reflect this lake evolution, while also exhibiting similar changes in stacking patterns between stratigraphic sections. The spectral gamma ray data collected from outcrop can

also be beneficial for interpreting and correlating subsurface standard gamma ray data from the Green River Formation in other parts of the basin.

Short-term climatic changes influence variations in the sediment supply regime, specifically during Eocene hyperthermal events that were characterized by seasonal, flashy fluvial discharge, or monsoonal episodes. Lean zones were dominated by high fluvial and siliciclastic input, with lower accommodation. The base of the lean zones are marked by regionally extensive surfaces of erosion, overlain by progradationally stacked coarsening upwards mouthbar and terminal distributary channel packages. Rich zones are characterized by low siliciclastic input and higher rates of carbonate production and accommodation. Rich zones contain regionally extensive flooding surfaces at their base that record increased accommodation and relative lake level rise, and are overlain by aggradational to retrogradational stacked shallowing upwards carbonate dominated packages. The regional lateral continuity of rich and lean zones and the stacking patterns of their comprising packages, as well as the regional extent of erosion and flooding surfaces support an allocyclic control on deposition. Specifically, the amount of fluvial sediment delivery into the lake from the hinterland varied systematically as a result of climate changes.

Longer-term tectonically induced subsidence determined accommodation space and interbasin lake communication. Identifying the role of climatic and tectonic drivers in deposition provides a genetic stratigraphic model and an understanding of lateral facies architecture that can be used to better evaluate the valuable resources of the Green River Formation in the Uinta Basin. If this stratigraphic model can be applied and correlated

throughout the basin, then the most economic oil shale targets can be laterally traced and identified.

APPENDIX

DETAILED MEASURED SECTIONS

Key:

Symbols:

- Horizontal, planar lamination
- Low angle planar lamination
- Trough cross-bedding
- Low angle planar dipping surfaces
- Accretionary surfaces
- Siltstone and/or heterolithic rip-up clast
- Carbonate rip-up clast
- Organic-Rich clast
- Current ripple cross-lamination
- Combined flow ripple cross-lamination
- Climbing ripple cross-lamination
- Wavy bedding
- Convolute bedding
- De-watering structures
- P — Pyrite Crystals
- E — Saline Minerals
- Load casting
- Concretion
- Shell material
- Garr fish scales
- *Lithophypoderm sp.* ("Botfly" Larvae)
- Ooids
- Ostracods
- Thrombolites
- Stromatolites
- Petrified wood, logs or debris
- Plant debris
- Insect fossils
- Root traces
- Mudcracks

Lithology:

- Claystone/ Siltstone
- Sandstone
- Carbonate
- Microbialite
- V — Tuff
- Paleosol
- Organic Rich
- Covered Section/ Unslabbed Core

Section Name: Asphalt Wash-1 Core
Location (lat/long): N39°52'37.4" W109°16'12.3" Total Thickness Measured: 1138 ft (~347 m)
Date Measured: 1/9-2/15/2012 Measured By: Morgan Rosenberg

Thick. Feet (m)	Graphic Log	Stratigraphic Zone	Additional Notes
13360 ft (407.2 m)		Douglas Creek Member	Coarsening siltstone to very fine sandstone, carbonate cement, de-watering structures, thin stromatolite layer, shell debris
13480 ft (410.9 m)			Paleosol with root structures
			Siltstone to very fine sandstone, low angle to plane parallel laminations, ripples present
			Very fine sandstone, low angle laminations with some ripples
13640 ft (415.7 m)			Siltstone to claystone to siltstone, wavy laminations and some ripples present, small clasts at bottom, fish scales, plant debris, and insect fossils present, some de-watering structures
	**Gap in Core		
20070 ft (611.7 m)			Fine sandstone, low angle laminations, clay rich towards top, wavy
			Claystone, low angle laminations, wood debris
20240 ft (616.9 m)			Fine sandstone, climbing ripples present
			Wavy siltstone with ripples. some fish fossils and fine sandstone clasts, sandstone and siltstone interbedded at top
20400 ft (621.8 m)			Silty, fine sandstone, wavy laminations, de-watering structures
			Clay rich fine sandstone with ripples, wavy laminations
			Claystone to siltstone, wavy and low angle laminations, some ripples present
20560 ft (626.7 m)			Wavy contact at base, clay rich fine sandstone with ripples and low angle laminations, some dewatering structures
			Clay rich sandstone with ripples, low angle laminations
20720 ft (631.5 m)			Concretions
			Vf sandstone with ripples
			Wavy Bedding
			Fish Scales
			Silty claystone at bottom
20880 ft (636.4 m)			Silty claystone; low angle/ wavy laminations; fish scales

clay mdst silt wkst v.f.sand pkst f.sand grst m.sand c.sand v.c.sand GPCB gravel

Section Name: Asphalt Wash-1 Core
Location (lat/long): N39°52'37.4" W109°16'12.3" Total Thickness Measured: 1138 ft (~347 m)
Date Measured: 1/9-2/15/2012 Measured By: Morgan Rosenberg

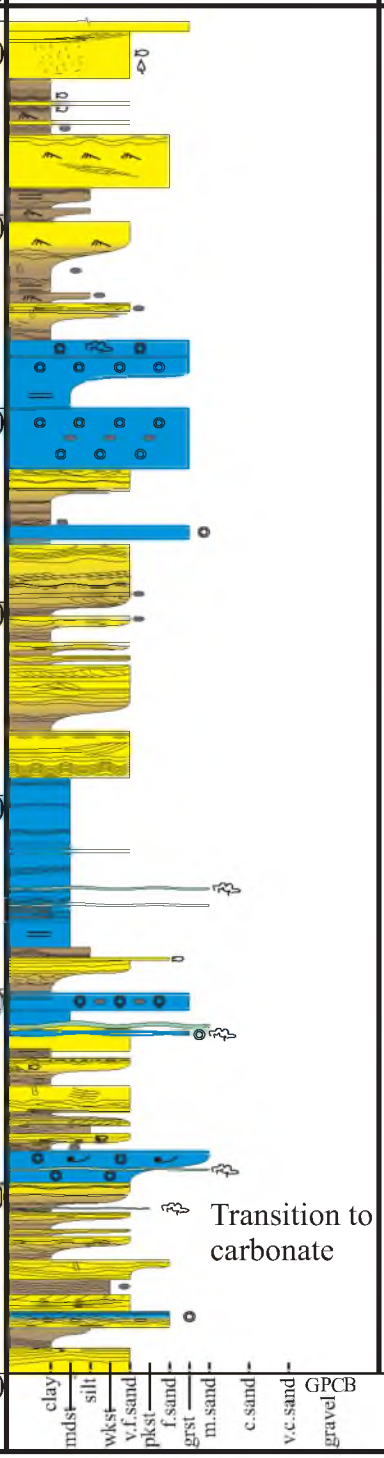

Stratigraphic Zone	Additional Notes
Douglas Creek Member	Very fine sandstone with some carbonate grains, carbonate cement, organic debris throughout (fish & plant), low angle laminations of organic material at top
	Fine sandstone with some carbonate grains, massive at bottom to low angle laminations, ripples and wavy laminations at top
	Claystone to siltstone, some soft sediment def.
	Claystone to very fine sandstone with carbonate cement, ripples and wavy laminations, massive towards top
	Claystone to v.f. sandstone (carb. cement), scour surfaces present, de-watering structure
	Carbonate mudstone to ooid grainstone with microbiolite clasts
	Coarsening upward ooid grainstone, clasts throughout
	Silty claystone to very fine sandstone, layer with rip up clasts at base
	Fining ooid grainstone
	Very fine sandstone with carbonate cement. wavy laminations and ripples, layer of clasts
	Silty claystone to very fine sandstone, wavy
	Silty, very fine sandstone, carbonate cement, few ripples, wavy at bottom to plane parallel laminations at top
	Carbonate mudstone, low angle laminations
	Interbedded carbonate mudstone and clay stone, ripples
	Silty claystone to very fine sandstone (carb. cement), wavy laminations, ripples
	Ooid grainstone with pebble clasts, clay layer
	Microbiolite layer with ooids, rip ups
	Claystone to very fine sandstone (carb. cement), scour surface filled with fish debris
	Very fine sandstone, carb. cement, fracture
	Claystone to very fine sandstone, granule clasts at base, fish debris at top Ooid grainstone with shell fragments
	Coarsening claystone to very fine sandstone packages, carbonate cement
	Sandy siltstone with slightly wavy bedding some pebble clasts
	Fine sandstone with brecciated layers of flattened grains, carbonate cement, transitions to ooid grainstone, wavy

Section Name: Asphalt Wash-1 Core
Location (lat/long): N39°52'37.4" W109°16'12.3" Total Thickness Measured: 1138 ft (~347 m)
Date Measured: 1/9-2/15/2012 Measured By: Morgan Rosenberg

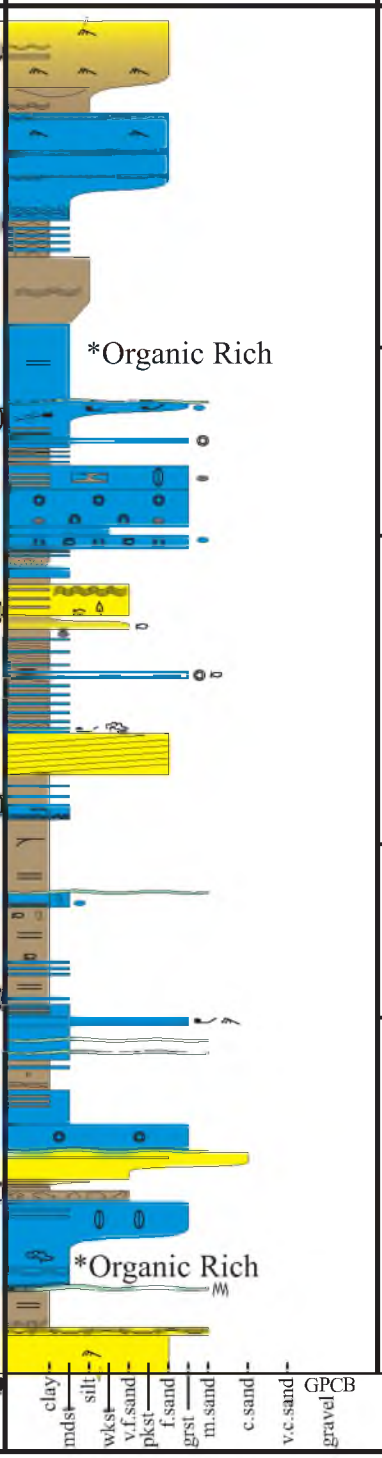

Stratigraphic Zone	Additional Notes
L3	Siltstone to fine sandstone, small clay channel form at base, wavy laminations and ripples
	Carbonate mudstone to fine grained carbonate grainstone, organic debris in mudstone, wavy laminations, ripples at top
R3	Dark carbonate mudstone
	Carbonate grainstone, few shell fragments, pebbles, SSD
	Ostracod grainstone, some claystone layers, SSD
L2	Ooid grainstone, some fish debris and pebble clasts
	Claystone with marcasite grains
	Interbedded very fine sandstone and claystone, wavy laminations, fish and plant debris at base
	Carbonate mudstone, shell, microbiolite debris
	Fine sandtone, low angle crossbedding, some carbonate cement
R2	Interbedded silty claystone and carbonate mudstone, plane parallel laminations to low angle
	Interbedded silty claystone and carbonate mudstone, light to dark, de-watering structures and ripples present
Douglas Creek Member	Carbonate grainstone with shell fragments, gastropod fossil, ripples at top
	Interbedded claystone and carbonate mudstone, pyrite present
	Coarsening upward ooid grainstone
	Very fine to coarse, angular sandstone, few carbonate grains present
	Claystone breccia
	Carbonate mudstone with some microbialite clasts to ostracodal grainstone
	Dark organic rich carbonate mudstone
	Fine to medium sandstone, mostly massive with few ripples to wavy

Section Name: Asphalt Wash-1 Core
Location (lat/long): N39°52'37.4" W109°16'12.3" Total Thickness Measured: 1138 ft (~347 m)
Date Measured: 1/9-2/15/2012 Measured By: Morgan Rosenberg

Thick. Feet (m)	Graphic Log	Stratigraphic Zone	Additional Notes
1000.0 ft (304.8 m)	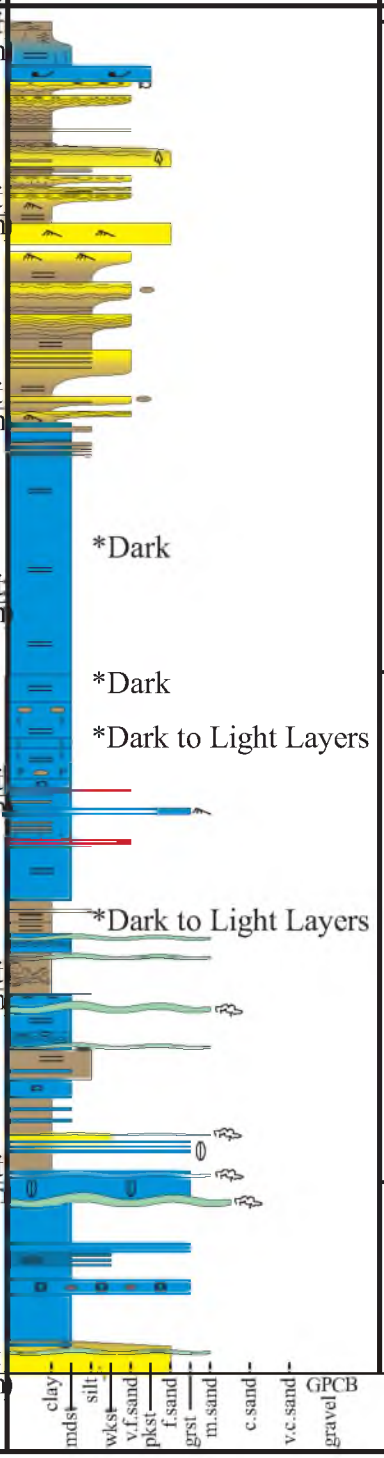	L4	Dark, silty claystone with soft sediment deformation over carbonate mudstone Carbonate packestone with shell fragments Interbedded claystone to siltstone and very fine to fine sandstone, some plant debris, fish scales, and ripples, wavy laminations
1016.0 ft (309.7 m)			Fine sandstone with ripples (Above small gap in core) Siltstone to very fine sandstone with few ripples and pebble clasts Silty claystone to very fine sandstone with few ripples and pebble clasts
1032.0 ft (314.6 m)			Dark, finely laminated carbonate mudstone, plane parallel laminations, increasing siltstone towards top
1048.0 ft (319.4 m)		R4	Dark to light carbonate mudstone with abundant soft sediment deformation and pebble clasts, some pyrite & fish scales present Carbonate mudstone to grainstone with ripples at top Dark to light silty claystone layers Silty slaystone w/ soft sediment deformation Dark carbonate mudstone with microbialite layers and flattened pebble grains Some interbedded carbonates and claystone siltstone, few fish scales in carbonate mudstone layer
1064.0 ft (324.3 m)			
1080.0 ft (329.2 m)			
1096.0 ft (334.1 m)		L3	Carbonate mudstone to grainstone, fractures in mudstone
1112.0 ft (338.9 m)			

Section Name: Asphalt Wash-1 Core
Location (lat/long): N39°52'37.4" W109°16'12.3" Total Thickness Measured: 1138 ft (~347 m)
Date Measured: 1/9-2/15/2012 Measured By: Morgan Rosenberg

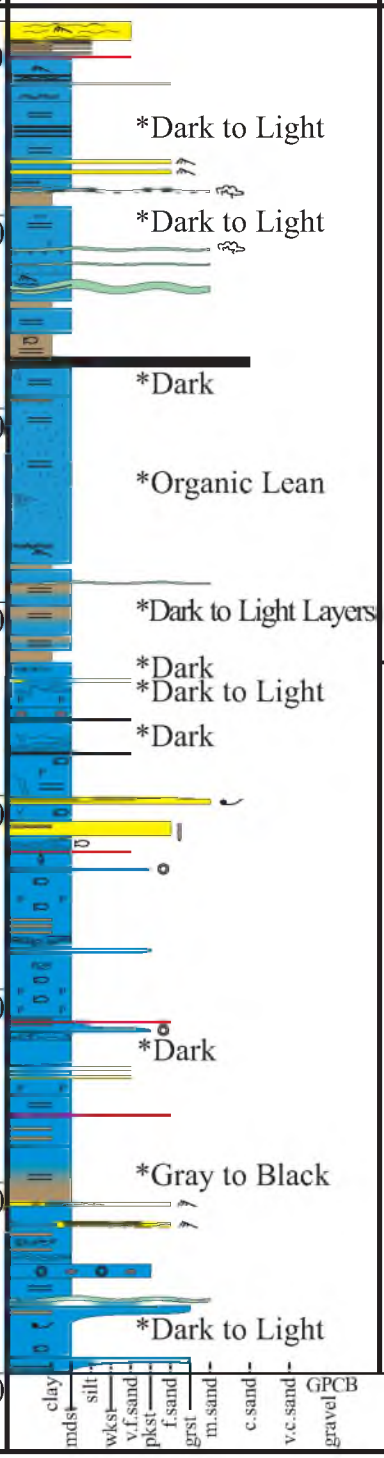

Thick. Feet (m)	Graphic Log	Stratigraphic Zone	Additional Notes
888.0 ft (270.7 m)		L5	Carbonate mudstone to silty claystone to very fine sandstone with ripples and wavy laminations
	*Dark to Light		Dark to light carbonate mudstone w/some thin sandstone layers & thin stromatolite layers, three extremely organic rich layers
904.0 ft (275.5 m)	*Dark to Light		
			Interbedded carbonate mudstone and claystone, tar sand layer and microbialite layer with interbedded carbonate mudstone
920.0 ft (280.4 m)	*Dark		
	*Organic Lean		Light, organic lean carbonate mudstone, abundant marcasite crystals, plane parallel laminations, some wavy laminations & ripples at bottom, carbonate nodule present
936.0 ft (285.3 m)	*Dark to Light Layers		Dark carbonate mudstone to light claystone layers, plane parallel laminations
	*Dark		
	*Dark to Light		
	*Dark	R5	Dark carbonate mudstone with abundant fish scales & pyrite, abundant SSD, some de-watering structures, some sandstone layers, two with tar, one with shell clasts, one with a burrow at bottom
952.0 ft (290.2 m)			
			Dark carbonate mudstone with abundant fish scales and pyrite, some layers of SSD, thin carbonate packestone layers and claystone layers
968.0 ft (295.0 m)			
	*Dark		Carbonate mudstone with some dark, organic rich layers, some pyrite present, de-watering structures, some claystone and very fine sandstone layers
984.0 ft (299.9 m)	*Gray to Black		Carbonate mudstone w/ some thin fine sandstone & claystone layers, soft sediment deformation and wavy laminations in mudstone
			Carbonate packestone with few ooids and pebble clasts
	*Dark to Light		Carbonate mudstone to grainstone, few thin claystone layers, some fish scales and shell fragments in dark mudstone
1000.0 ft (304.8 m)			

Section Name: Asphalt Wash-1 Core
Location (lat/long): N39°52'37.4" W109°16'12.3" Total Thickness Measured: 1138 ft (~347 m)
Date Measured: 1/9-2/15/2012 Measured By: Morgan Rosenberg

Thick. Feet (m)	Stratigraphic Zone	Additional Notes
776.0 ft (236.5 m)	Middle R6	Siltstone with plane parallel laminations and dewatering structures
		Carbonate mudstone, top has oil-stained fracture plane
		Siltstone with wavy laminations
792.0 ft (241.4 m)		Carbonate mudstone with some SSD below thin microbialite layer, some marcasite crystals
		Claystone with increasing siltstone, plane parallel laminations to wavy laminations
808.0 ft (246.3 m)		Dark to light carbonate mudstone with thin gilsonite vein at top, plane parallel laminations
		Medium sandstone to silty claystone to dark to light carbonate mudstone, very organic rich fine sandstone at top (tar sand)
824.0 ft (251.2 m)		Unsplit core, siltstone with slight reaction, plant debris and some organic matter present
840.0 ft (256.0 m)		Siltstone with wavy laminations
856.0 ft (260.9 m)	Lower R6	
		Dark carbonate mudstone, few carbonate nodules and fish scales, plane parallel laminations, some SSD at top with some low angle laminations and gilsonite veins
872.0 ft (265.8 m)	L5	
		Dark carbonate mudstone with pyrite crystals to light carbonate wackestone with wavy laminations
		Dark to light carbonate mudstone layers some very fine sandstone layers
888.0 ft (270.7 m)		

Section Name: Asphalt Wash-1 Core
Location (lat/long): N39°52'37.4" W109°16'12.3" Total Thickness Measured: 1138 ft (~347 m)
Date Measured: 1/9-2/15/2012 Measured By: Morgan Rosenberg

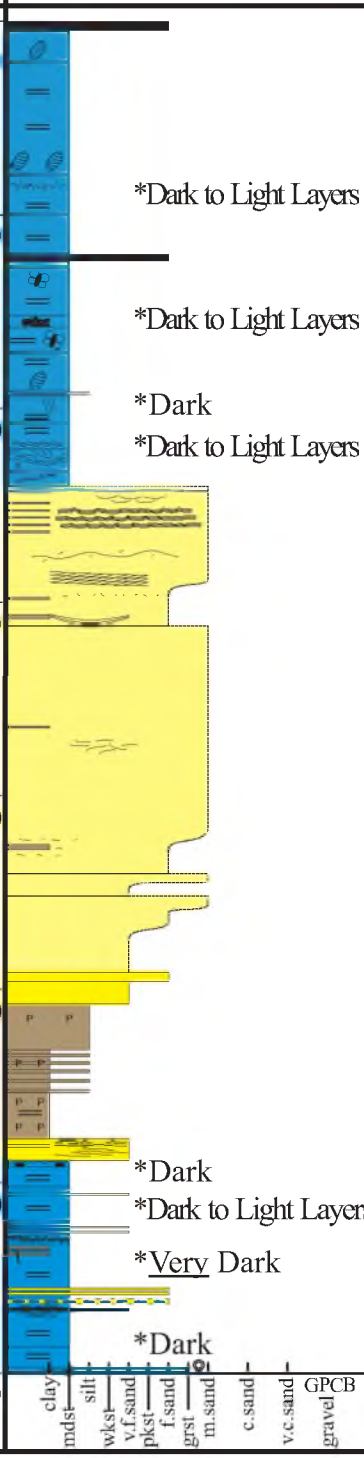

Thick. Feet (m)	Graphic Log	Stratigraphic Zone	Additional Notes
664.0 ft (202.4 m)		Upper R6	
680.0 ft (207.3 m)	*Dark to Light Layers		Dark to light carbonate mudstone, plane parallel laminations, botfly larvae fossils and other organic debris
	*Dark to Light Layers		Dark to light carbonate mudstone, plane parallel laminations, bug and tree limb fossils, thin fine tar sand layer
696.0 ft (212.1 m)	*Dark *Dark to Light Layers		Dark to light carbonate mudstone, SSD and wavy laminations, some dewatering structures, botfly larvae
712.0 ft (217.0 m)			Unsplit core, fine sandstone to medium sandstone, some claystone, organic matter, and some layers of ripples
728.0 ft (221.9 m)			Unsplit core, fine sandstone to medium sandstone, some claystone, organic matter, and few possible ripples
744.0 ft (226.8 m)			Unsplit core, very fine sandstone to medium sandstone
			Claystone to siltstone to vf sandstone to f sandstone, mostly massive with some plane parallel laminations, some pyrite crystals
			Very fine sandstone with low angle laminations and some thin claystone layers
760.0 ft (231.6 m)	*Dark		Organic rich carbonate mudstone, some SSD, tar sand clasts at top
	*Dark to Light Layers		Very dark carbonate mudstone, some claystone at top with dewatering structure, oil-shale breccia layer at bottom
	*Very Dark		Dark carbonate mudstone, some SSD
776.0 ft (236.5 m)	*Dark		Thin ooid grainstone layer

Section Name: Asphalt Wash-1 Core
Location (lat/long): N39°52'37.4" W109°16'12.3" Total Thickness Measured: 1138 ft (~347 m)
Date Measured: 1/9-2/15/2012 Measured By: Morgan Rosenberg

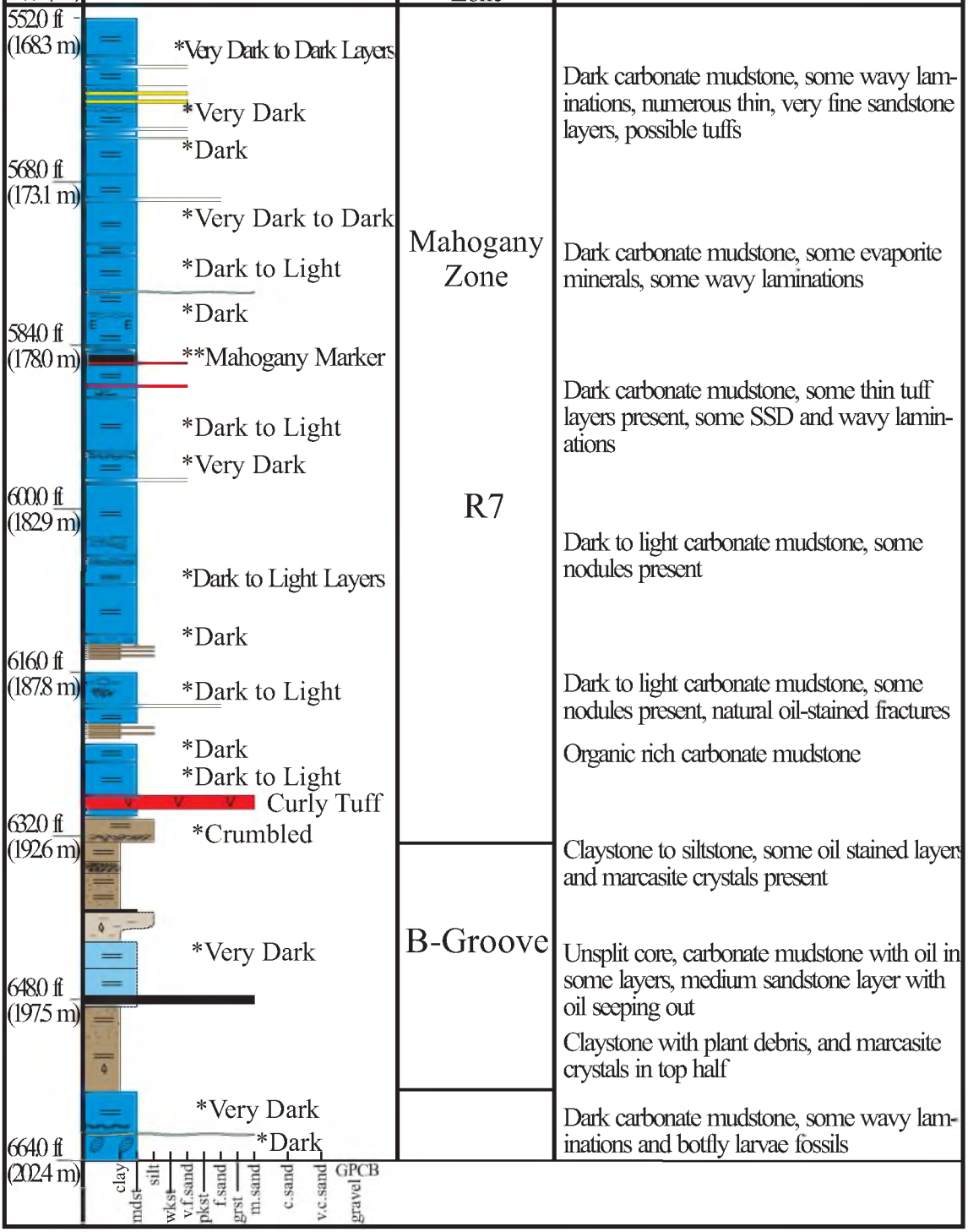

Section Name: Asphalt Wash-1 Core
Location (lat/long): N39°52'37.4" W109°16'12.3" Total Thickness Measured: 1138 ft (~347 m)
Date Measured: 1/9-2/15/2012 Measured By: Morgan Rosenberg

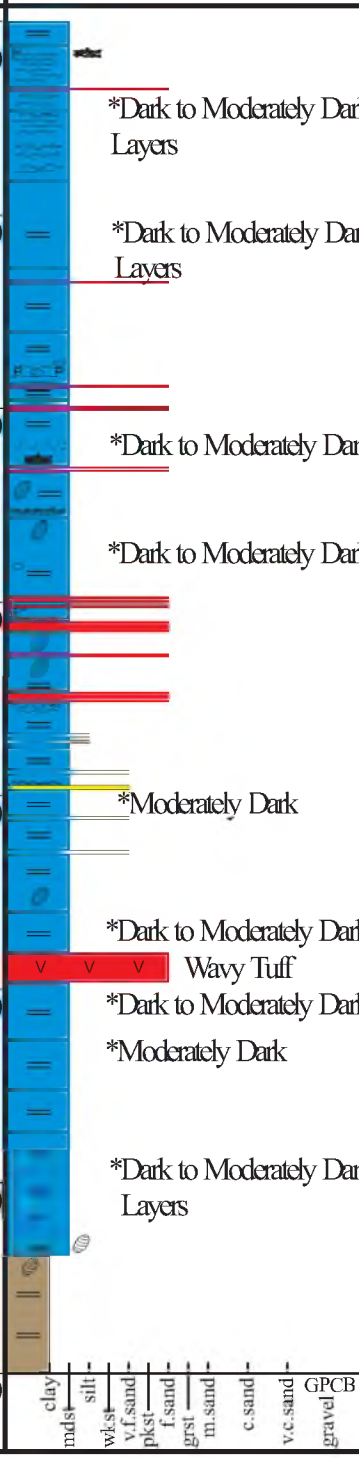

Section Name: Asphalt Wash-1 Core
Location (lat/long): N39°52'37.4" W109°16'12.3" Total Thickness Measured: 1138 ft (~347 m)
Date Measured: 1/9-2/15/2012 Measured By: Morgan Rosenberg

Thick. Feet (m)	Graphic Log	Stratigraphic Zone	Additional Notes
328.0 ft (100.0 m)	*Dark *Dark to Moderately Dark *Dark	Saline Zone	Dark to moderately dark carbonate mudstone with some SSD, wavy to parallel laminations, evaporate minerals and plant debris present
344.0 ft (104.9 m)	*Dark to Light		Dark to light carbonate mudstone, some plant debris
360.0 ft (109.7 m)	*Very Dark to Light		
	*Dark to Moderately Dark		
376.0 ft (114.6 m)		R8	
	*Dark to Moderately Dark		
392.0 ft (119.5 m)	*Dark to Moderately Dark Layers		Dark to moderately dark carbonate mudstone, wavy to plane parallel laminations, some thin tar sand layers
408.0 ft (124.4 m)	*Dark		Dark carbonate mudstone, plane parallel laminations, some thin tar sand layers
424.0 ft (129.2 m)	*Dark		Dark carbonate mudstone, plane parallel laminations, some pyrite at bottom
440.0 ft (134.1 m)	clay mds silt wkst v.f.sand pkst f.sand grst m.sand c.sand v.c.sand GPCB gravel		

Section Name: Asphalt Wash-1 Core
Location (lat/long): N39°52'37.4" W109°16'12.3" Total Thickness Measured: 1138 ft (~347 m)
Date Measured: 1/9-2/15/2012 Measured By: Morgan Rosenberg

Thick. Feet (m)	Graphic Log	Stratigraphic Zone	Additional Notes
307.0 ft (93.6 m)		R8 Saline Zone	Dark carbonate mudstone, plane parallel laminations, very abundant evaporate minerals, some layers of plant debris
312.0 ft (95.1 m)			
328.0 ft (100.0 m)			

Section Name: Evacuation Creek/ Condo Section Total Thickness Measured: 134.8 m
Location (lat/long): N39°50'3.0" W109°6'59.7" Morgan Rosenberg, Ryan O'Hara, Lauren Birgenheier,
Date Measured: 7/26-27/2011 Measured By: Mike Vanden Berg, Kati Tanavsuu-Milkeviciene

Thick. Feet (m)	Graphic Log	Stratigraphic Zone	Additional Notes
34.4 m 30 m 25 m	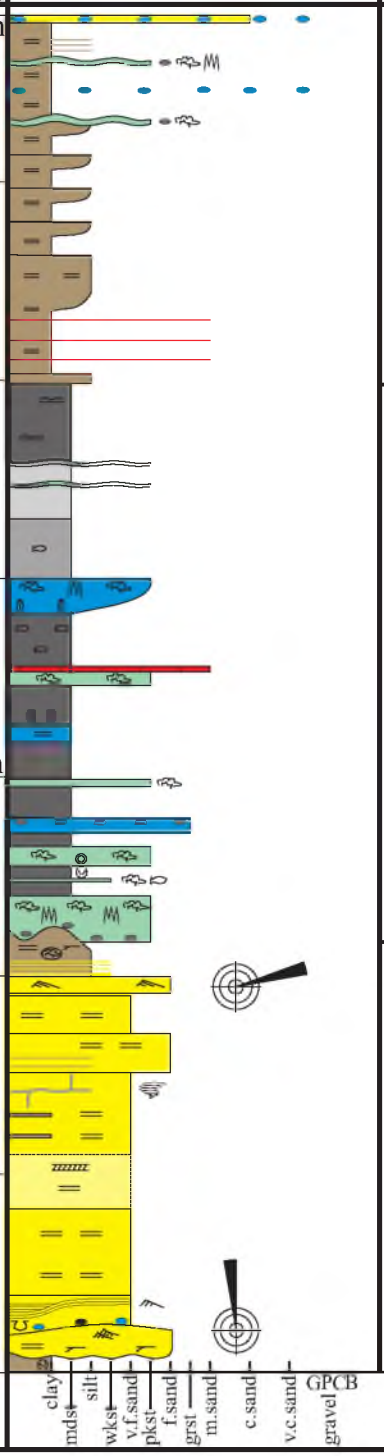	L5	Brecciated, carbonate, granular size rip-up clasts Flat laminated claystone with two thin microbialite layers (containing rip up clasts), layer of carbonate clasts Five coarsening upward packages of claystone to siltstone, flat laminated Bottom package: slight reaction with acid and contains few thin tuff layers
20 m 15 m		R5	Wavy bedded organic rich carbonate mudstone with thin microbialite layers at bottom Moderately organic rich carbonate mudstone with fish scales at bottom Ostracodal grainstone to stromatolite/ thrombolite Fish and crocodile scales in organic rich carbonate mudstone Thin tuff layer above stromatolitic microbialite Ostracods at bottom of organic rich carbonate mudstone Organic rich carbonate mudstone with microbialite and carbonate layers Small rip-up clasts at top of carbonate grainstone Thrombolitic and stromatolitic microbialite, rip up clasts at base
10 m 5 m 0 m		L4	Sandy siltstone at bottom, stromatolite nodule present Wave ripples present Thin to medium bedded sandstone with thin siltsone interbeds, minor calcium content Thin to medium bedded vf sandstone with thin claystone interbeds, dewatering structures Covered, very fine sandstone, trough cross stratification Very thinly bedded vf ss, top half poorly exposed Vf ss, channel cut-in, carbonate and oil shale rip-ups Claystone base with chert nodules Thickly bedded fine sandstone, channel shaped

Section Name: Evacuation Creek/ Condo Section Total Thickness Measured: 134.8 m

Location (lat/long): N39°50'3.0" W109°6'59.7" Morgan Rosenberg, Ryan O'Hara, Lauren Birgenheier,

Date Measured: 7/26-27/2011 Measured By: Mike Vanden Berg, Kati Tanavsuu-Milkeviciene

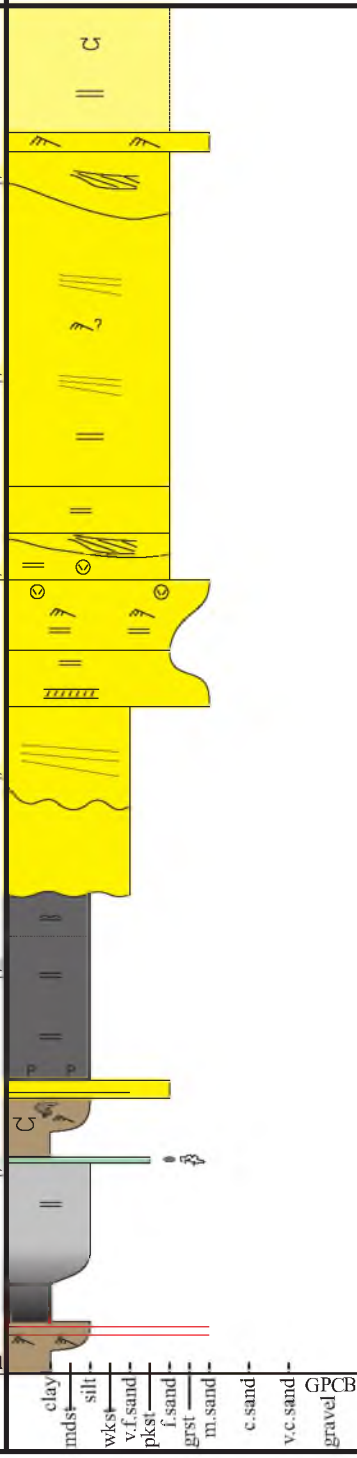

Thick. Feet (m)	Graphic Log	Stratigraphic Zone	Additional Notes
64.4 m		Middle R6	Covered, fine sandstone, planar laminations, load casts present
			Medium sandstone with current ripples
			Fine sandstone with high angle accretion surfaces with channelized base cut into layer below
59.4 m			Fine sandstone, flat laminated to low angle laminations with possible current ripples
			Fine sandstone, flat laminated
54.4 m			Channel with accretion surfaces cutting into fine, planar bedded ss with concretion layer
			Coarsening sandstone from fine to medium, current ripples with possible wave modification, concretion layer near top
			Fining upward sandstone from medium to fine, trough cross stratification at bottom to planar laminations
49.4 m			Very fine sandstone, channel form, low angle laminations
			Very fine sandstone, massive, red/green/orange color, deep channel
		Lower R6	Very finely laminated, "papershale"
44.4 m			Organic rich siltstone, plane parallel laminations, Pyrite crystals at bottom
			Massively bedded fine sand with thin vf layer
		L5	Coarsening upward claystone to siltstone, de-watering structures, ripples, and loadcasts
39.4 m			Sandy stromatolite with rip-up clasts
			Coarsening upward claystone to siltstone, leaning upward from organic rich to fairly rich, flat laminated
			Coarsening upward claystone to siltstone, layer of ripples present, two thin possible tuffs at top
34.4 m			

Section Name: Evacuation Creek/ Condo Section Total Thickness Measured: 134.8 m
Location (lat/long): N39°50'3.0" W109°6'59.7" Morgan Rosenberg, Ryan O'Hara, Lauren Birgenheier,
Date Measured: 7/26-27/2011 Measured By: Mike Vanden Berg, Kati Tanavsuu-Milkeviciene

Thick. Feet (m)	Graphic Log	Stratigraphic Zone	Additional Notes
	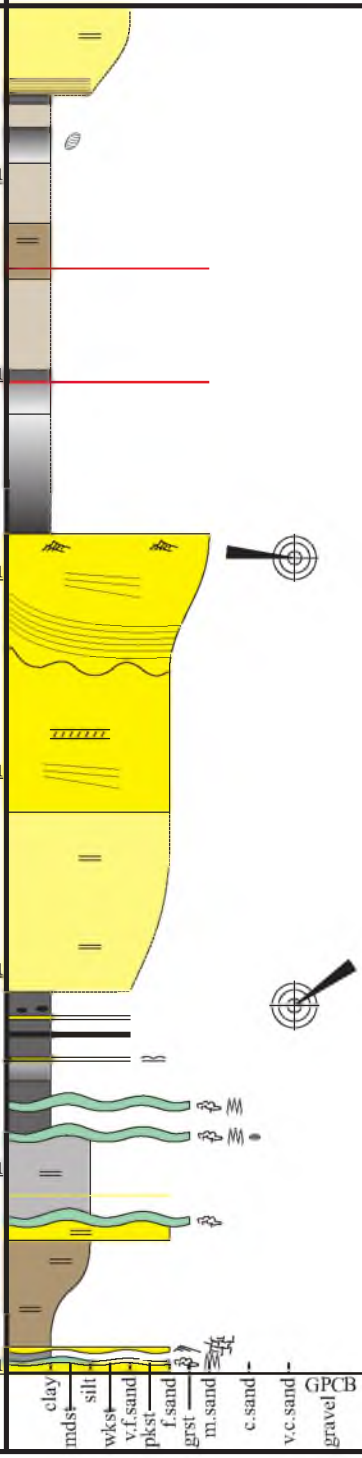	B-Groove	Partly covered very fine silty sandstone to fine sandstone
98.8 m		Upper R6	Moderately rich to organic rich mudstone, bottfly larvae at top
			Covered mudstone, possibly organic rich
			Lean, flat laminated mudstone with thin tuff bed
			Partly covered mudstone, possibly organic rich
93.8 m			Moderately rich to organic rich mudstone with possible tuff layer at top
			Mostly covered, organic rich to moderately rich mudstone
88.8 m			Fine to medium sandstone, channelized base, low angle to planar (more angular on one side), climbing wave ripples at top, organic material present in some foresets
83.8 m			Fine sandstone, low angle to plane parallel laminations, trough cross stratification
			Covered very fine to fine sandstone, thinly bedded, planar, variable thickness laterally
78.8 m			Oil shale breccia clasts
			Very fine tar-sand
			Organic rich mudstone with thin, wavy, vf sandstone bed
73.8 m			Moderately organic rich siltstone, flat laminated, microbialite on each side
		Middle R6	Coarsening upward siltstone to fine sandstone, flat laminated
68.8 m			Fine sandstone with mudcracks (some tar), with moderately organic claystone and stromatolitic and thrombolitic microbialite

clay mdst silt wkst v.f.sand pkst f.sand grst m.sand c.sand v.c.sand GPCB gravel

Section Name: Evacuation Creek/ Condo Section Total Thickness Measured: 134.8 m
Location (lat/long): N39°50'3.0" W109°6'59.7" Morgan Rosenberg, Ryan O'Hara, Lauren Birgenheier,
Date Measured: 7/26-27/2011 Measured By: Mike Vanden Berg, Kati Tanavsuu-Milkeviciene

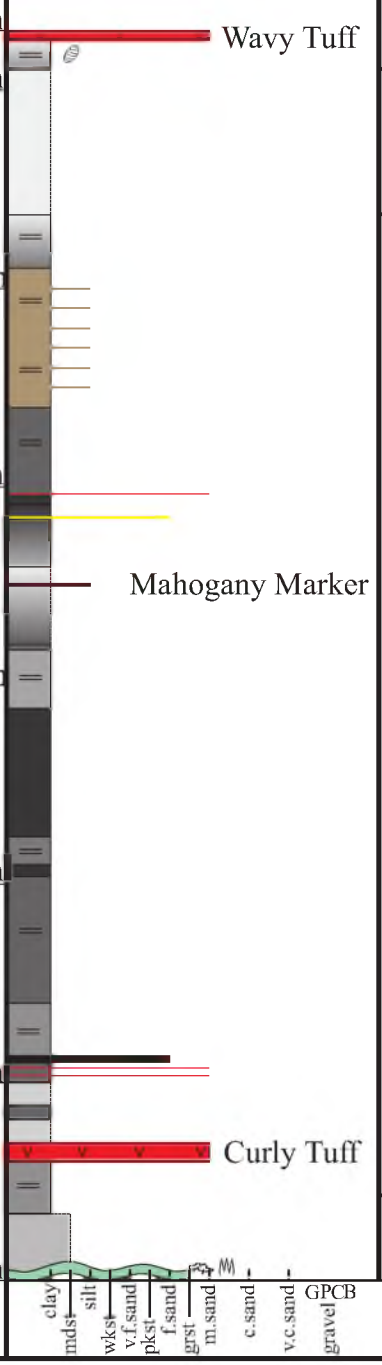

Stratigraphic Zone	Additional Notes
Lower R8	Organic rich to lean mudstone, botfly larvae present
A-Groove	Partly covered, lean
	Organic rich to lean mudstone
	Lean, silty claystone
Mahogany Zone	Partly covered
	Mostly very organic rich mudstone, some covered with thin tuff beds
R7	
	Moderately organic rich mudstone
	Mostly covered, carbonate mudstone, fairly organic
	Stromatolitic/ thrombolitic microbialite

Section Name: Evacuation Creek/ Flash Flood Section
Location (lat/long): N39°49'31" W109°6'6" Total Thickness Measured: 180.3 m
Date Measured: 7/28-30/2011 Measured By: Morgan Rosenberg

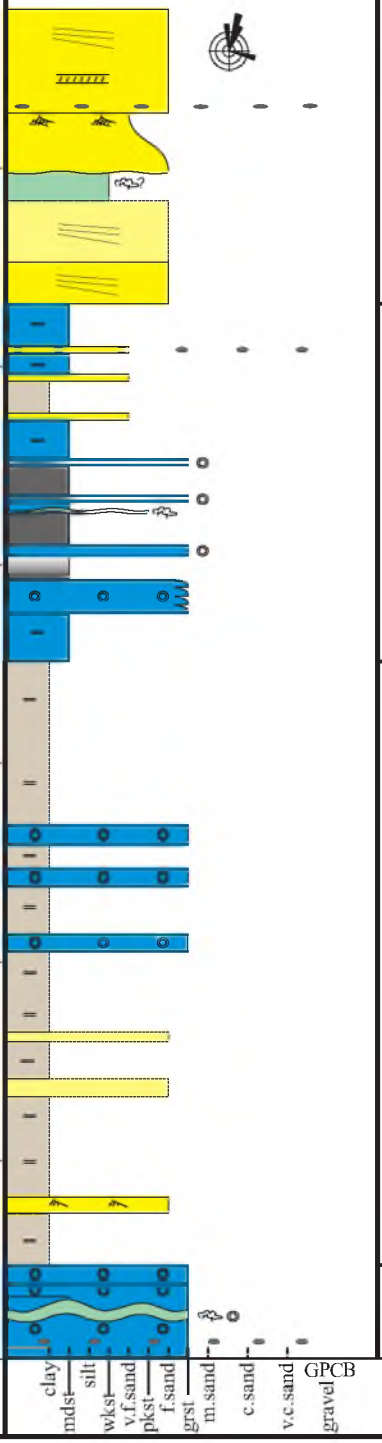

Stratigraphic Zone	Additional Notes
L3	Fine sandstone, trough cross bedding at base to low angle laminations towards top, dark organic matter in some laminations, rounded nodules at bottom paleocurrent data taken
	Fining upward sandstone, climbing current ripples at top
	Microbialite, possibly stromatolitic
	Mostly covered fine sandstone
	Fine sandstone with low angled surfaces
R3	Carbonate mudstone with thin, very fine sandstone layer that contains flattened clasts
	Mostly covered claystone, possibly carbonate mudstone, with thin, very fine sandstone on either side
	Organic rich carbonate mudstone with three thin ooid grainstone layers and one stromatolitic microbialite (middle ooid layer fines upward slightly)
	Organic rich to lean carbonate mudstone
	Ooid grainstone, 4 to 5 fining upward sequences
L2	Carbonate mudstone, beds thin upward
	Mostly covered claystone, possibly carbonate mudstone with multiple ooid grainstone layers
	Covered claystone, possibly lean carbonate mudstone
	Partly covered fine sandstone beds
	Mostly covered claystone, possibly carbonate mudstone
	Partly covered claystone, possibly lean carbonate mudstone
	Fine sandstone with ripples present
	Mostly covered claystone, possibly lean carbonate mudstone
R2	Ooid grainstone with few thin mudstone and microbialite beds
	Ooid grainstone with thin clay layer, granule lag above clay layer

Section Name: Evacuation Creek/ Flash Flood Section
Location (lat/long): N39°49'31" W109°6'6" Total Thickness Measured: 180.3 m
Date Measured: 7/28-30/2011 Measured By: Morgan Rosenberg

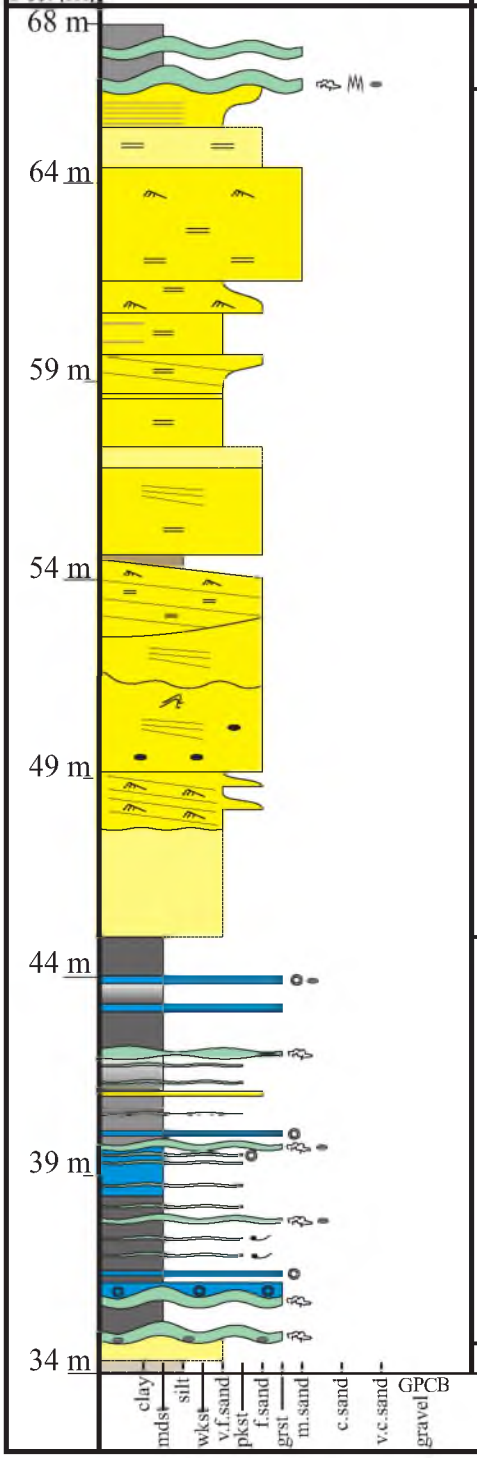

Stratigraphic Zone	Additional Notes
R5	Moderately organic rich carbonate mudstone with multiple microbialite layers
	**White, thrombolitic microbialite
L4	Silty, very fine sandstone, thinly bedded, coarsening upward
	Covered fine sandstone, possibly interbedded with siltstone
	Medium sandstone with plane parallel laminations at bottom to current ripples towards top
	Fining upward sandstone with current ripples at bottom to planar laminations
	Vf sandstone with thin claystone layers
	Coarsening upward sandstone, slightly dipping beds with plane parallel laminations
	Very fine sandstone, thinly bedded, parallel laminations, not well exposed
	Covered fine sandstone
	Fine sandstone, low angle to plane parallel laminations
	Siltstone parting
	Fine sandstone, possible channelized base, parallel laminations, small current ripples
	Fine sandstone, channelized base, planar to low angle laminations
	Fine sandstone, low angle laminations, organic rich rip-up clasts, soft sediment deformation towards top, truncation by above layer
	Two fining upward sequences from fine to very fine sandstone, layers of ripples present
	Covered very fine sandstone, possibly interbedded with siltstone due to consistent slope forming
R4	Organic rich zone with ooid grainstone beds
	Large stromatolite heads
	**Possibly tuff layer being dated
	Organic rich zone with many thin microbialite and other carbonate layers
	Two thin microbialite/ shell layers
	Stromatolitic microbialite with stromatolite rip-ups at base
	Covered siltstone to very fine sandstone

Section Name: Evacuation Creek/ Flash Flood Section
Location (lat/long): N39°49'31" W109°6'6" Total Thickness Measured: 180.3 m
Date Measured: 7/28-30/2011 Measured By: Morgan Rosenberg

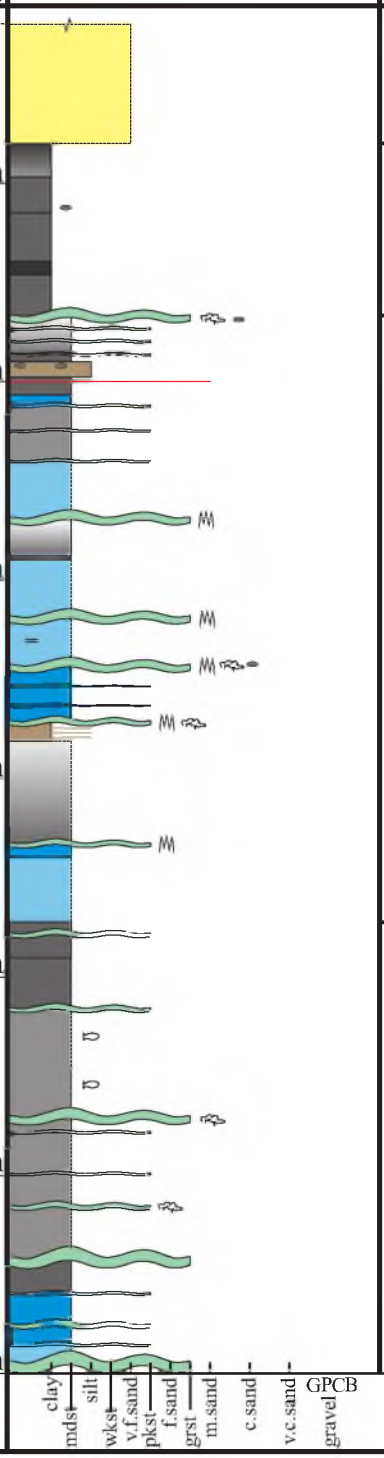

Thick. Feet (m)	Graphic Log	Stratigraphic Zone	Additional Notes
102 m		Middle R6	Covered very fine sandstone
			Moderately rich to organic rich mudstone
98 m		Lower R6	Large concretion nodules Covered organic rich mudstone
			Very rich mudstone
			Organic rich to lean carbonate mudstone with multiple microbialite layers
93 m			Thin tuff bed
			Moderately rich organic mudstone with thin microbialite layers
			Partly covered carbonate mudstone
		L5	Organic rich to lean carbonate mudstone
88 m			Carbonate mudstone with multiple microbialite layers
			Silty claystone
83 m			Partly covered, leaning upward organic-rich carbonate mudstone
			Covered to exposed, lean carbonate mudstone
78 m			Organic rich carbonate mudstone with multiple, thin microbialite layers (some mudstone layers partly covered)
			Fish scales present
		R5	
73 m			Organic rich carbonate mudstone with multiple, thin microbialite layers (some mudstone layers partly covered)
			Carbonate mudstone with many thin microbialite layers
68 m			

Section Name: Evacuation Creek/ Flash Flood Section
Location (lat/long): N39°49'31" W109°6'6" Total Thickness Measured: 180.3 m
Date Measured: 7/28-30/2011 Measured By: Morgan Rosenberg

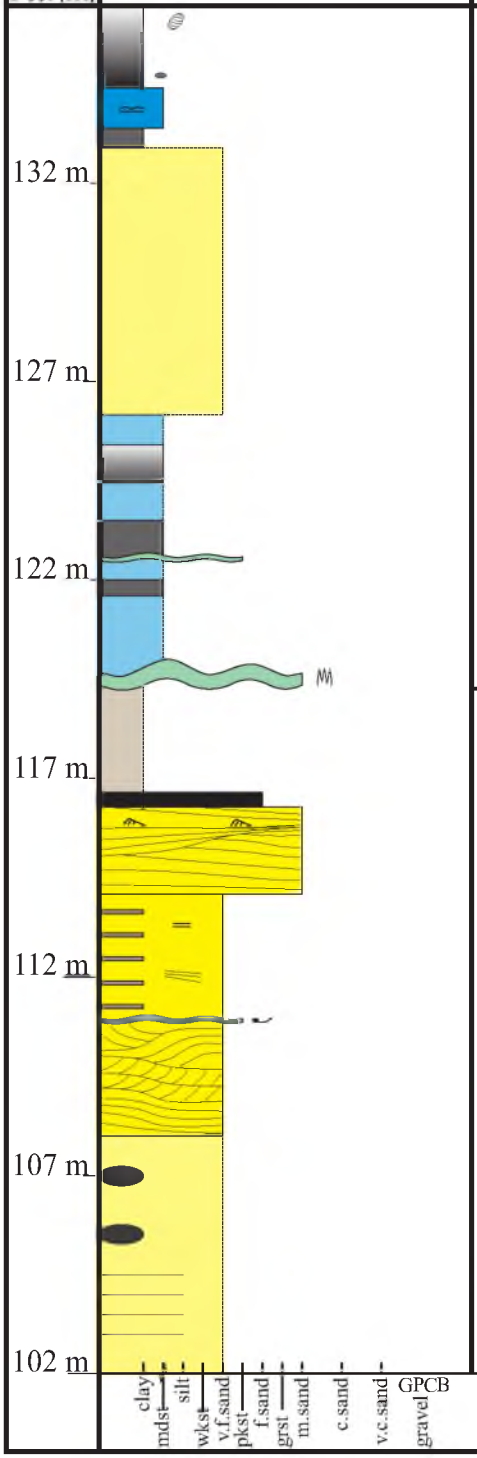

Section Name: Evacuation Creek/ Flash Flood Section
Location (lat/long): N39°49'31" W109°6'6" Total Thickness Measured: 180.3 m
Date Measured: 7/28-30/2011 Measured By: Morgan Rosenberg

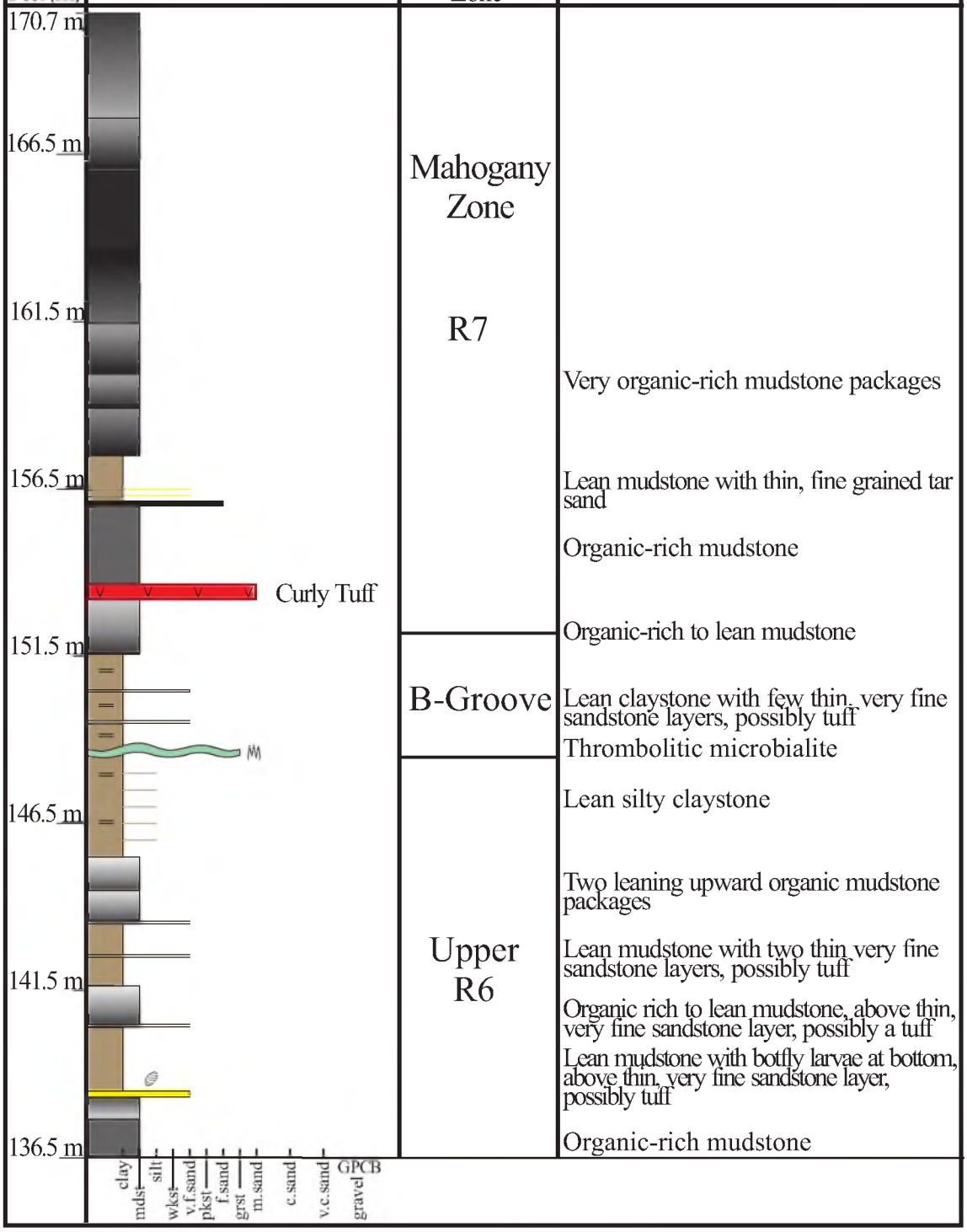

Section Name: Evacuation Creek/ Flash Flood Section
Location (lat/long): N39°49'31" W109°6'6" Total Thickness Measured: 180.3 m
Date Measured: 7/28-30/2011 Measured By: Morgan Rosenberg

Thick. Feet (m)	Graphic Log	Stratigraphic Zone	Additional Notes
180.3 m	Wavy Tuff	Lower R8	
175.7 m		A-Groove	
170.7 m			

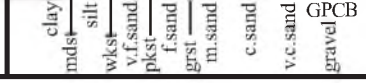

Section Name: Evacuation Creek/ Temple Section
Location (lat/long): N39°48'46.2" W109°5'27.1" Total Thickness Measured: 205.5 m
Date Measured: 7/31-8/4/2011, 10/30/2011 Measured By: Morgan Rosenberg, Jon Primm

Thick. Feet (m)	Graphic Log	Stratigraphic Zone	Additional Notes
34.2 m	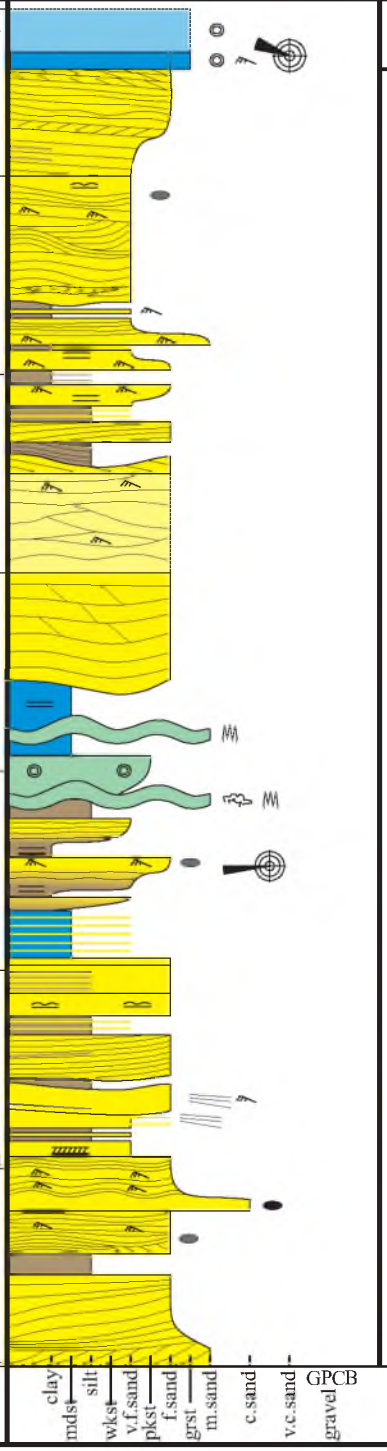	R2	Covered ooid grainstone
			Ooid grainstone with low angle laminations and ripples
30 m		Douglas Creek Member	Coarsening upward sand with low angle to wavy laminations with few ripple layers, some thin clay layers and round cobbles
			Layer of ripples, amalgamation surface
			Planar/ low angle laminations, multidirectional flow
25 m			Alternating claystone and sandstone layers, sands contain ripples. Bottom sandstone layer coarsens while other sandstone layers fine upward.
			Fine sandstone, low angle/ plane parallel laminations
20 m			Partially covered fine sand with low angle laminations and few ripples
			Channelized fine sandstone with wavy laminations and some isolated current ripples
			Carbonate mudstone with thrombolitic microbialite
15 m			Coarsening upward ooid/ microbialite
			Two coarsening upward sands, bottom layer contains ripples and accretion nodules at top, reacts slightly to acid, top layer has low angle laminations
			Coarsening upward sand
			Sandy carbonate mudstone
10 m			Silty f sandstone
			Very wavy laminations
			Vf sandy siltstone
			Low angle laminations, thin siltstone layer
			Low angle vf ss with thin coarser layers
5 m			Trough cross bedding
			Coarse lag with organic clasts fining into fine sand with wavy laminations and ripples
			Low angle to plane parallel laminations with layer of current ripples and clasts
0 m			Low angle channel laminations, more angled at bottom to planar at top

clay mdst silt wkst v.f.sand pkst f.sand grst m.sand c.sand v.c.sand gravel GPCB

Section Name: Evacuation Creek/ Temple Section
Location (lat/long): N39°48'46.2" W109°5'27.1" Total Thickness Measured: 205.5 m
Date Measured: 7/31-8/4/2011, 10/30/2011 Measured By: Morgan Rosenberg, Jon Primm

Thick. Feet (m)	Graphic Log	Stratigraphic Zone	Additional Notes
68.1 m	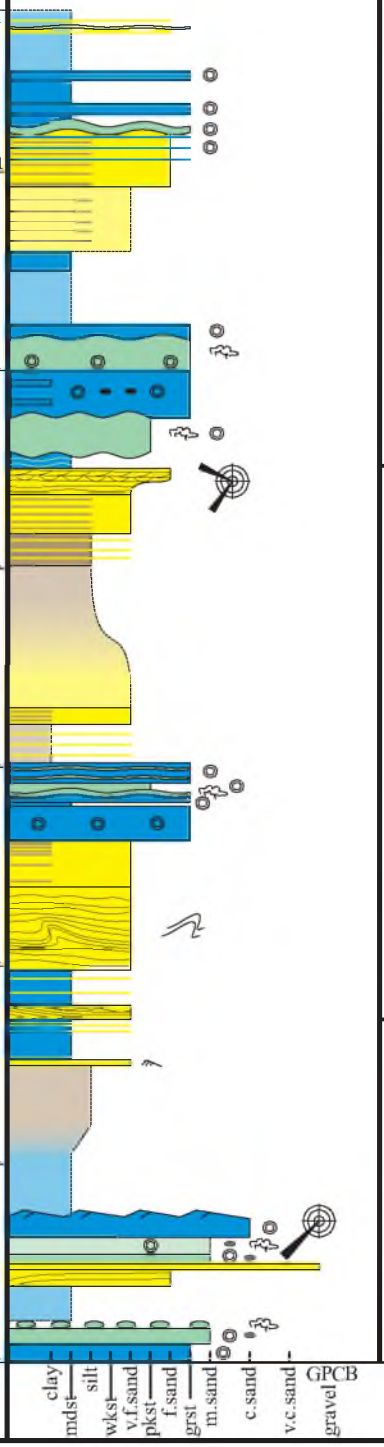	R3	Covered, sandy carbonate mudstone with thin microbialite bed at top Alternating carbonate mudstone and ooid grainstone layers Microbialite with ooids Silty sandstone with thin ooid grainstone beds towards top Covered silty sandstone Carbonate mudstone Covered carbonate mudstone Ooid microbialite to ooid, stromatolitic microbialite to ooidal grainstone Ooid grainstone with two carbonate mudstone interbeds, pebble sized clasts Ooid, stromatolitic microbialite Carbonate mudstone with few microbialite layers Coarsening upward sand with low angle laminations to trough cross stratification Siltstone to sandstone Covered sandstone to siltstone Clay rich sandstone Covered sandy claystone Alternating ooid grainstone and microbialite beds Clay-rich sandstone, increasing clay towards top Low angle/ planar laminations at bottom to wavy, soft sediment deformation features Silty carbonate mudstone with few ss beds Low angle laminations, possible trough X-strat at top Carbonate mudstone, increasing sandstone towards top Covered carbonate mudstone to siltstone Ooid grainstone with few pebble interbeds, wave ripples on top Partially covered carbonate mudstone Ooid grainstone to thrombolites, stromatolite heads
64.2 m			
59.2 m			
54.2 m		L2	
49.2 m			
44.2 m			
39.2 m		R2	
34.2 m			

Section Name: Evacuation Creek/ Temple Section
Location (lat/long): N39°48'46.2" W109°5'27.1" Total Thickness Measured: 205.5 m
Date Measured: 7/31-8/4/2011, 10/30/2011 Measured By: Morgan Rosenberg, Jon Primm

Thick. Feet (m)	Graphic Log	Stratigraphic Zone	Additional Notes
101.4 m	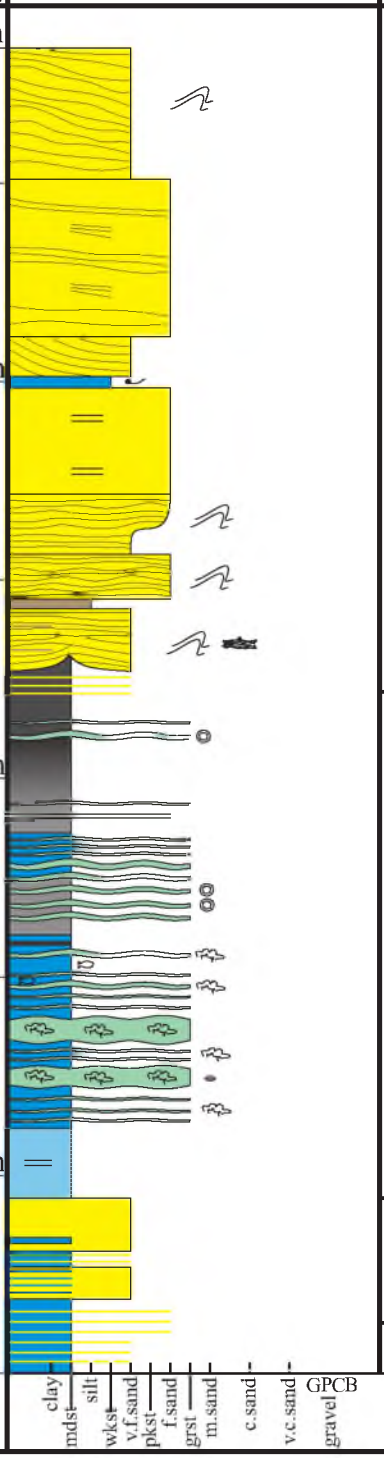		
		L4	Low angle to planar laminations, soft sediment deformation
98.1 m			Few planar to low angle laminations
			Low angle laminations
93.1 m			Thin, "shelly" carbonate layer
			Fairly massive sand, few possible planar laminations
			Coarsening upward ss, planar to low angle laminations, soft sediment deformation
88.1 m			Wavy, low angle to planar laminations, soft sediment deformation
			Loading structure at bottom where sand thins and pushes on either side, clay rich sand with internal scours and pieces of wood, flat laminated
83.1 m		R4	Moderately-rich to organic-rich carbonate mudstone with few microbialite layers and increasing ss towards the top
			Thin sand layer, possible tuff
			Carbonate mudstone with many thin microbialite beds
78.1 m			Moderately organic carbonate mudstone with many thin ooid microbialite beds
			Carbonate mudstone with many stromatolitic microbialite layers, fish scales towards top, thin organic-rich layer at top
73.1 m			Partially covered carbonate mudstone
		L3	Sandstone with thin carbonate mudstone layer at bottom, reacts slightly with acid
			Sandy carbonate mudstone
			Sandstone with thin carbonate mudstone layers
68.1 m			Sandy carbonate mudstone

clay mdst silt wkst v.f.sand pkst f.sand grst m.sand c.sand v.c.sand gravel GPCB

Section Name: Evacuation Creek/ Temple Section
Location (lat/long): N39°48'46.2" W109°5'27.1" Total Thickness Measured: 205.5 m
Date Measured: 7/31-8/4/2011, 10/30/2011 Measured By: Morgan Rosenberg, Jon Primm

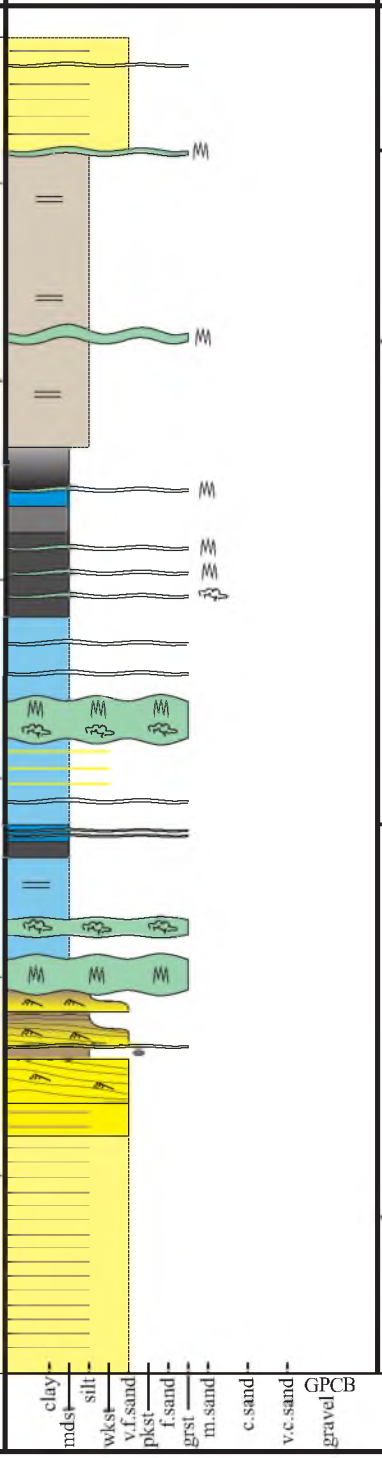

Thick. Feet (m)	Graphic Log	Stratigraphic Zone	Additional Notes
135.1 m		Middle R6	Covered silty sandstone with few microbialite layers
131.4 m		Lower R6	Covered carbonate mudstone, few thrombolitic microbialite beds
126.4 m		L5	Organic-rich to lean carbonate mudstone (mod. to lean); thrombolite at top Covered moderately organic carbonate mudstone Organic-rich carbonate mudstone with thin stromatolitic and thrombolitic microbialite beds Stromatolitic and thrombolitic microbialite Covered carbonate mudstone with thin microbialite layer at bottom and increasing sandstone towards top
116.4 m		R5	Carbonate mudstone with thin microbialite layers Covered carbonate mudstone with stromatolitic microbialite layer **White, thrombolitic microbialite Two fining upward packages with low angle laminations and current ripples Low angle laminations with few ripples Silty sandstone
111.4 m			
106.4 m		L4	Covered silty sandstone
101.4 m			

Section Name: Evacuation Creek/ Temple Section
Location (lat/long): N39°48'46.2" W109°5'27.1" Total Thickness Measured: 205.5 m
Date Measured: 7/31-8/4/2011, 10/30/2011 Measured By: Morgan Rosenberg, Jon Primm

Thick. Feet (m)	Graphic Log	Stratigraphic Zone	Additional Notes
167.5 m	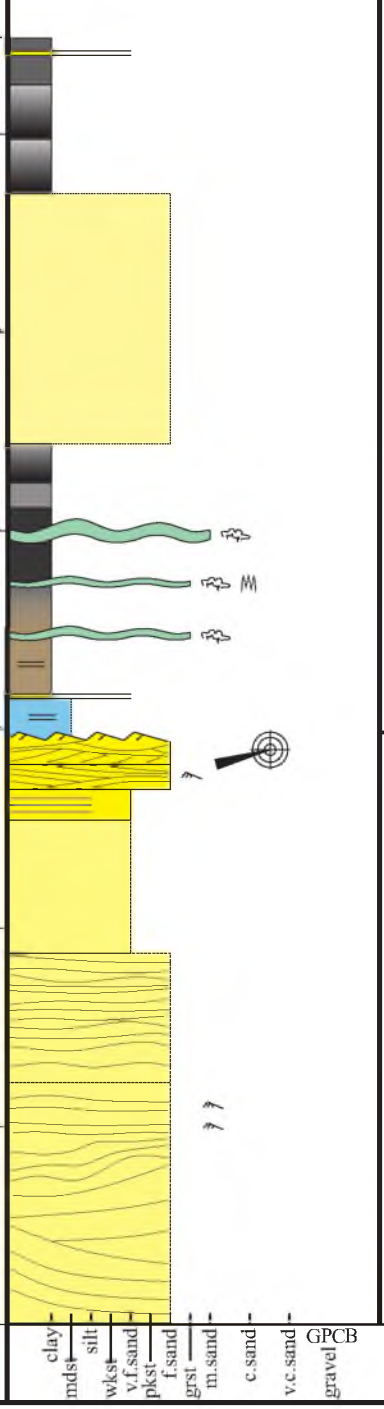	Upper R6	Organic-rich mudstone with thin, very fine sandstone layer, possible tuff
165.1 m			Very rich to moderately rich mudstone Top layer contains feather fossil
160.1 m			Covered, thinly bedded fine sandstone
155.1 m			Very rich to moderately rich mudstone Covered, moderately rich mudstone Very rich, very fissile mudstone Organic lean to very rich, thinly bedded mudstone Thin, very fine sandstone towards bottom, possible tuff Few microbialite beds
150.1 m			Covered, lean carbonate mudstone
145.1 m		Middle R6	Fine sandstone with high angle cross stratification at bottom to low angle laminations with ripples at top Covered vf sandstone
140.1 m			Partly covered fine sandstone, low angle to plane parallel laminations
135.1 m			Partly covered fine sandstone, low angle channel laminations at bottom to low angle/ plane parallel laminations with few ripples at top

Section Name: Evacuation Creek/ Temple Section
Location (lat/long): N39°48'46.2" W109°5'27.1" Total Thickness Measured: 205.5 m
Date Measured: 7/31-8/4/2011, 10/30/2011 Measured By: Morgan Rosenberg, Jon Primm

Stratigraphic Zone	Additional Notes
	Lean to moderately rich carbonate mudstone
	Organic-rich mudstone
Mahogany Zone	Moderately rich to very organic-rich mudstone
	Moderately rich mudstone with thin tuff bed
	Moderately rich to organic-rich mudstone
	Very organic-rich mudstone
R7	Very organic-rich mudstone
	Moderately organic-rich mudstone
	Very rich to rich mudstone
	Moderately organic-rich mudstone
	Fine grained tar-sand
	Organic-rich to moderately rich mudstone
	Moderately rich to organic-rich mudstone
	Medium sandstone
	Moderately organic dolostone
B-Groove	
	Stromatolitic/ thrombolitic microbialite
	Covered, lean carbonate mudstone
Upper R6	Lean to very organic-rich mudstone, numerous botfly larvae present towards top

Section Name: Evacuation Creek/ Temple Section
Location (lat/long): N39°48'46.2" W109°5'27.1" Total Thickness Measured: 205.5 m
Date Measured: 7/31-8/4/2011, 10/30/2011 Measured By: Morgan Rosenberg, Jon Primm

Thick. Feet (m)	Graphic Log	Stratigraphic Zone	Additional Notes
205.5 m	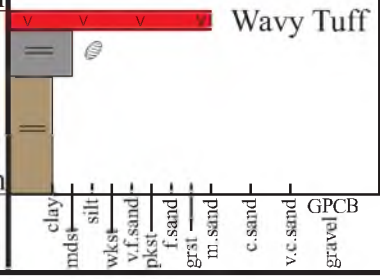	Lower R8	Moderately organic-rich carbonate mudstone, botfly larvae fossils present
200.9 m		A-Groove	Claystone

Section Name: Evacuation Creek/ Gray Huts Section
Location (lat/long): N39°48'29" W109°4'48.4" Total Thickness Measured: 216.8 m
Date Measured: 10/27-10/29/2011 Measured By: Morgan Rosenberg, Jon Primm

Thick. Feet (m)	Graphic Log	Stratigraphic Zone	Additional Notes
34 m	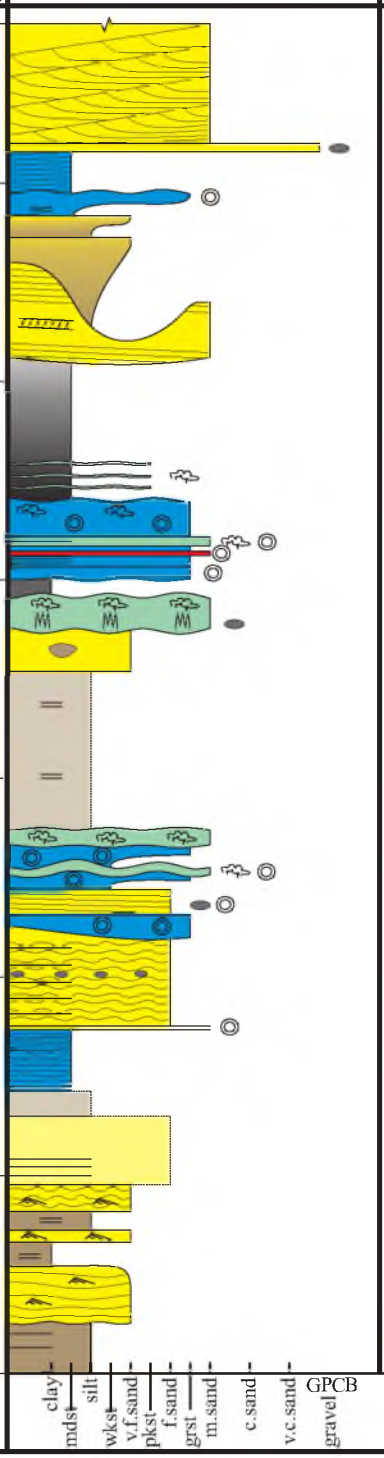	Douglas Creek Member	Medium sandstone with low-angle cross stratifications, possible troughs
30 m			Wavy carbonate mudstone and ooid grainstone with wave influenced ripples on bedding plane
			Coarsening sandstone beds in channel forms, some trough cross stratification present
25 m			
			Interbedded microbialites and carbonate grainstone to organic-rich carbonate mudstone
20 m			
			Very fine sandstone with siltstone lense (possible sulfur present)
			Mostly covered, thinly laminated siltstone
15 m			
			Interbedded coarsening ooid to peloid grainstone and microbialites
			Fine sandstone with low angle laminations
			Ooid grainstone, bed thickness fluctuates
10 m			
			Silty, fine sandstone with wave ripple laminations and thin beds of rip up clasts
			Fissile, carbonate mudstone
5 m			
			Interbedded claystone/ siltstone and very fine sandstone, sandstone has abundant wave-ripple laminations
0 m			

Section Name: Evacuation Creek/ Gray Huts Section
Location (lat/long): N39°48'29" W109°4'48.4" Total Thickness Measured: 216.8 m
Date Measured: 10/27-10/29/2011 Measured By: Morgan Rosenberg, Jon Primm

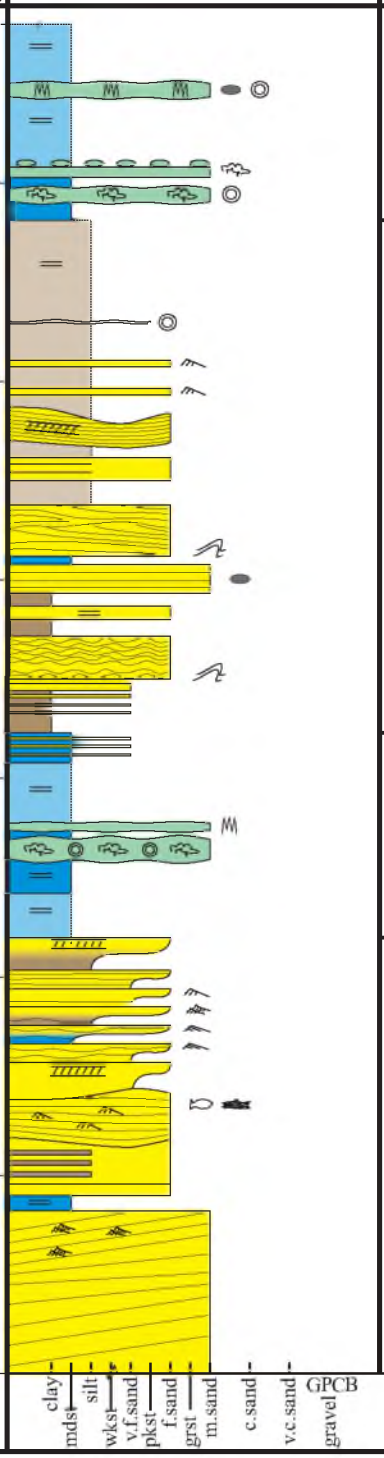

Stratigraphic Zone	Additional Notes
R3	Interbedded carbonate mudstone and microbialites, some ooid grains present in microbialite beds, well defined stromatolite heads (up to 20 cm in diameter)
L2	Mostly covered siltstone with thin microbialite beds present Thin, fine sandstone layers with ripples Interbedded covered siltstone and fine sandstone, low angle laminations present in bottom sandstone possibly broad troughs, top sandstone channelized with trough cross stratifications Interbedded claystone and sandstone, up to medium sandstone, abundant soft sediment deformation present, rip up clasts present towards top
R2	Thinly bedded carbonate mudstone with ooid grainstone and microbialite beds
Douglas Creek Member	Numerous, thin coarsening upward packages from mudstone/ siltstone to fine sandstone with current ripples, some climbing Fine sandstone body of fluctuating thickness, current ripples present, fish scale and tree limb fossils Medium sandstone with low angle to plane parallel laminations, climbing current ripples present at top

Section Name: Evacuation Creek/ Gray Huts Section
Location (lat/long): N39°48'29" W109°4'48.4" Total Thickness Measured: 216.8 m
Date Measured: 10/27-10/29/2011 Measured By: Morgan Rosenberg, Jon Primm

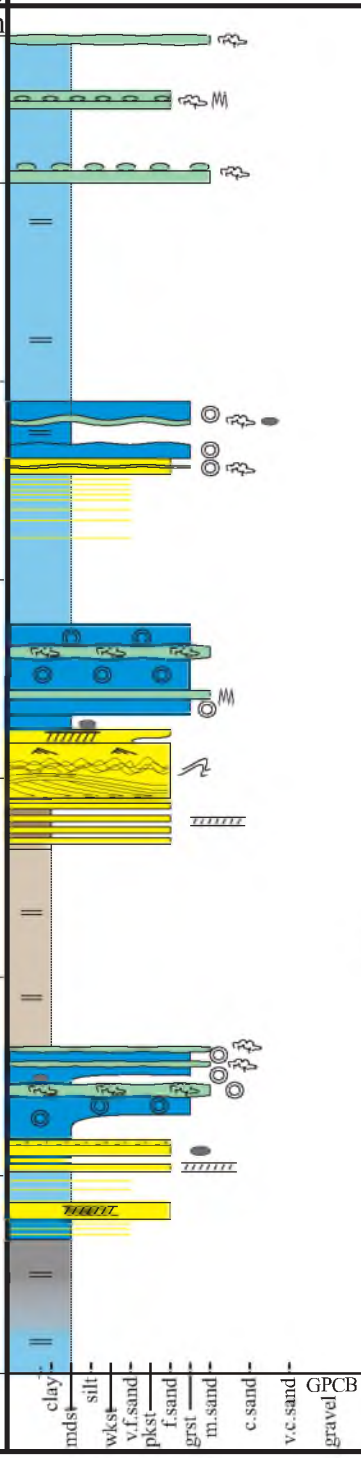

Section Name: Evacuation Creek/ Gray Huts Section
Location (lat/long): N39°48'29" W109°4'48.4" Total Thickness Measured: 216.8 m
Date Measured: 10/27-10/29/2011 Measured By: Morgan Rosenberg, Jon Primm

Thick. Feet (m)	Graphic Log	Stratigraphic Zone	Additional Notes
135.1 m	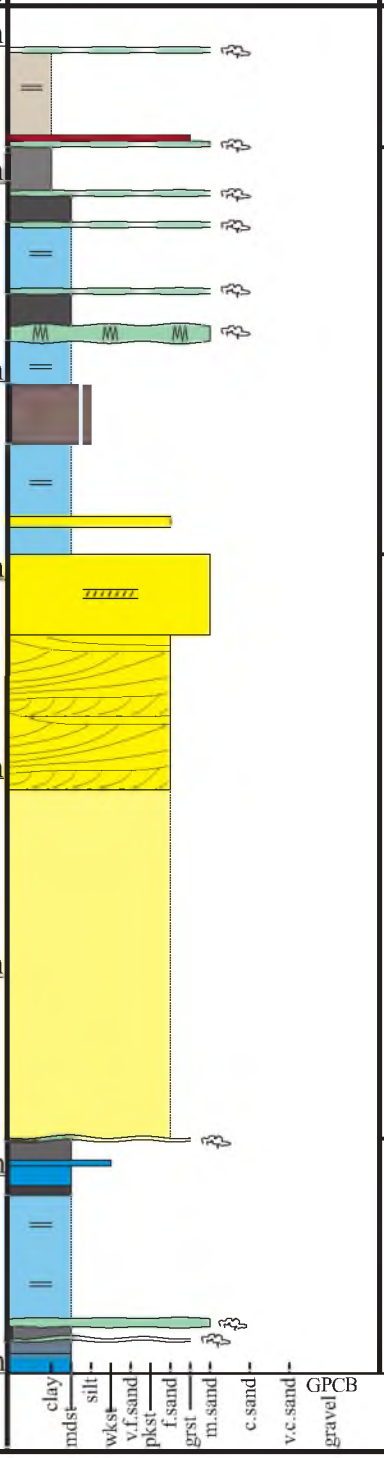	L5	Mostly covered claystone, plane parallel laminations
131.7 m		R5	Possibly same thick microbialite as in Condo Section (base of R5)
126.7 m			Mostly covered, lean carbonate mudstone with numerous thin microbialite beds, some beds organic-rich
121.7 m		L4	Mostly covered fine sandstone, some trough cross stratification present towards top, grains coarsen to medium at top
116.7 m			
111.7 m			
106.7 m		R4	Carbonate mudstone with some thin microbialite beds, some thin organic rich beds
101.7 m			

Section Name: Evacuation Creek/ Gray Huts Section
Location (lat/long): N39°48'29" W109°4'48.4" Total Thickness Measured: 216.8 m
Date Measured: 10/27-10/29/2011 Measured By: Morgan Rosenberg, Jon Primm

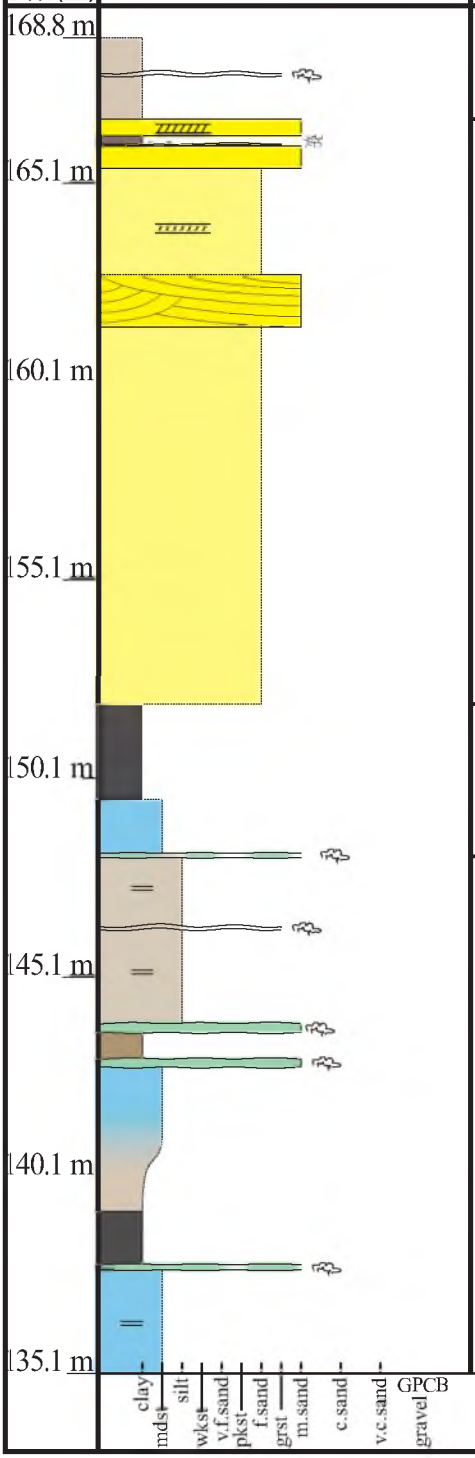

Stratigraphic Zone	Additional Notes
Upper R6	Medium sandstone with trough cross stratification, mudcracks at base in silty mudstone below microbialites under mud cracks
Middle R6	Covered fine to medium sandstone with trough cross stratification Medium sandstone with trough cross stratification Covered fine sandstone
Lower R6	Lean to organic-rich carbonate mudstone
L5	Mostly covered claystone to siltstone with some thin microbialites Crystal-like pattern on top of microbialites Mostly covered carbonate mudstone, some microbialite and claystone beds present, mostly lean, but some organic-rich beds

Section Name: Evacuation Creek/ Gray Huts Section
Location (lat/long): N39°48'29" W109°4'48.4" Total Thickness Measured: 216.8 m
Date Measured: 10/27-10/29/2011 Measured By: Morgan Rosenberg, Jon Primm

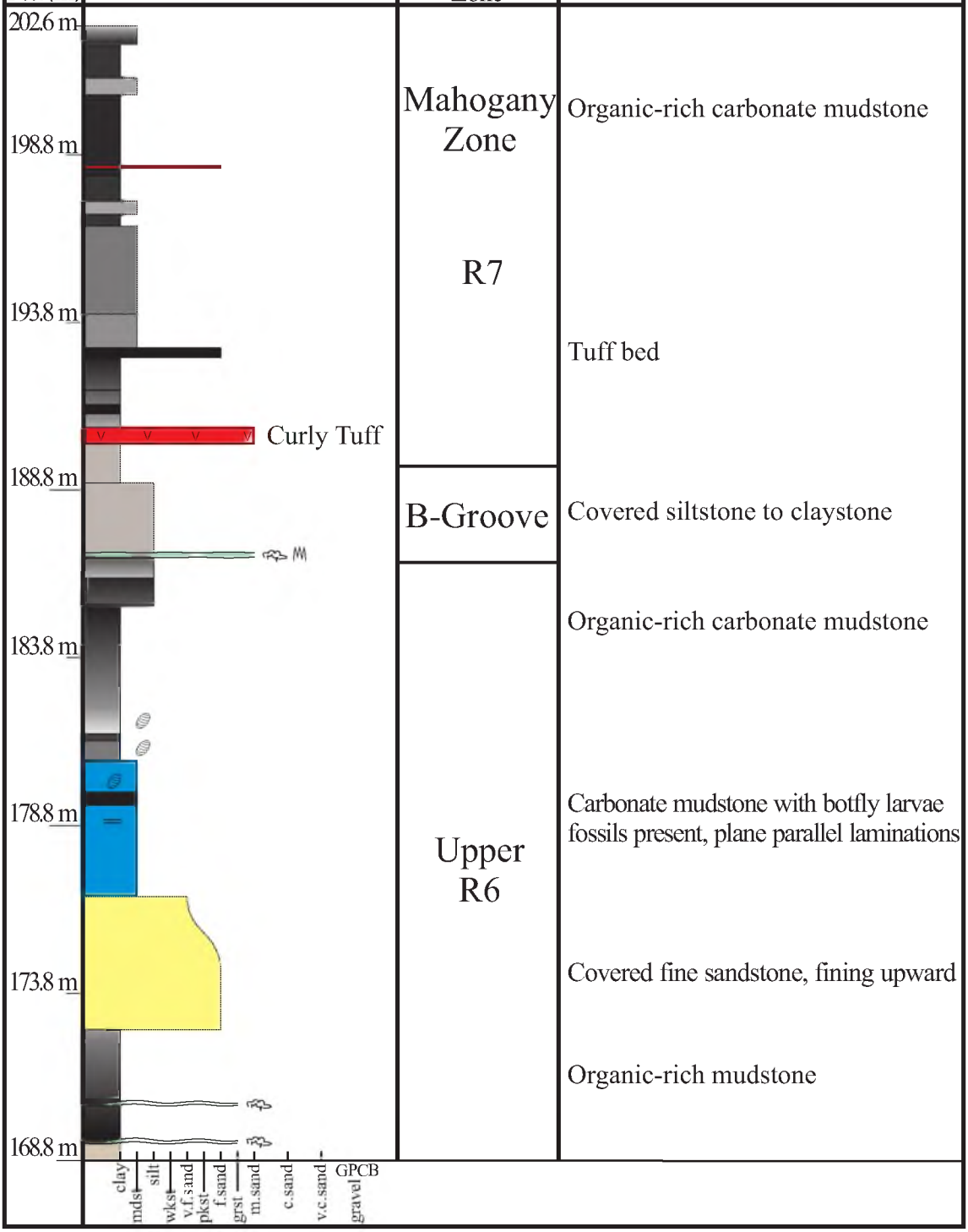

REFERENCES

Abbott, W., 1957, Tertiary of the Uinta Basin: Guidebook to the geology of the Uinta Basin; Eighth Annual Field Conference.

Abels, H.A., Clyde, W.C., Gingerich, P.D., Hilgen, F.J., Fricke, H.C., Bowen, G.J., and Lourens, L.J., 2012, Terrestrial carbon isotope excursions and biotic change during Palaeogene hyperthermals: Nature Geoscience, v. 5, no. 5, p. 326–329, doi: 10.1038/ngeo1427.

Andrews, A., 2006, Oil Shale: History, incentives, and policy: Congressional Research Service, 1–32 p.

Aswasereelert, W., Meyers, S.R., Carroll, A.R., Peters, S.E., Smith, M.E., and Feigl, K.L., 2013, Basin-scale cyclostratigraphy of the Green River Formation, Wyoming: Geological Society of America Bulletin, v. 125, no. 1-2, p. 216–228, doi: 10.1130/B30541.1.

Bader, J.W., 2009, Structural and tectonic evolution of the Douglas Creek arch, the Douglas Creek fault zone, and environs, northwestern Colorado and northeastern Utah: Implications for petroleum accumulation in the Piceance and Uinta basins: Rocky Mountain Geology, v. 44, no. 2, p. 121–145.

Bhattacharya, J.P., and Giosan, L., 2003, Wave-influenced deltas: geomorphological implications for facies reconstruction: Sedimentology, v. 50, p. 187–210.

Birgenheier, L. P., Plink-Bjorklund, P., and Golab, J., 2009, Geochemical and sedimentary record of climate change from the Paleocene-Eocene Colton and Green River Formations, Southwestern Uinta Basin, Utah: American Association of Petroleum Geologists Annual Meeting.

Birgenheier, L., and Vanden Berg, M., 2011, Core-based integrated sedimentologic, stratigraphic, and geochemical analysis of the oil shale bearing Green River Formation, Uinta Basin, Utah: United States Department of Energy DE-FE0001243, 1–30 p.

Birgenheier, L., Plink-Bjorklund, P., Vanden Berg, M.D., Rosenberg, M., Toms, L., and Golab, J., 2013, A genetic stratigraphic framework of the Green River Formation, Uinta Basin, Utah: The impact of climatic controls on lake evolution: American Association of Petroleum Geologists Annual Meeting.

Blackstone, D.L., Jr, 1983, Laramide compressional tectonics, southeastern Wyoming: Contributions to Geology, University of Wyoming, v. 22, no. 1, p. 1–38.

Blakey, R.C., and Ranney, W., 2008, Ancient landscapes of the Colorado Plateau: Grand Canyon Association, Grand Canyon, AZ.

Carroll, A.R., and Bohacs, K.M., 1999, Stratigraphic classification of ancient lakes: Balancing tectonic and climatic controls: Geology, v. 27, no. 2, p. 99–102.

Cashion, W.B., 1967, Geology and fuel resources of the Green River Formation southeastern Uinta Basin Utah and Colorado: United States Department of the Interior: Geological Survey Professional Paper, Washington DC.

Crews, S.G., and Ethridge, F.G., 1993, Laramide Tectonics and humid alluvial fan sedimentation, Ne Uinta Uplift, Utah and Wyoming: Journal of Sedimentary Petrology, v. 63, no. 3, p. 420–436.

DeCelles, P.G., 1994, Late Cretaceous-Paleocene synorogenic sedimentation and kinematic history of the Sevier thrust belt, northeast Utah and southwest Wyoming: Geological Society of America Bulletin, v. 106, p. 32–56.

Dickinson, W.R., Klute, M.A., Hayes, M.J., Janecke, S.U., Lundin, E.R., McKittrick, M.A., and Olivares, M.D., 1988, Paleogeographic and paleotectonic setting of Laramide sedimentary basins in the central Rocky Mountain region: Geological Society of America Bulletin, v. 100, p. 1023–1039.

Dyni, J.R., 2006, Geology and resources of some world oil-shale deposits: USGS Scientific Investigations Report 2005-5294, p. 1–49.

Fahey, J.J., 1962, Saline minerals of the Green River Formation: United States Department of the Interior: Geological Survey Professional Paper, Washington D.C.

Foreman, B.Z., Heller, P.L., and Clementz, M.T., 2012, Fluvial response to abrupt global warming at the Palaeocene/Eocene boundary: Nature,, p. 1–4, doi: 10.1038/nature11513.

Fouch, T.D., 1975, Lithofacies and related hydrocarbon accumulations in Tertiary strata of the Western and Central Uinta Basin, Utah, *in* Bolyard, D.W. ed., Deep drilling frontiers in the Central Rocky Mountains: Rocky Mountain Association of Geologists Symposium, Denver, p. 163–173.

Fouch, T.D., Nuccio, V.F., Osmond, J.C., MacMillan, L., Cashion, W.B., and Wandrey, C.J., 1992, Oil and gas in uppermost Cretaceous and Tertiary rock, Uinta Basin, Utah:, p. 1–40.

Glover, P., 2000, Spectral Gamma Ray Log, *in* Petrophysics MSc Course Notes, p. 111–120.

Hagen, E.S., Shuster, M.W., and Furlong, K.P., 1985, Tectonic loading and subsidence of intermontane basins: Wyoming foreland province: Geology, v. 13, p. 585–588.

Johnson, R.C., 1985, Early Cenozoic history of the Uinta and Piceance Creek Basins, Utah and Colorado, with Special Reference to the Development of Eocene Lake Uinta: Rocky Mountain Section (SEPM),, p. 1–30.

Keighley, D., Flint, S., Howell, J., and Moscariello, A., 2003, Sequence stratigraphy in lacustrine basins: A model for part of the Green River Formation (Eocene), Southwest Uinta Basin, Utah, U.S.A.: Journal of Sedimentary Research, v. 73, no. 6, p. 987–1006.

Keighley, D., Flint, S., Howell, J., Andersson, D., Collins, S., Moscariello, A., and Stone, G., 2002, Surface and subsurface correlation of the Green River Formation in central Nine Mile Canyon, SW Uinta Basin, Carbon and Duchesne Counties, East-Central Utah: Utah Geological Survey Miscellaneous Publication, v. 02-1, p. 1–66.

Moncure, G., and Surdam, R.C., 1980, Depositional environment of the Green River Formation in the vicinity of the Douglas Creek Arch, Colorado and Utah: Contributions to Geology, University of Wyoming, v. 19, p. 9–24.

Moore, J., Taylor, A., Johnson, C., Ritts, B.D., and Archer, R., 2012, Facies analysis, reservoir characterization, and LIDAR modeling of an Eocene Lacustrine Delta, Green River Formation, Southwest Uinta Basin, Utah, *in* Baganz, O.W., Bartov, Y., Bohacs, K., and Nummedal, D. eds., Lacustrine sandstone reservoirs and hydrocarbon systems: AAPG Memoir 95, p. 183–208.

Morgan, C.D., Chidsey, T.C., Jr, McClure, K.P., Bereskin, S.R., and Deo, M.D., 2003, Reservoir characterization of the Lower Green River Formation, Uinta Basin, Utah: Utah Geological Survey 411, 1–140 p.

Olariu, C., and Bhattacharya, J.P., 2006, Terminal distributary channels and delta front architecture of River-Dominated Delta Systems: Journal of Sedimentary Research, v. 76, no. 2, p. 212–233, doi: 10.2110/jsr.2006.026.

Osmond, J.C., 1965, Geologic History of Site of Uinta Basin, Utah: AAPG Bulletin, v. 49, no. 11, p. 1957–1973.

Picard, M.D., and High, L.R., Jr, 1972, Paleoenvironmental reconstructions in an area of rapid facies change, Parachute Creek Member of Green River Formation (Eocene),Uinta Basin, Utah: Geological Society of America Bulletin, v. 83, p. 2689–2708.

Plink-Bjorklund, P., Birgenheier, L., and Golab, J., 2009, Alluvial Depositional Models Consortium Year End Report.

Plink-Bjorklund, P., Birgenheier, L., and Golab, J., 2010, Separating allogenic and autogenic controls in a super-greenhouse fluvial system, *in* New Orleans, p. 1–27.

Plink-Bjorklund, P., and Birgenheier, L.P., 2012, Extreme seasonality during Early Eocene hyperthermals: American Geophysical Union Annual Convention.

Renaut, R.W., and Gierlowski-Kordesch, E.H., 2010, Lakes, *in* James, N.P. and Dalrymple, R.W. eds., Facies models 4, Geological Association of Canada, St. John's, p. 541–575.

Rider, M., 2008, The gamma ray and spectral gamma ray log, *in* The geological interpretation of well logs, Rider-French Consulting Ltd., Sutherland, p. 67–90.

Ruble, T.E., and Philp, R.P., 1998, Stratigraphy, depositional environments and organic geochemistry of source-rocks in the Green River Petroleum System, Uinta Basin, Utah (J. K. Pitman & A. R. Carroll, Eds.): Modern and Ancient Lake Systems; Utah Geologic Association Guidebook 26,, p. 289–321.

Ryder, R.T., Fouch, T.D., and Elison, J.H., 1976, Early Tertiary sedimentation in the western Uinta Basin, Utah: Geological Society of America Bulletin, v. 87, no. 60402, p. 496–512.

Schomacker, E.R., Kjemperud, A.V., and Nystuen, J.P., 2010, Recognition and significance of sharp-based mouth-bar deposits in the Eocene Green River Formation, Uinta Basin, Utah: Sedimentology, v. 57, no. 4, p. 1069–1087, doi: 10.1111/j.1365-3091.2009.01136.x.

Smith, M.E., Carroll, A.R., and Singer, B.S., 2008, Synoptic reconstruction of a major ancient lake system: Eocene Green River Formation, western United States: Geological Society of America Bulletin, v. 120, no. 1-2, p. 54–84, doi: 10.1130/B26073.1.

Smith, M.E., Chamberlain, K.R., Singer, B.S., and Carroll, A.R., 2010, Eocene clocks agree: Coeval 40Ar/39Ar, U-Pb, and astronomical ages from the Green River Formation: Geology, v. 38, no. 6, p. 527–530, doi: 10.1130/G30630.1.

Smith, M.E., Singer, B.S., and Carroll, A.R., 2003, 40 Ar/39 Ar geochronology of the Eocene Green River Formation, Wyoming: Geological Society of America Bulletin, v. 115, p. 549–565.

Surdam, R.C., and Stanley, K.O., 1980, Effects of changes in drainage-basin boundaries on sedimentation in Eocene Lakes Gosiute and Uinta of Wyoming, Utah, and Colorado: Geology, v. 8, p. 135–139.

Taylor, A.W., and Ritts, B.D., 2004, Mesoscale heterogeneity of fluvial-lacustrine reservoir analogues: Examples from the Eocene Green River and Colton Formations, Uinta Basin, Utah, USA: Journal of Petroleum Geology, v. 27, p. 3–26.

Tänavsuu-Milkeviciene, K., and Sarg, F.J., 2012, Evolution of an organic-rich lake basin - stratigraphy, climate and tectonics: Piceance Creek basin, Eocene Green River Formation: Sedimentology, v. 59, no. 6, p. 1735–1768, doi: 10.1111/j.1365-

3091.2012.01324.x.

Vanden Berg, M., 2008, Basin-wide evaluation of the uppermost Green River Formation's Oil-Shale Resource, Uinta Basin, Utah and Colorado: Natural Resources Map and Bookstore, 1–31 p.

Vanden Berg, M.D., Anderson, P., Wallace, J., Morgan, C.D., and Carney, S., 2012, Water-related issues affecting conventional oil and gas recovery and potential oil-shale development in the Uinta Basin, Utah: United States Department of Energy DE-NT0005671, 1–267 p.

Williamson, C.R., and Picard, M.D., 1974, Petrology of carbonate rocks of the Green River Formation (Eocene): Journal of Sedimentary Petrology, v. 44, p. 738–759.

Witkind, I.J., 1995, Geologic map of the Price 1^{o} x 2^{o} quadrangle, Utah.